UNIVERSITAT
POLITÈCNICA
DE VALÈNCIA

Modelling the hydraulic response of permeable pavements: a numerical and experimental approach for model comparison and sensitivity analysis to design parameters

June 2023

Author: Eneko Madrazo Uribeetxebarria

Supervisors: Maddi Garmendia Antín
Jabier Almandoz Berrondo
Ignacio Andrés Doménech

Abstract / Resumen / Resum

Abstract

Permeable Pavements (PP) are a Sustainable Urban Drainage System (SUDS) technique. Unlike other such techniques, it provides a transitable hard surface while managing surface stormwater, being its hydraulic properties fundamental for its performance as a SUDS. This dissertation explores the hydraulic performance of PPs, based on the hydrologic-hydraulic model of PP provided in the widely used Storm Water Management Model (SWMM). The dissertation is presented in a *three-paper* format. Accordingly, after an approach to the general research question given in the first introductory chapter, the second chapter of the document analyses which parameters are the most influential and which are negligible in the model by providing a general sensitivity analysis. The next chapter explores the relation between the PP model from SWMM and the widely used Curve Number (CN) model regarding runoff generated by both models and examines the relationship between both approaches based on the pavement permeability variable. The fourth chapter analyses the PP response under controlled experimental conditions and compares it with the PP model given in SWMM. After a general discussion of the results in the fifth chapter, general conclusions are given in the last chapter. The dissertation deepens the understanding of the hydraulic behaviour of PPs to help practitioners and researchers with its characterisation.

Keywords: permeable pavement, hydrological modelling, sensitivity analysis, SWMM, curve number.

Resumen

Los Pavimentos Permeables (PP) son una técnica de los denominados Sistemas Urbanos de Drenaje Sostenible (SUDS). A diferencia de otras técnicas de este tipo, proporciona una superficie dura transitable a la vez que gestiona las aguas pluviales superficiales, siendo sus propiedades hidráulicas fundamentales para su rendimiento como SUDS. Esta tesis explora el rendimiento hidráulico de los PP, basándose en el modelo hidrológico-hidráulico de PP proporcionado en el ampliamente utilizado Storm Water Management Model (SWMM). La tesis se presenta en un formato de tres artículos. Así, tras una aproximación a la pregunta general de investigación dada en el primer capítulo introductorio, el segundo capítulo del documento analiza qué parámetros son los más influyentes y cuáles son despreciables en el modelo, proporcionando un análisis de sensibilidad general. El siguiente capítulo explora la relación entre el modelo de PP de SWMM y el modelo de número de curva (CN), ampliamente utilizado, en lo que respecta a la escorrentía deducida por ambos modelos en función de la permeabilidad del pavimento. En el cuarto capítulo se analiza la respuesta del PP en condiciones experimentales controladas y se compara con el modelo de PP dado en SWMM. Tras una discusión general de los resultados en el quinto capítulo, se ofrecen unas conclusiones generales en el último. La tesis profundiza en el conocimiento del comportamiento hidráulico de los PP para ayudar a profesionales e investigadores en su caracterización.

Palabras clave: pavimento permeable, modelización hidrológica, análisis de sensibilidad, SWMM, número de curva.

Resum

Els Paviments Permeables (PP) són una tècnica dels denominats Sistemes Urbans de Drenatge Sostenible (SUDS). A diferència d'altres tècniques d'aquest tipus, proporciona una superfície dura transitable alhora que gestiona les aigües pluvials superficials, sent les seues propietats hidràuliques fonamentals per al seu rendiment com SUDS. Aquesta tesi explora el rendiment hidràulic dels PP, basant-se en el model hidrològic-hidràulic de PP proporcionat en l'àmpliament utilitzat Storm Water Management Model (SWMM). La tesi es presenta en un format de tres articles. Així, després d'una aproximació a la pregunta general d'investigació donada en el primer capítol introductori, el segon capítol del document analitza quins paràmetres són els més influents i quins són menyspreables en el model, proporcionant una anàlisi de sensibilitat general. El següent capítol explora la relació entre el model de PP de SWMM i el model de número

de corba (CN), àmpliament utilitzat, pel que fa a l'escolament deduït per tots dos models en funció de la variable permeabilitat del paviment. En el quart capítol s'analitza la resposta del PP en condicions experimentals controlades i es compara amb el model de PP donat en SWMM. Després d'una discussió general dels resultats en el cinqué capítol, s'ofereixen unes conclusions generals en l'últim. La tesi aprofundix en el coneixement del comportament hidràulic dels PP per a ajudar a professionals i investigadors en la seua caracterització.

Paraules clau: paviment permeable, modelització hidrològica, anàlisi de sensibilitat, SWMM, número de corba.

Zuena ere bada,
–Izar, Lur, Martin eta Naiara–
zuen denborarekin egina baita.

Acknowledgements

I would like to thank the Donostia City Council, especially Joseba, who is devoted to SUDS, for making this research possible. Without their help, this dissertation would not be possible.

I also would like to thank my three directors. Someone told me, in the very early stages of the dissertation, that it was not advisable to have so many directors because I would go mad with different indications. Now I have finished, I have to thank all three, each of them has been very helpful in his/her area of expertise, respecting other directors' decisions and guiding me in the right direction.

Finally, my biggest thanks to my family. To my kids for not getting angry with me when I have not devoted the appropriate attention to them, and, to my wife, for all the support she gave me from the beginning.

Authorization

Dr. Ignacio Andrés Doméch, Tenured Lecturer of the School of Civil Engineering in the Department of Hydraulic Engineering and Environment, Universitat Politècnica de València, AUTHORISE:

The presentation of the Doctoral Thesis entitled *Modelling the hydraulic response of permeable pavements: a numerical and experimental approach for model comparison and sensitivity analysis to design parameters*, carried out by Eneko Madrazo Uribeetxebarria, and presented in the form of a compendium of articles, under the direction and supervision of Maddi Garmendia Antín (UPV/EHU), Jabier Almandoz Berrondo (UPV/EHU), and me, in the Water and Environmental Engineering programme by the Universitat Politècnica de València.

In compliance with current legislation, I sign this authorization in València.

Ignacio Andrés Doménech
igando@hma.upv.es

Research outputs

This section lists the main outputs related to the Ph.D. dissertation, materialised during the research period. The output items are grouped in research papers, conference presentations at national and international levels, research projects related to SUDS investigation, and a research visit to an international laboratory.

A. Research papers

Article 1: urban water management general analysis

Garmendia Antín, M. & Madrazo Uribeetxebarria, E. (2020). Ura eta hirigintza. Paradigma-aldaketaren bidean hiri-uren kudeaketan (Water and urban planning. Towards a paradigm shift in urban water management). Aldiri. Arkitektura eta abar, I(41), pp. 8-11. https://www.buruxkak.eus/aldiri/aldiri-41-ura-gara/160

Article 2: review on permeable pavements

Madrazo-Uribeetxebarria, E., Garmendia Antín, M. & Meaurio Arrate, M. (2022). Permeable pavements as integrated elements of urban stormwater network. Ekaia. https://doi.org/10.1387/ekaia.23083

Article 3: sensitivity analysis of permeable pavement model

Madrazo-Uribeetxebarria, E., Garmendia Antín, M., Almandoz Berrondo, J., & Andrés-Doménech, I. (2021). Sensitivity analysis of permeable pavement hydrological modelling in the Storm Water Management Model. Journal of Hydrology, 600, 126525. `https://doi.org/10.1016/j.jhydrol.2021.126525`

Article 4: numerical comparison with the CN

Madrazo-Uribeetxebarria, E., Garmendia Antín, M., Almandoz Berrondo, J., & Andrés-Doménech, I. (2022). Modelling runoff from from permeable pavements: A link to the Curve Number method. Water, 15(1), 160. `https://doi.org/10.3390/w15010160`

Article 5: experimental analysis of the model

Madrazo-Uribeetxebarria, E., Garmendia Antín, M., Alberro Eguilegor, G., & Andrés-Doménech, I. (2023). Analysis of the hydraulic performance of permeable pavements on a layer-by-layer basis. Construction and Building Materials, 387, 131587. `https://doi.org/10.1016/j.conbuildmat.2023.131587`

B. Conference presentations

Conference 1: relation between PP model and CN

Madrazo-Uribeetxebarria, E., Garmendia Antín, M., Almandoz Berrondo, J., & Andrés-Doménech, I. (2020). Modelling impervious pavements with the Low Impact Development module of the Storm Water Management Model. In M. Kalinowska (Ed.), 6th IAHR Europe Congress. Abstract Book (pp. 806–807). `https://addi.ehu.es/handle/10810/54908`

Conference 2: experimental data analysis for permeable pavements

Madrazo-Uribeetxebarria, E., Garmendia Antín, M., Almandoz Berrondo, J., & Andrés-Doménech, I. (2019). Hydraulic performance of permeable asphalt and PICP in SWMM, validated by laboratory data. In S. Mambretti & J. L. Miralles i Garcia (Eds.), WIT Transactions on Ecology and the Environment (Vol. 238, pp. 569–579). WIT Press. https://doi.org/10.2495/SC190491

Conference 3: hydraulic data analysis for subsurface cells

Madrazo-Uribeetxebarria, E., Garmendia Antín, M., Almandoz Berrondo, J., & Andrés-Doménech, I. (2019). Análisis hidráulico y modelización de geoceldas de drenaje subsuperficial en pavimentos permeables. In J. González, A. Galán, & A. Díaz (Eds.), VI Jornadas de Ingeniería del Agua 2019. . Libro de resúmenes (pp. 314-316). Universidad de Castilla-La Mancha. https://addi.ehu.es/handle/10810/35744

Conference 4: SUDS space allocation

Madrazo-Uribeetxebarria, E., Garmendia Antín, M., Almandoz Berrondo, J., & Andrés-Doménech, I. (2022). Influence of SUDS Allocated Area on Runoff Reduction in Developing Urban Catchments: a Case Study in San Sebastian (Spain). In M. Ortega-Sánchez (Ed.), Proceedings of the 39th IAHR World Congress - IAHR 2022 (pp. 6948–6954). International Association for Hydro-Environment Engineering and Research-IAHR. https://doi://10.3850/IAHR-39WC2521716X2022282

Conference 5: experimental site construction

Garmendia Antín, M., Madrazo Uribeetxebarria, E., Martín-Garín, A., & Millán, J. A. (5-6 October). Progress towards sustainable stormwater management: Field monitoring of permeable pavements. EESAP13. Abstract Book. 13th Edition of the International Congress on Energy Efficiency and Sustainability in Architecture and Urban Planning (EESAP 13), Donostia.

Conference 6 (accepted): performance after implementation

Madrazo-Uribeetxebarria, E., Garmendia Antín, M., Andrés-Doménech, I., Lekuona Orkaizagirre, A., Meaurio, M., & Gredilla, A. (2023). Permeable pavement flood control performance for several layouts in an Atlantic climate site. Novatech 2023.

C. Research projects

Project 1: PP model calibration and validation.

Calibración y validación de un modelo matemático para el análisis de la respuesta hidráulica y de retención de contaminantes de pavimentos permeables a partir de la monitorización de una zona experimental en Txomin-Enea (Donostia- San Sebastián). Duration: 2 years (29/11/2019 to 28/11/2021). Budget: 18 000 euro.

Project 2: several PP performance analysis.

Gestión sostenible del agua de escorrentía urbana. Duration: 2 years (01/11/2022 to 01/11/2024). Budget: 24 772 euro.

Project 3: SUDS design with students.

EHUsuds: Integrar los Sistemas Urbanos de Drenaje Sostenible (SUDS) en los campus de la UPV/EHU. Duration: 1 year (01/11/2020 to 01/11/2021). Budget: 1900 euro.

Project 4: SUDS design with students.

EHUsuds: Integrar los Sistemas Urbanos de Drenaje Sostenible (SUDS) en los campus de la UPV/EHU. Duration: 1 year (01/11/2021 to 01/11/2022). Budget: 2000 euro.

Project 5: SUDS design with students.

EHUsuds: Integrar los Sistemas Urbanos de Drenaje Sostenible (SUDS) en los campus de la UPV/EHU. Duration: 1 year (01/11/2022 to 01/11/2023). Budget: 1680 euro.

D. Visiting Research laboratories

Stay 1: INSA Lyon, DEEP laboratory.

Laboratoire Déchets Eaux Environnement Pollutions (DEEP), Institut National des Sciences Appliquées de Lyon (INSA Lyon). Duration: 1 month (03/01/2022 to 03/02/2022). Topic: SUDS modelling. Host researcher: Gislain Lipeme Kouyi.

Contents

List of Figures

List of Tables

Chapter 1

Introduction

1.1 Context

Traditionally, urban drainage systems have been designed to direct surface waters to the conveyance network and prevent flooding. These systems face many challenges, but climate change and urban growth are identified as the most critical factors impacting their performance (Arnone et al. 2018).

In order to mitigate the undesirable effects of climate change, making the drainage infrastructure less vulnerable to uncertain future climate, several adaptative strategies were proposed in recent studies (Yazdanfar and Sharma 2015): implementation of sustainable technologies and management, focus on integrated urban water management strategies, improve uncertainty reduction techniques for climate projections, update of the design procedure, and use of long-term continuous simulation for system design.

In that regard, Sustainable Urban Drainage Systems (SUDS) are structural measures for stormwater management, an additional planning tool to design more resilient urban systems, increasingly recommended at both strategic planning and implementation levels (Pappalardo and La Rosa 2020).

More specifically, SUDS involve several technologies that replicate the natural water cycle in the urban environment, which are typically configured to work together, creating a management train (Fletcher et al. 2015). Hence, from a hydrological point of view, SUDS enhance infiltration, evaporation, retention, and detention. However, SUDS advantages are not just hydraulic or related to flooding; they also positively affect water quality, biodiversity, aesthetics, or recreational aspects (Charlesworth and Wade 2014).

Despite the recognised advantages, there are still multiple factors limiting its implementation. Those barriers, rather than technical, are mainly socio-institutional (Brown and Farrelly 2009). This is the situation, for instance, at a local level in Spain, where the lack of national standards developing the general technical criteria for design was identified as the main barrier (Andrés-Doménech et al. 2021).

1.2 Research motivation

In this context, researchers from the University of the Basque Country (UPV/EHU) and the Donostia/San Sebastián City Council agreed to collaborate in the SUDS investigation to promote its implementation at a city level. The overall objective for the collaboration was to promote the use of SUDS, aiming to overcome reluctance to long-term efficiency and encourage coordination between municipal services.

As a starting point, city council technicians focused on a new local development, Txominenea, with severe flooding episodes in the last decades. As a first approach, it was considered that a mathematical model for the new development should contribute to analysing the influence of hypothetical SUDS implemented into the new development and, hence, quantify the hydraulic benefits derived from their use. For that purpose, the Storm Water Management Model was selected because it is one of the most popular among scientists and integrates several SUDS models into a more general hydrologic-hydraulic model (Kaykhosravi, Sahereh, Khan, Usman T, and Jadidi, Amaneh 2018). Consequently, a model was created for the entire Txominenea plot, which shall facilitate obtaining specific conclusions at the municipal level and, where possible, broader ones.

However, several uncertainty sources emerge while using models (Radwan, Willems, and Berlamont 2004), and ours was no exception. In order to reduce uncertainty, models are usually calibrated and validated, and a sensitivity analysis is performed previously. However, the municipality did not have any data

at that moment. Hence, UPV/EHU researchers suggested creating a monitored site in the new development under construction, a decision the municipality approved. Nevertheless, as urbanisation construction had already begun, the proposed SUDS should have to adhere to provided urban land uses. Therefore, permeable pavement (PP) was considered the most appropriate SUDS type because PPs, unlike other such techniques, provide a transitable hard surface while managing surface stormwater (Kuruppu, Rahman, and Rahman 2019), making it a very beneficial solution in highly urbanised areas. Therefore, the research focused on this specific SUDS technique.

On the other hand, SWMM provided the PP model to analyse SUDS's performance and study its implementation in new plots. This PP model is defined on a layer basis, similar to other SUDS types in SWMM, although the PP model has two notable characteristics if compared to other SUDS: it is the only one implementing the pavement layer, and it is also the only one giving the soil layer as optional (Rossman 2015). However, as mentioned before, there was a gap not only in understanding its hydraulic response but also in the values given to the model parameters.

Consequently, it was considered of great value to deepen the model performance. Exploring the model by analysing its parameters was essential as a first step. Some numerical analyses were designed for that purpose, and bibliographical research was conducted. In addition, materials implemented in the experimental site were collected and transported to the university facilities. These samples were used to design laboratory experiments to understand the implemented materials' hydraulic response. To this end, an existing hydrological bench had to be transformed into a controlled rain and slope test bench.

In parallel, the construction of the new experimental plot continued, which shall also be monitored. UPV/EHU researchers were involved in all stages of the design and implementation of the PP site, which demanded selecting the relevant parameters to be measured and designing the required equipment to measure those parameters precisely. Figure 1.1 provides pictures of the construction site and includes elements implemented in the new plot and used in laboratory experiments.

(a) Experimental site construction.

(b) Experimental site waterproofing.

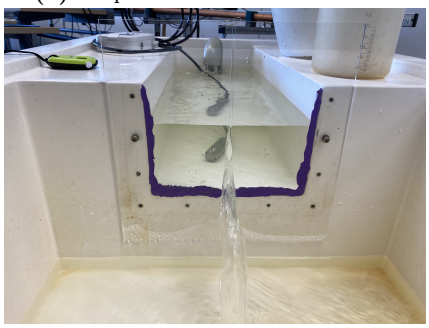

(c) Weir design and calibration.

(d) Rain simulator construction.

Figure 1.1: Pictures related to the experimental implementation.

1.3 General and specific objectives

Given the above explained precedents, this thesis aims to study the hydraulic response of permeable pavements, both numerically and experimentally, to facilitate its implementation into wider models. Hence, based on that initial global objective, where several SUDS implementation was to be analysed, the scope has been narrowed to the permeable pavement technique, based on a modelling approach focused on the water quantity variable.

To achieve that goal, the dissertation also sets some partial goals. The first is to explore how different factors influence the model's output, identifying which parameters are the most important and which may be neglected. The second partial objective is to compare the runoff created by the model with another widely used model to characterise generated runoff. The third and last one is to test the model against laboratory data obtained under specific controlled conditions. As an overview of the document structure and objectives, a graph-

ical summary is given in Figure 1.2, including the main outputs derived from the research work, with references to the Research Outputs section, at the beginning of the document.

1.4 Structure of the thesis

The dissertation is presented in a paper compilation format based on the three main accepted articles:

Article 1: Madrazo-Uribeetxebarria, E., Garmendia Antín, M., Almandoz Berrondo, J., & Andrés-Doménech, I. (2021). Sensitivity analysis of permeable pavement hydrological modelling in the Storm Water Management Model. *Journal of Hydrology*, 600. `https://doi.org/https://doi.org/10.1016/j.jhydrol.2021.126525`

Article 2: Madrazo-Uribeetxebarria, E., Garmendia Antín, M., Almandoz Berrondo, J., & Andrés-Doménech, I. (2022). Modelling runoff from from permeable pavements: A link to the Curve Number method. *Water*, 15(1), 160. `https://doi.org/10.3390/w15010160`

Article 3: Madrazo-Uribeetxebarria, E., Garmendia Antín, M., Alberro Eguilegor, G., & Andrés-Doménech, I. (2023). Analysis of the hydraulic performance of permeable pavements on a layer-by-layer basis. *Construction and Building Materials*, 387, 131587. `https://doi.org/10.1016/j.conbuildmat.2023.131587`

Chapter 1 describes the context and motivation for the research, as well as the general and specific objectives of the dissertation.

Chapter 2 corresponds to *Article 1* (or Article 3 in Figure 1.2). The chapter provides a global sensitivity analysis of the PP model in the Storm Water Management Model, as necessary to detect the primary parameters to be considered in further stages.

Chapter 3 corresponds to *Article 2* (or Article 4 in Figure 1.2). The chapter provides a comparison between the Curve Number model and the PP model from the Storm Water Management Model, facilitating model application by making it easier to switch between permeable and traditional pavement scenarios and deepening the understanding of the PP model.

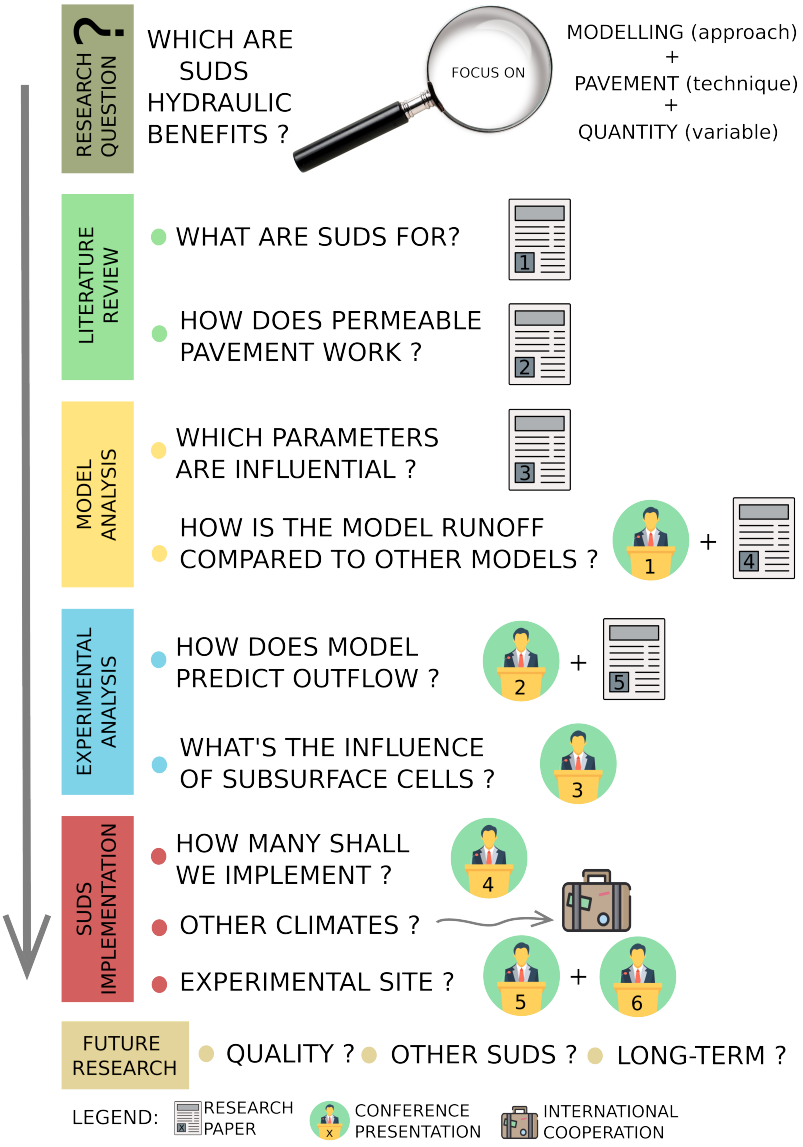

Figure 1.2: Graphical introduction and dissertation outcomes, with reference numbers to those given in the initial Research Outputs section.

Chapter 4 corresponds to *Article 3* (or Article 5 in Figure 1.2). The chapter provides the experimental laboratory study to test the hydraulic performance for several materials and layouts, comparing results with the model.

Chapter 5 chapter presents a discussion of the results from the three previous chapters but also integrates some preliminary results from the Txominenea experimental plot published in several conferences. These are Conferences 3, 4, 5, and 6, detailed in Figure 1.2, which are included as appendixes A to D.

Chapter 6 summarises the main conclusions from the dissertation, mainly focused on the three published articles.

Chapter 2

Model sensitivity analysis

The Storm Water Management Model (SWMM), widely used by engineers to design or analyse stormwater networks, allows to model the so-called Low Impact Development (LID) controls, which reduce the flow conveyed to traditional networks. But, values for LID control parameters are often unknown. Furthermore, it is not always easy to link the cross-section materials to those provided by the model, particularly in the soil layer. This article provides a global sensitivity analysis for the PP type of LID control, in order to support practitioners in calibration tasks. The analysis explores what factors are the most influential and which can be fixed while calibrating a model. In particular, flow volume and peak are studied but the analysis also explores the influence of storm length and drain layer, which is optional. At the end, the most influential parameters, and those that can be neglected are presented, showing that we can focus on quite less parameters than initially given when calibrating a PP model in SWMM.

Original article 1

Madrazo-Uribeetxebarria, E., Garmendia Antín, M., Almandoz Berrondo, J., & Andrés-Doménech, I. (2021). Sensitivity analysis of permeable pavement hydrological modelling in the Storm Water Management Model. Journal of Hydrology, 600. https://doi.org/https://doi.org/10.1016/j.jhydrol.2021.126525

2.1 Introduction

Sustainability issues are gaining increasing attention from society (Biswas 2020), and authorities are encouraged to consider environmental dimensions of their practices, stormwater projects being no exception (Geyler, Bedtke, and Gawel 2019). In that context, Sustainable Urban Drainage Systems (SUDS) or Low Impact Development controls (LID controls) are techniques that provide an improved rainwater management at source, in order to get the hydrological behaviour of urbanised land closer to predeveloped situation.

Permeable pavement (PP) is one type of such LID technique, characterised by generating a porous but, at the same time, accessible surface for pedestrians and vehicles. PPs consist of several porous layers laid over the natural soil, with a cover layer of pavement at the top allowing water to flow through. The layers are usually referred to, from the top-down: pavement, bedding, base, subbase and subgrade (natural soil) layers. The section may also include one or more geotextile layers and one or multiple drains. In any case, there is no unique layout or cross-section, as solutions adopted by practitioners are usually multiple, depending on the structural and hydrological requirements of a given application (Rodríguez-Rojas et al. 2020; Kuruppu, Rahman, and Rahman 2019; Woods Ballard et al. 2015; Mullaney and Lucke 2014; Scholz and Grabowiecki 2007), but also adapted to local materials and conditions.

For stormwater designing purposes or to forecast the response of a given network facing predicted weather events, it is common for practitioners to rely on mathematical models. There are several available models for the analysis of the PPs, widely detailed previously (Kaykhosravi, Sahereh, Khan, Usman T, and Jadidi, Amaneh 2018), but few allow for an integrated hydrological-hydraulic modelling of LIDs incorporated within catchments, being Storm Water Management Model (SWMM) one of them. Hence, SWMM is a powerful instrument to carry out different studies related to various types of LID (Andres-Domenech et al. 2018), including PP. Several studies use SWMM for analysing LIDs effects on urban flooding (Qin, Li, and Fu 2013), hydrologic response of an urban catchment under different scenarios (Palla and Gnecco 2015), or prioritising sites and types for LID practices (Liao et al. 2018; Song and Chung 2017). Besides SWMM being recommended for preliminary and detailed design objectives, it is also one of the most popular models among scientists (Kaykhosravi, Sahereh, Khan, Usman T, and Jadidi, Amaneh 2018).

Similarly to other types of LID present in SWMM, PPs are defined by overlapping several layers: surface, pavement, soil, storage and drain. Figure 2.1.a illustrates the layer layout but, in order to run the model, it is necessary to

fix the parameters defined in each of the layers (see Table 2.1). It is then, when allocating values to the parameters provided by SWMM, that doubts arise about which may be those that fit better to the real pavement characteristics. This is due to the lack of information on the physical properties of the materials used or, alternatively, because the layout (see Figures 2.1.b, .c and .d as an example) do not match predefined layers in the SWMM LID model.

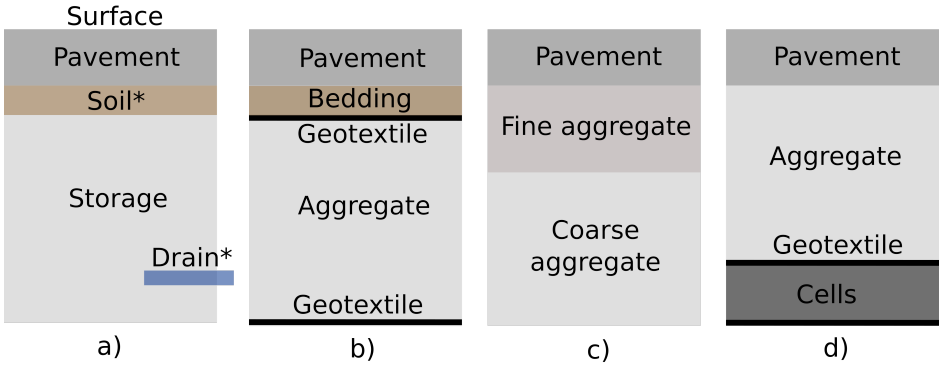

Figure 2.1: PP cross-sections (a) as defined in the SWMM model (b) with bedding layer and geotextiles, (c) various aggregate types, and (d) cells below aggregate with geotextiles.

With such difficulties, it is of great value knowing in advance which are the most influential parameters during model calibration. In essence, while setting up and using numerical simulation models, Sensitivity Analysis (SA) methods are invaluable tools (Iooss and Lemaître 2015). In hydrological modelling, the most frequent reason for conducting SA is to select the most sensitive parameters to vary during model calibration (Gupta and Razavi 2018). Global approaches are required to perform a valid SA when models feature nonlinearities and interactions (Saltelli et al. 2019), although there are three main obstacles to perform such analysis: the computation time, the number of inputs, and the size of the input space (Pujol 2009).

Various SA have recently been carried out on PPs based on HYDRUS model (Costa et al. 2020; Brunetti et al. 2018; Turco et al. 2017; Brunetti, Šimůnek, and Piro 2016), but the analysed parameters or inputs differ from those used in SWMM. Also, several SA have been carried out previously in SWMM, a detailed list can be found in Niazi et al. (2017), but few have carried out such an analysis focusing just on LID controls and its parameters (Panos, Wolfand, and Hogue 2020; Xu et al. 2019b; Leimgruber et al. 2018; Peng and Stovin 2017; Krebs et al. 2016), and most of them did it as a previous step

before calibrating a certain model. Randall et al. (2020) are the only ones that explored the PP, but they did not use a global SA, as they explored parameter variability for three cross-sections used in their study. In addition, they focused on the underdrain flow exclusively.

Besides, PPs have two particular characteristics that differentiate them from other types of LID controls (Rossman 2015): the pavement layer is used exclusively in this type of LID control and, moreover, it is the only one where the soil layer is optional. Thus, the analysis of PP LID type would be of great value, since none of the previous studies provided a general vision for PPs in SWMM, not just valid for a particular case, but as a universal instrument for all real cases that may emerge when calibrating PPs in SWMM. If that data may be available, it could potentially be used directly by practitioners to improve the quality and efficiency of their SWMM modelling.

Therefore, the aim of this study is to investigate the influence of multiple factors on the hydrological response of PPs in both short- and long-term modelling scenarios by using the rainfall-runoff model SWMM. The problem is addressed in the following way. First, minimum and maximum values were set for explored parameters. Then, considered cases are defined, in terms of analysis length, optional layers and analysed outputs. Finally, sensitivity indices and their confidence intervals are calculated for each case. Consequently, the objectives set for the study are: (a) to check if there are differences between parameter sensitivities for the several cases studied, (b) to identify negligible and most influential parameters, and (c) to compare those parameters with the ones identified on previous SA studies.

2.2 Methodology

This section describes the methodology used in the three fundamental steps followed: (1) characterise the variance based SA, (2) characterise the LID model defined in SWMM, and (3) define the terms in which SA is performed.

2.2.1 Variance based sensitivity analysis

The Sobol method is a variance based sensitivity method (Sobol' 1990), which decomposes the model output variance into relative contributions from individual parameters and parameter interactions, as shown in Equation (2.1). As a result, the sensitivity of a given parameter is quantified by the ratio of its contribution to the output variance, which ranges from 0 to 1 (Shin et al.

2013). The first term of the equation indicates the addition of the variance for each factor i, named $V_i(Y)$, being these variances exclusive to that factor. The second term indicates the variance due to combinations of two factors i and j, named $V_{ij}(Y)$, and so on.

$$V(Y) = \sum_{i=1}^{k} V_i(Y) + \sum_{i<j}^{k} V_{ij}(Y) + \ldots V_{12\ldots k}(Y) \tag{2.1}$$

Those $V_i(Y)$ terms constitute the *main effect* or the variance of the average output when the input factor X_i is fixed. The second one, constitutes the *second order effect* or the variance of the average output when the input factors X_i and X_j are fixed. Thus, if we consider how much of the total variance is due to main effect, we can define the *first-order index* given in Equation (2.2), which represents the main effect contribution of each input factor to the variance of the output (Saltelli et al. 2008). Higher-ranking indices may be defined in the same way, such as *second-order indices* or S_{ij}.

$$S_i = \frac{V_i(Y)}{V(Y)} \tag{2.2}$$

In case we consider the total contribution of the factor X_i to the output variance, we also have to consider the interactions of X_i with other factors, which accounts not only for the main effect, but also the higher-order effects. That will be the *total effect* of the factor X_i. Hence, *total index* S_{T_i} can be defined as shown in Equation (2.3). Total effect will give, then, how much the output variance is reduced on average when factor X_i is fixed.

$$S_{T_i} = 1 - \frac{V_{\sim i}(Y)}{V(Y)} \tag{2.3}$$

In practice, when k is large, only the main effects and the total effects are computed, obtaining a good information on the model sensitivities. In addition, S_i and S_{Ti} are closely linked to a couple of extremely significant sensitivity settings in the calibration context: *factor fixing* and *factor prioritisation* (Ratto et al. 2007). *Factor fixing* refers to the identification of those input factors, if any, which have no influence on the model output and therefore can be fixed to any value within their feasible range, but with negligible implications on the output. *Factor prioritisation* describes the ordering of the input factors

according to their relative influence on the model output (Sarrazin, Pianosi, and Wagener 2016).

First-order index being zero, $S_i = 0$, is a necessary but insufficient condition to identify the factor X_i as non-relevant and fix it. In such case, the factor may be involved in interactions with other factors, so there might be higher-order terms (Saltelli et al. 2008). Instead, $S_i > 0$ is a good value to qualify a factor as influential, as a factor prioritisation setting.

On the other hand, total indices are suitable for the factor fixing setting (Saltelli et al. 2008), being $S_{T_i} = 0$ a necessary and sufficient condition in order to fix X_i as a noninfluential factor. If $S_{T_i} \cong 0$, then X_i can be fixed at any value within its range of uncertainty without appreciably affecting the value of the output variance $V(Y)$. As $S_{Ti} = 0.01$ is generally used as a threshold for factor fixing (Sarrazin, Pianosi, and Wagener 2016), both obtained S_{T_i} and S_i values are rounded to the second decimal.

For additive models and under the assumption of orthogonal input factors, S_{Ti} and S_i are equal and the sum of all S_i (and thus all S_{Ti}) is 1. For non-additive models interactions exist: S_{Ti} is greater than S_i and the sum of all S_i is less than 1, and, also, the sum of all S_{Ti} is greater than 1. By analysing the difference between S_{Ti} and S_i, the impact of the interactions between parameter X_i and the other parameters can be determined.

For calculating both S_i and S_{T_i}, the procedure suggested by Saltelli (2002) has been used, at the cost of $N(k + 2)$ simulations, being N the base sample. Samples are generated with the Latin Hypercube sampling method (McKay and Beckman 1979). Although commonly suggested N value in literature is 1000, Sarrazin, Pianosi, and Wagener (2016) found that high N values ($N >>$ 1000) are necessary for sensitivity indices to converge. However, they found that much lower N is enough when the goal is factor prioritisation or fixing. As the objective of the article is factor prioritisation and factor fixing, a value of N=2000 is used and confidence intervals are calculated.

Confidence intervals for the sensitivity indices are estimated with the bootstrap technique (Efron 1979). A confidence interval of 95% is given for the sensitivity indices, where limits are computed with the basic method (Davison and Hinkley 1997). For that purpose, a number of 1000 replicates is considered enough (Archer, Saltelli, and Sobol 1997).

2.2.2 Storm Water Management Model

SWMM is a dynamic rainfall-runoff simulation model used for single event or long-term (continuous) simulation, where LID units can be modelled and added to a certain subcatchment (Rossman and Huber 2015). Conceptually a generic LID unit can be represented by a number of vertical layers (Rossman 2010), combined to create the various LID controls. PP type LID control combines Surface, Pavement, Soil, Storage and Drain layers (Figure 2.2), being Soil and Drain layers optional. In this article a square subcatchment of $100\,\mathrm{m}^2$ has been generated for the simulations, all occupied by a LID control of the PP type.

As illustrated in Figure 2.2, PP can receive water from precipitation (i) or inflows ($q0$) from other areas. That water on the surface can evaporate ($e1$), infiltrate to pavement layer ($f1$), or flow out from the pavement as runoff ($q1$). Water in the pavement layer can also evaporate ($e4$), or percolate to the soil layer ($f4$). Something similar happens in the soil layer beneath; water can percolate to storage layer ($f2$), or evaporate ($e2$). In the storage layer, water can exfiltrate to native soil ($f3$), evaporate ($e3$), or be directed to another area or conveyance through the drain ($q3$). In this article $q0$ will not be considered, and regarding the analysed outputs covered in Section 2.2.3, outflow from the PP will be the sum of $q1$ and $q3$.

The hydrologic performance of the LID control is modelled by solving simple mass balance equations, given in the Equations (2.4), (2.5), (2.6) and (2.7), that express the change in water volume in each layer over time as the difference between the inflow water flux rate and the outflow flux rate (Rossman 2010). The flux terms (q, e, and f) in these equations are functions of the current water content in the various layers (d_i and θ_i) and specific site and soil characteristics. Both d_i and θ_i represent stored water, first one as depth (mm) and second one as moisture content (volume of water / total volume of soil). D_i are layer thicknesses and ϕ_i are layer porosities. The rest of parameters are specified in the Table 2.1, presented in Section 2.2.3, as they are model parameters.

$$\frac{d(d_1)}{dt} = i + q_0 - e_1 - f_1 - q_1 \tag{2.4}$$

$$D_4 \cdot (1 - F_4) \cdot \frac{d\theta_4}{dt} = f_1 - e_4 - f_4 \tag{2.5}$$

$$D_2 \cdot \frac{d\theta_2}{dt} = f_4 - e_2 - f_2 \tag{2.6}$$

$$\phi_3 \cdot \frac{d(d_3)}{dt} = f_2 - e_3 - f_3 - q_3 \tag{2.7}$$

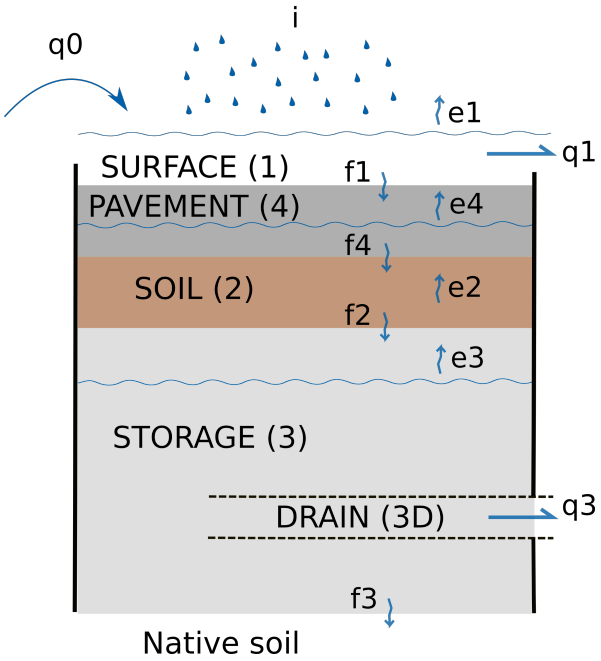

Figure 2.2: SWMM layers and flux terms for PP.

Evaporation rates are calculated based on potential evaporation, $E_o(t)$, detailed in Section 2.2.3. Evaporation on the top layer or surface will be the minimum of $E_o(t)$ and available water. For layers below, evaporation will be the minimum of available water and the fraction of potential evaporation that did not materialise in the upper layers.

Water flow from surface is computed with Manning Equation (2.8). Infiltration to pavement layer depends on available water volume on the surface layer, as shown in Equation (2.9). Percolation from pavement layer is the pavement permeability, as shown in Equation (2.10). Percolation from soil layer is calculated with Equation (2.11), which will occur only if water content is higher than field capacity. In that case, percolation is modelled using Darcy's law. Flow from drain, Equation (2.12), is computed as flow from an orifice, being h_3 the hydraulic head seen by the underdrain. Exfiltration to native soil is the seepage rate of the storage layer, as shown in Equation (2.13).

$$q_1 = \frac{1.49 \cdot W \cdot S^{1/2}}{A \cdot n} \cdot (d_1 - D_1)^{5/3} \tag{2.8}$$

$$f_1 = i + q_0 + \frac{d_1}{\Delta t} \tag{2.9}$$

$$f_4 = K_4 \tag{2.10}$$

$$f_2 = \begin{cases} \text{if } \theta_2 > \theta_{fc} \text{ then,} & K_{2S} \cdot e^{(-HCO \cdot (\phi_2 - \theta_2))} \\ \text{if } \theta_2 \leq \theta_{fc} \text{ then,} & 0 \end{cases} \tag{2.11}$$

$$q_3 = C_{3D} \cdot (h_3)^{K_{3D}} \tag{2.12}$$

$$f_3 = K_{3S} \tag{2.13}$$

This set of equations can be solved numerically at each runoff time step to determine how an inflow hydrograph to the LID unit is converted into some combination of runoff hydrograph, sub-surface storage, sub-surface drainage, and infiltration into the surrounding native soil. Certain limitations are imposed on the above-mentioned water volumes, defined by the capacity of each layer in terms of available space to keep water, or present water volume. More details about the equations to compute moisture balance in each layer can be found on Rossman and Huber (2016).

2.2.3 Model settings and sensitivity analysis

Climatological data

This study is undertaken with data gathered in Donostia/San Sebastián (Spain), located facing the Bay of Biscay, in an area with an Atlantic climate. Data from two weather stations has been gathered: one of them is Igeldo weather station (43°19′0″N, 2°0′0″W), with a large historical data, and the other one is Miramon weather station (43°17′20″N, 1°58′16″W), a newer weather station with 10 minutes time interval accessible data.

The sensitivity analysis is conducted studying the hydraulic response of the PP facing two kinds of events: short-term and long-term. As it is common for practitioners to check the performance of the network for a certain event, which is also a simple method for LID volumetric design purposes, a 100 years return period and 6 hour rainfall event has been considered for the short-term analysis (Woods Ballard et al. 2015). A synthetic single event is generated from data available at the Igeldo weather station. Based on the IDF curves representing a return period of 100 years, the precipitation depth for a 6 hours

duration storm is 90.7 mm. The design storm has been set with the alternating block method (Chow 2010), considering 15 minutes steps.

The aforementioned method does not address a continuous scenario, in which one storm may follow another, and the system may not have time to drain; henceforth, its potential to handle a new event will be limited. That is why the performance for the system facing continuous events should also be examined. As 5 years is considered the minimum period required for securing sensitivity analysis results that are stable in subcatchments (Shin et al. 2013), that period is also considered as sufficient for the defined subcatchment. For the long-term analysis, 5 years series recorded at the Miramon weather station have been gathered, both temperature and precipitation collected in 10-minutes intervals. Figure 2.3 shows gathered time series, but with daily precipitation and average daily temperature data to improve the visibility. Average rainfall is 1507 mm/year, with 196 days per year with measured rainfall, and average temperature is 14.2 °C.

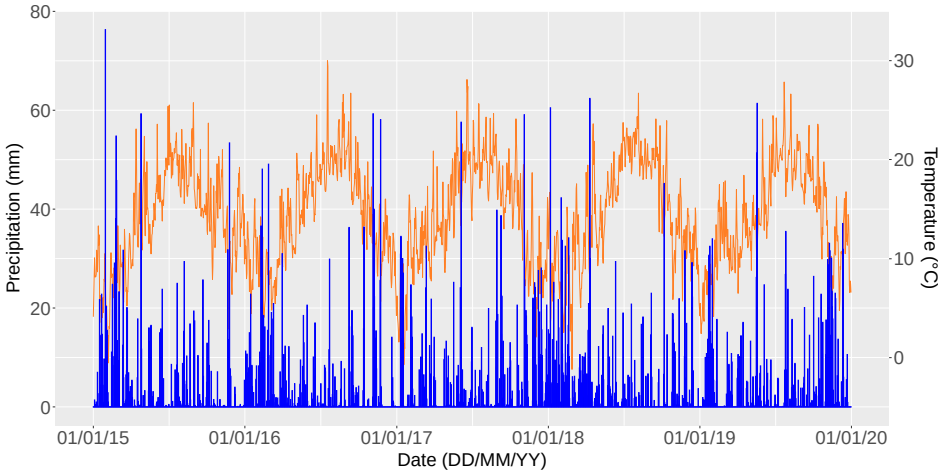

Figure 2.3: Daily precipitation (blue/left axis) and daily average temperature (brown/right axis) for the long-term modelling scenario.

Potential evaporation in the long-term is computed from daily maximum and minimum data, based on the Hargreaves method (Hargreaves and Samani 1985) and the latitude. For the long-term, the considered time steps for computing runoff when modelling have been 2:30 minutes for Wet Weather and 10:00 minutes for Dry Weather. For the short-term, time step for both cases has been 1:00 minute. Reporting time step is 5:00 minutes for short-term and 10:00 minutes for long-term.

Selected optional layers for LID control

As mentioned before, there are two optional layers in the PP type LID control: soil layer and drain. The soil layer or bedding layer beneath the pavement, fine gravel or clean sand in practice, is a common layer for PICP in order to laying the pavers on a evener surface than the one given by bigger gravel. Although soil layer is not always placed (Randall et al. 2020; Kayhanian et al. 2019; Tennis, Leming, and Akers 2004), soil layer has not been considered as an optional layer. Thus two cases are studied: one with Drain option deactivated, named as *SO* and, a second one with Drain activated, labelled as *SODR*.

Selected input parameters for LID control

The inputs or parameters given to SWMM, which are used to compute the mentioned water balances to get the outputs, are listed on the Table 2.1. The table also indicates which parameters have been used in the following SA. Vegetation Volume Fraction from the Surface layer, which refers to the volume occupied by stems and leaves over the surface (Rossman 2015), has been excluded from the SA, as it is very unusual case in PPs (this parameter is general for all LID control types). Parameters that reduce permeability in the long-term, such as clogging factor, regeneration interval and regeneration fraction, have not been considered.

In the storage layer, the parameter that considers the reduction of the seepage rate has not been considered either: clogging factor. Finally, the parameters that control the opening and closing of the drain have not been considered: open level, closed level and control curve. All those values have been ignored while calculating PP performance.

Table 2.1 also gives the range for each parameter value while performing the SA, maximum and minimum are given, considering a uniform distribution. Most parameter ranges are taken from the SWMM manuals (Rossman 2015; Rossman and Huber 2016). Some are modified, such as Surface Berm Height (SUbh) top value, which is set to 150 mm, as it is common value for the curb height which might work as a berm. Another revised value is Surface Roughness (SUro), as values given by the manual are considered typical for traditional pavements. Therefore, as pervious pavements are more rough than traditional ones, unfinished concrete value of 0.02 is used as a high value for roughness (Chow 1959). Another modified value is the Surface Slope (SUsl). A top value of 10% is selected, as it is not usual to design higher slopes, mainly because of accessibility issues. In Spain, for example, the different regional

regulations do not exceed 8% in general, and allow slopes of up to 12% for ramps (Alonso López 2010).

The Soil layer and its parameters are, probably, the most unknown to practitioners, since they are defined with soil parameters such as wilting point or suction head. Some Soil parameters are also changed, Soil Thickness (SOth) for example. In that sense, as mentioned in the introduction, it is considered that there is a wide variety of cross sections that can be modelled in many different ways. For that reason, a maximum thickness of 200 mm is considered (Woods Ballard et al. 2015). Field Capacity (SOfc) and Wilting Point (SOwp) are also modified, as it is considered that those materials may be clean gravel/sand type. Therefore, a 0.06/0.20 range is considered for the first parameter and 0.01/0.05 for the second one (Pardossi et al. 2009).

In the Storage layer, seepage rate is also modified, considering it up to 1000 mm/h (Woods Ballard et al. 2015). In the Drain layer, the Flow Coefficient (DRfc) is considered up to 1000 (Zhang and Guo 2015). It should be noted that the Offset value from the drain layer is not given in mm, but as a percentage of the total thickness of the Storage layer.

Although SWMM contains some parameters related to the LID control in a subcatchment, such as Subcatchment Area, Surface Width per Unit, % Initially Saturated, % Impervious Area Treated and % Pervious Area Treated, these parameters have not been considered in the SA, since the study focused on studying specifically the LID control and its parameters.

Hydrological outputs and data treatment

When carrying out a sensitivity analysis it is essential to define its objective in advance, i.e. which variable or model result is going to be analysed. SA results may vary depending on targeted output: each target function is insensitive to some, often different, parameters, particularly for those models with more than a handful of parameters (Shin et al. 2013).

The aim of this study is to explore the impact of design parameters on the hydraulic response of the PP. To this end, the outputs analysed are those related with the generated outflow from the PP site: outflow volume and outflow peak. For that purpose, outflow will be the sum of q_1 and q_3 from Figure 2.2, that is, superficial runoff and drain outflow.

All outflow data managed by the PP, used to evaluate sensitivity indices, is obtained from the report file generated by SWMM. Data related to the volumes

Table 2.1: SWMM parameters for PP type LID control.

LAYER / Parameter	Symbol	*Code*	*Units*	*Min.*	*Max.*
SURFACE					
Berm Height^{sa}	D_1	SUbh	mm	0	150
Vegetation Volume Frac.	$1-\phi_1$	SUvf	-	0	0
Roughness^{sa}	n	SUro	Manning n	0.01	0.02
Slope^{sa}	S	SUsl	%	0	10
PAVEMENT					
Thickness^{sa}	D_4	PAth	mm	60	250
Void Ratio^{sa}	$\phi_4/(1-\phi_4)$	PAvr	Voids/Solids	0.3	0.8
Impervious Surf. Frac.^{sa}	F_4	PAis	-	0	0.95
Permeability^{sa}	K_4	PApe	mm/h	0.01	40000
Clogging Factor	-	PAcf	-	0	0
Regeneration Interval	-	PAri	days	0	0
Regeneration Fraction	-	PArf	-	0	0
SOIL					
Thickness^{sa}	D_2	SOth	mm	0	200
Porosity^{sa}	ϕ_2	SOpo	vol. frac.	0.25	0.35
Field Capacity^{sa}	θ_{fc}	SOfc	vol. frac.	0.06	0.20
Wilting Point^{sa}	θ_{wp}	SOwp	vol. frac.	0.01	0.05
Conductivity^{sa}	K_{2S}	SOco	mm/h	100	800
Conductivity Slope^{sa}	HCO	SOcs	-	20	60
Suction Head^{sa}	ψ_2	SOsh	mm	40	120
STORAGE					
Thickness^{sa}	D_3	STth	mm	100	1000
Void Ratio^{sa}	$\phi_3/(1-\phi_3)$	STvr	Voids/Solids	0.2	0.8
Seepage Rate^{sa}	K_{3S}	STsr	mm/h	0	1000
Clogging Factor	-	STcf	-	0	0
DRAIN					
Flow Coefficient^{sa}	C_{3D}	DRfc	-	0	1000
Flow Exponent^{sa}	K_{3D}	DRfe	-	0	30
Offset^{sa}	D_{3D}	DRof	mm	0	100*
Open Level	-	DRol	mm	0	0
Closed Level	-	DRcl	mm	0	0
Control Curve	-	DRcc	-	-	-

*: this value is given as a percentage of Storage Thickness.
^{sa}: included in the sensitivity analysis.

is read from the LID Performance Summary section. Data relative to peak flows is collected from the same file but, in this case, from the Node Inflow Summary, as runoff and drain flows are diverted in the model to a couple of nodes for that purpose.

By evaluating a total of two outputs across four cases, sixteen indices are calculated for each LID parameter: a first-order one (S_i) and a total effect one (S_{Ti}) for each parameter. As analysed input/output cases are multiple, values are compared graphically.

The data has been gathered with the version 5.1.015 of SWMM (Rossman 2015). The analysis of the data has been carried out using the open-source programming language R (R Core Team 2023). For modelling purposes *swmmr* package has been used, which interfaces the SWMM with R (Leutnant, Döring, and Uhl 2019). For the sensitivity analysis, the *sensitivity* package has been used (Iooss et al. 2020), and for sample generating the *pse* package (Chalom and Prado 2017).

2.3 Results and Discussion

The results are presented into several sections. First, some general data description is given. Later, (1) differences between short- and long-term are discussed, (2) the influence of the drain layer is analysed, and (3) differences between selected outputs are discussed. At the end, (4) global analysis is performed.

Although a total of 164 000 simulations are done across various cases while performing the global SA and, in addition, the 1-in-100 years storm is simulated for the short-term analysis, few outflow values are computed. On average, just 0.93% of the simulations produced any outflow. In particular, the short-term analysis created any outflow five times more than the long-term, which appears to be intuitive, since the short-term precipitation is higher. Something similar happened with the optional layers, SODR created outflow almost eight times the SO option did. That also appears to be intuitive, since active drainage layer allows underdrain flow. The most remarkable aspect of this data is that it shows how effective can PP be reducing the contribution to the stormwater network, no matter how the PP is designed. The reason for that is that rain intensity is usually lower than pavement permeability and its storage capacity allows infiltration to native soil before flow is diverted from the drain.

Once SA is performed, some S_i values are found to be close to zero but negative. That is consistent with previous findings, as Saltelli et al. (2008) described negative signs due to numerical errors in the estimates when analytical sensitivity indices are close to zero. In addition, obtained confidence intervals were very large in all modelling scenarios, as convergence was not obtained for calculated sensitivity indices. To avoid those negative values and high confidence inter-

vals, sample size should be increased until convergence, which is considered unnecessary for factor fixing and prioritisation. Also, the methodology used to obtain confidence intervals yielded negative values or indices higher than one. As those are considered meaningless, those values are not represented on the figures.

Before proceeding with a global discussion considering all the cases, conducted at the end of this section, three previous analyses have been performed from the calculated indices. For those mentioned reviews, plots with values for first-order indices (S) and total effect indices (ST) are created. For that purpose, Table 2.2 is also built, giving the sum of all indices across cases. Values from that table will be discussed in the next sections. In addition, that table confirms that the model is nonadditive, as the sum of S_i is smaller than one for all cases. Also, the sum of S_{Ti} is greater than one for all considered cases.

Table 2.2: Sum of first-order indices, $\sum_{i=1}^{k} S_i$, and total-effect indices, $\sum_{i=1}^{k} S_{Ti}$, for each modelling scenario.

INPUT	Short-term (6 hours)				Long-term (5 years)			
	SO		SODR		SO		SODR	
OUTPUT	Vol.	Peak	Vol.	Peak	Vol.	Peak	Vol.	Peak
$\sum_{i=1}^{k} S_i$	0.12	0.06	0.00	0.00	0.66	0.44	0.63	0.21
$\sum_{i=1}^{k} S_{Ti}$	2.42	2.81	9.84	9.84	1.34	1.78	1.76	2.63

2.3.1 Analysis of short- or long-term influence

Regarding to the analysis of storm length, some differences arise between short-term and long-term. The Figure 2.4 and values from Table 2.2 show that long-term outflows are much more influenced by single parameters, without considering any interactions. For the short-term, 4.5% of the variance can be explained, on average, by one parameter (SOth). On the other hand, for the long-term outflow 48.5% of its variance can be explained, on average, by two variables (SOth and STsr). In summary, parameter interaction plays a significant role on the short-term.

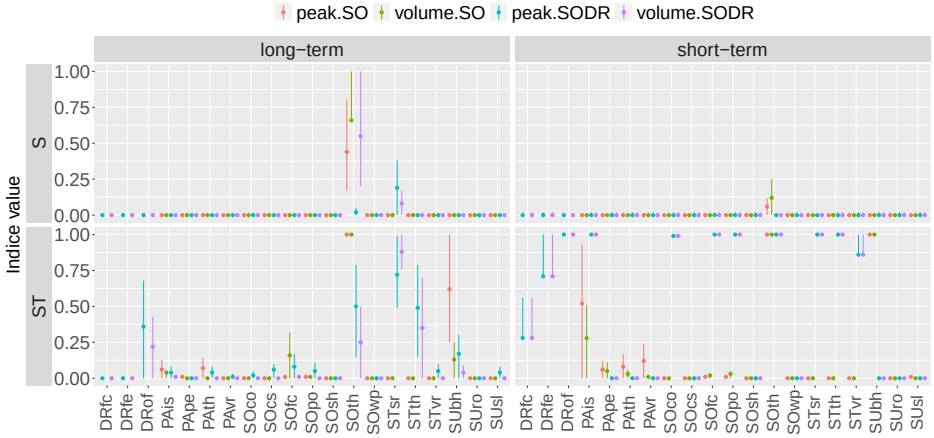

Figure 2.4: Estimated total (ST) and first-order (S) effects with their confidence intervals for the long (left) and short-term (right) modelling scenarios. Different colours are shown for scenarios including (SODR) and excluding (SO) the effects of drain and measuring outflow peak or volume.

2.3.2 Analysis of drain influence

If the sensitivity indices are examined according to whether the drain layer is active or not, the individual influence of parameters is similar to the previous case. As shown in Figure 2.5 and values from Table 2.2, outflow variance in the SO case is explained on, as average, by one variable (SOth) in a 32%, while in the SODR case is explained by two variables (SOth and STsr) in a 21%. That means that interactions are more relevant when Drain layer is active, which seems reasonable, as outflow is also controlled by the drain parameters, and, overall, influence of the SOth is reduced.

In that sense, the number of parameters that may be fixed without affecting the outflow, with a $S_T \approx 0$, increases in the SO case. However, it is interesting how these parameters differ from case to case. For the SO case, all parameters other than SOth and SOfc may be fixed in the Soil layer. On the contrary, for SODR case, almost all parameters may be fixed in the Pavement layer. That shows that when Drain layer is active, other soil parameters different from Thickness have also influence in the outflow, which also accounts for drain flow. But, when Drain layer is not active and outflow accounts just for runoff, Soil layer parameters loose its influence and Pavement layer parameters influence is notable. That appears to be intuitive, since pavement parameters control runoff or at what extent there will be infiltration to the layers below.

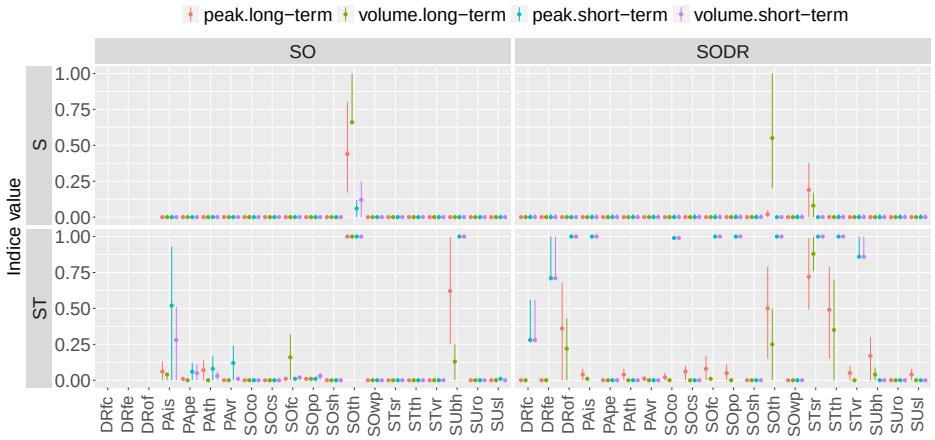

Figure 2.5: Estimated total (ST) and first-order (S) effects with their confidence intervals for scenarios excluding (SO), on the left, and including (SODR), on the right, the effects of drain. Different colours are shown for scenarios considering the long- or short-term modelling and measuring outflow peak or volume).

2.3.3 Analysis of peak or volume

With regard to the output values, Figure 2.6 and values from Table 2.2 show that, on average, 35.2% of the outflow variance is explained by two parameters for the outflow volume, but that value decreases to the 18.8% when the analysed output is the peak flow, while the variables remain the same (SOth and STsr). Also, interactions play a smaller role on the volume outflow than in the peak flow. It is also interesting to see how the number of values which can be fixed without affecting the output is higher for the runoff volume. For runoff peak the are three parameters with a $S_T \approx 0$, while for the volume there are six, which includes all the previous three.

2.3.4 General analysis

Finally, all cases are compared at once in Figure 2.7, which is also used to identify the most important parameters and those that can be neglected or fixed when calibrating the model, no matter what input/output case we consider. Those parameters are summarised in Table 2.3.

The graph clearly shows that only two parameters have a influence by themselves on the evaluated outputs. SOth and STsr alone can explain, as average, 26.5% of the output variance. On the contrary, there are clearly three param-

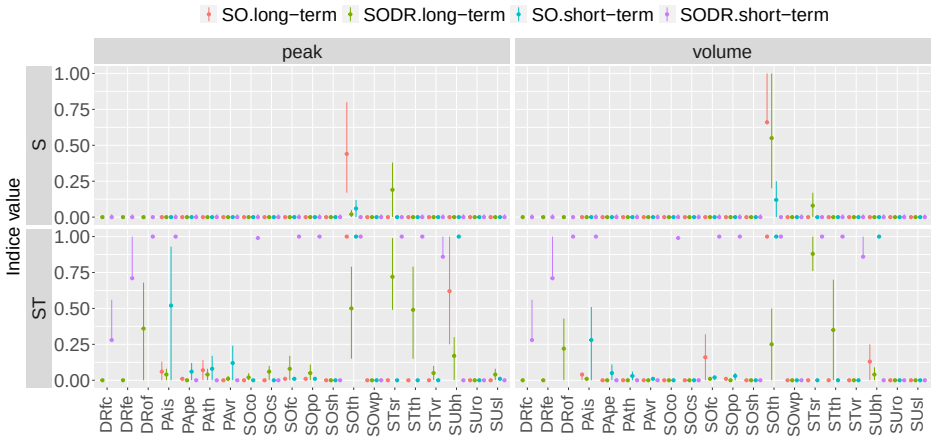

Figure 2.6: Estimated total (ST) and first-order (S) effects with their confidence intervals for scenarios measuring outflow peak (left) and outflow volume (right). Different colours are shown for scenarios including (SODR) and excluding (SO) the effects of drain and considering the short- or long-term modelling.

eters that do not affect the output variance: SOsh, SOwp and SUro. First two parameters will be the most obvious candidates for the influential ones, and last three will be set as the ones without any influence.

If examined by layer, surface parameters have no influence individually. On the contrary, SUbh presents high interactions with other parameters, thus, it can be considered as the most influential parameter of this layer. On the other hand, SUsl presents quite low interactions in just one case, so it will be considered as having low influence. It seems consistent SUbh being the most influential parameter, as it can restrict the output level and, consequently, the generated runoff and infiltration to layers below.

With regard to the Pavement layer, something similar happens with the individual influence, since all parameters show a first order index equal to zero. If total indices are examined and, thus, interactions, PAis is clearly the most influential parameter. The other three parameters present moderate interactions, enough not to be considered as non influential. To rank the other three parameters, the number of cases with the total effect index greater than zero and its value are checked. Hence, the most influential parameter is PAth, followed by PApe and, finally, PAvr. None has been considered as non influential at all, although PAvr could be considered as such in most of the cases. Again, it seems reasonable PAis being the most influential, as it controls the open

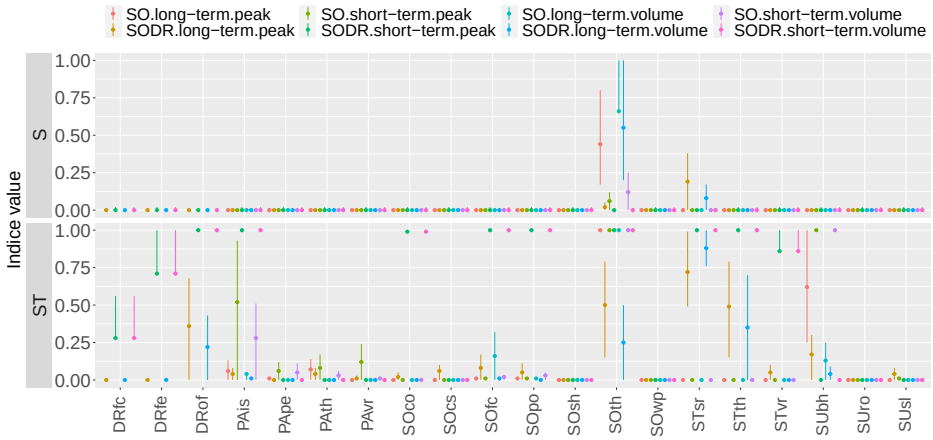

Figure 2.7: Estimated total (ST) and first-order (S) effects with their confidence intervals for all considered scenarios. Different colours are shown for scenarios including (SODR) and excluding (SO) the effects of drain, scenarios with long- or short-term modelling, and scenarios measuring outflow peak or volume.

space that water has on surface to penetrate into the pavement section before other parameters can have any influence.

The soil layer, the one with highest number of parameters, contains the most influential parameter by itself alone: SOth. This layer has also two parameters with no influence in the output: SOsh and SOwp. There is a third one, SOcs, that presents low interactions in just one case. As the number of parameters is high in this layer, this last parameter will also be considered as non-influential. Other three parameters show moderate interactions, variable over cases: SOfc clearly interacts more than SOpo and SOco. In this layer, as opposed to the other layers, there is no a clear physical explanation for SOth being the most influential one. An explanation may be that the layer thickness controls how water can percolate into lower layers and, thus, controls the amount of water on the surface that can turn into runoff.

The storage layer contains the second most influencing parameter overall: STsr. However, its individual influence arises when the Drain layer is active. The other two storage parameters present moderate and high interactions, so they can not be fixed. These interactions are also for the activated Drain layer option, indicating that storage layer parameters have influence, mainly, in the drain outflow. STth would be the most influential of both, and STvr the least. Here, again, it seems reasonable STsr to be the most influential, as it would

control outflow and, thus, water level on the layer, before there is outflow from the drain and other two parameters can have its role.

The last layer, the only one considered as optional, has no parameters influencing by themselves. On the contrary, all parameters show interactions. The most influential would be DRof, followed by DRfe and DRfc. Here, it also seems a reasonable outcome, as the drain offset controls the flow presence on the drain.

Table 2.3 summarises, for each layer, the most influential parameters, those with little influence and those that its value can be fixed. The table is the main objective of this article, and will provide practitioners calibrating a real pavement, or designing a new one, a helpful tool to focus their efforts on the most important parameters (Figure 2.7 can also be used for that purpose). The data is given as a general tool for runoff control purposes, no matter if the simulation is done in the long term/short term or if Drain optional layer is checked. The most influential parameters are given in the first column, and those parameters that have less influence, including interactions with other parameters, are given in the second one. The last column gives those parameters which value can be fixed and influence neglected. It is recommended to start with the most influential one and, if necessary, to follow with those who have less influence.

Table 2.3: Factors influence for PP type LID in SWMM.

LAYER	Most influential	Low influence	No influence
Surface	(1) SUbh	(2) SUsl	SUro
Pavement	(1) PAis	(2) PAth (3) PApe (4) PAvr	-
Soil	(1) SOth	(2) SOfc (3) SOpo (4) SOco	SOsh, SOwp, SOcs
Storage	(1) STsr	(2) STth (3) STvr	-
Drain	(1) DRof	(2) DRfe (3) DRfc	-

As mentioned in the introduction, Randall et al. (2020) are the only ones that studied PP, but they performed a One At a Time (OAT) SA for three cross-sections, focusing on their study, but not as a general tool. They performed the SA for a short-term event, and studied the underdrain flow, peak and volume, without considering the runoff. However, SOth is not identified as an influential parameter. If values from Figure 2.4 are analysed in detail, it can be seen that for the short-term and SODR case none of the parameters has $S_i > 0$, not even the SOth; that may explain the difference. Rest of the parameters seem to fit well with findings from Randall et al. (2020). Therefore, their findings are in line with the values obtained here.

2.4 Conclusion

Although PP is studied here and some other LID types previously were, it would be advisable, for future research, to analyse the sensitivity of LID modules that have not yet been studied (rain barrel, rooftoop disconnection, rain garden and vegetative swale).

The parameters that reduce the permeability of the different layers have not been analysed in this article, as that case may be related to the ageing of the pavement. It would be interesting to study how clogging may affect to other parameters. Similarly, the parameters associated with the assignment of LIDs to the subcatchment have not been studied, as those are the same for all LID types. Thus, it would also be interesting to examine their influence on the model output.

Moreover, as the soil layer parameters are quite unknown, particularly when applied to PPs, its properties should be further investigated, as it can not be characterised as a natural soil. Also, the study has been carried out with the data associated to a certain climate, so other rainfall could yield different results. It is recommended to study the influence of other rainfall regimes in the model.

Results show that, in general and regardless the type of storm analysed or whether the drain is active, there are a few parameters that control the value of the outflow from a PP site. There are certain differences among cases but the influential/negligible parameters are similar. Consequently, the most influential ones are berm height, impervious surface fraction of pavement, soil thickness, storage seepage rate and drain offset. On the contrary, surface roughness, soil suction head, soil wilting point and soil conductivity slope have negligible influence on the outflow.

Thus, the most sensitive and non-influential SWMM parameters corresponding to the PP type LID control are identified in this article. Although further research is needed, the parameter list given in this article may still be a helpful tool for practitioners while calibrating a PP, as data is given as a general tool, not specific to a case, considering long-term performance and most useful parameters for urban stormwater design.

Chapter 3

Model comparison

Many investigations compare the runoff created by the PP model and other models to extract broader conclusions without considering model equivalencies. This chapter explores the runoff computed by the widespread Curve Number (CN), set as a baseline, and the PP model provided in SWMM, also analysing the influence of storm depth, pavement slope, catchment shape, and PP type. The correlation was set by calibration, based on the Nash-Sutcliffe coefficient, using a single-event hydrograph. It also explores the peak and volume performances. The results showed that the runoff hydrographs computed with the PP model and those created with the CN method can be linked, although that relationship is only helpful for some of the CN range, practical for CNs higher than 88, but helpful for urban planners and researchers to compare several pervious/impervious scenarios in urban drainage models more robustly. One direct application is to compare the runoff computed by both models without changing the model.

Original article 2

Madrazo-Uribeetxebarria, E., Garmendia Antín, M., Almandoz Berrondo, J., & Andrés-Doménech, I. (2022). Modelling runoff from from permeable pavements: A link to the Curve Number method. *Water*, 15(1), 160. `https://doi.org/10.3390/w15010160`

3.1 Introduction

Authorities are increasingly implementing environmentally sustainable solutions in new and existing developments, and urban drainage systems are no exception. In this field, Sustainable Urban Drainage Systems (SUDS) have multiple advantages (Charlesworth 2010): they provide energy savings, they mitigate climate change by reducing greenhouse gases, they reduce the urban heat island effect, and they improve community livability by enhancing, among others, aesthetics, recreation possibilities, and biodiverse habitats. In addition, from the stormwater management point of view, SUDS reduce the volume and peak of generated runoff, being recognised as a sustainable strategy to mitigate floods in urban environments (Ciriminna et al. 2022; Qi et al. 2021; Liu et al. 2021; Huang et al. 2018; Woods Ballard et al. 2015; Fletcher et al. 2015; Fletcher, Andrieu, and Hamel 2013).

However, both stormwater management and flood mitigation require efficient mathematical models in order to promote sustainable urban environments (Qi et al. 2021). However, the increasing number of hydrological model applications in urban environments, together with the greater sustainability challenges, makes it essential to go further in the hydrological processes present in urban areas; hence, these models need to be further explored in order to face existing and new challenges (Salvadore, Bronders, and Batelaan 2015).

Regarding stormwater network contribution, runoff is currently the main parameter to characterise the hydrological response of an urban plot (Ahiablame and Shakya 2016). Hence, runoff simulation is a key component of the modelling process, together with the confluence process to the stormwater network. In that regard, hydrologic methods compute catchment runoff based on precipitation excess, with infiltration being the main process that creates precipitation losses. This infiltration can be computed based on several methods, although the relative efficiency of a particular method with respect to others cannot be determined in a definite manner (Luo et al. 2022).

On the other hand, models integrating SUDS are becoming increasingly common, as they contribute to the analysis of SUDS' impact at a catchment scale (Kaykhosravi, Sahereh, Khan, Usman T, and Jadidi, Amaneh 2018). These models have been extensively used as optimisation tools for different SUDS configurations, making them an extremely helpful decision resource to explore the hydraulic performance of several SUDS types, study their implementation, and check different setups (Qi et al. 2021). Yet, further research is recommended in order to improve modelling techniques for evaluating the performance of SUDS (Eckart, McPhee, and Bolisetti 2017).

Permeable Pavements (PP) are one of such SUDS and can be used in walkways, roads, playgrounds, or parking lots, among others (Kuruppu, Rahman, and Rahman 2019). PPs are quite different from other SUDS types, as they ensure a hard surface while providing infiltration and detention capacity, thus reducing additional land requirement for detention facilities and being an alternative for impervious surfaces. This is especially important in urban areas with high land price and highly impervious sites with little or no space for stormwater detention (Zhu et al. 2021; Li, Kayhanian, and Harvey 2013). Those implementation factors, together with their environmental benefits, have boosted its implementation (Chandrappa and Biligiri 2016).

Currently, there are several computational models available to simulate the hydrodynamic behaviour of PPs (Kuruppu, Rahman, and Rahman 2019; Elliott and Trowsdale 2007), with some of them being integrated into wider urban drainage models (Bach et al. 2014). However, as mentioned previously, methods for calculating infiltration in a certain subcatchment are diverse. Moreover, with the implementation of PP models, infiltration can also be computed with the recent, in addition to the *traditional*, thus overlapping several infiltration methods in the same model. Hence, in a particular urban plot, a traditional method can be selected to compute infiltration, but in the adjoining plot or even in a particular area of the former plot, a PP model may be applied to compute infiltration.

This is a quite common practice in order to study how a certain PP implementation affects the runoff created in a certain urban area. Palla and Gnecco (Palla and Gnecco 2015) compared runoff peak/volume/delay in a *do nothing* scenario with several *conversion scenarios* where PPs were applied. Jato-Espino et al. (Jato-Espino et al. 2016) tested the efficiency of PPs reducing the stormwater volume in the existing drainage system, for which *actual*/PP scenarios were defined. In addition, Lee et al. (Lee et al. 2022) created before/after PP situations to check how different climate change scenarios affected to the runoff reduction rate of PPs.

The previous cases are just some examples of how PP efficiency is analysed with a model defining a hypothetical PP scenario. Nevertheless, to analyse the effect of PPs, the same catchment has to be modelled with two different methods, a *traditional* one, to test current conditions, and the PP model, to test the hypothetical or future scenario. However, can results obtained from different models be directly compared in order to draw certain conclusions? The authors consider that an equivalency or link between models shall be established in order to obtain robust conclusions.

For that purpose, it is common to compare the performance of several models and decide which one is the most suitable for a certain application. In those cases, conclusions are often based on field data. Wilcox et al. (Wilcox et al. 1990) compared runoff prediction capabilities, without calibration, for the Soil Conservation Service Curve Number (SCS-CN) and Green–Ampt (GA) models in rural catchments based on real data from six catchments. They concluded that the SCS-CN model, although simpler, performs as well as more complex models. More recently, Ajmal et al. (Ajmal et al. 2015) compared the SCS-CN model with a proposed nonlinear model based on one parameter. Proposed nonlinear models, overall, performed better than the SCS-CN model for studied watersheds. In addition, Hu et al. (Hu et al. 2021) developed a new urban hydrological model that represents nonlinear rainfall–runoff relationships for different urban surfaces and compared it with two commonly used urban hydrological models: the Horton and SCS-CN models. The results showed that their proposed model outperformed the other two models in terms of total runoff and peak flow.

However, measured data are not the only way to produce relevant outcomes: infiltration models can also be compared on a theoretical basis. Zhang and Guo (Zhang and Guo 2015) compared the runoff reduction performance of a certain area when infiltration was controlled by the PP model or by the GA model. They found inconsistent results for the PP model for low pavement heights, low drains, and large time steps, so they recommended using the GA method to model PPs. On the other hand, Baiamonte (Baiamonte Giorgio 2019) established, assuming constant rainfall intensity, an analytical link between SCS-CN and GA infiltration models, which allowed for an interoperability between both.

Despite its limitations, the SCS-CN method is a popular model compared to those *traditional* ones because it is simple, predictable, and stable and also because it relies on only one parameter that responds to major properties producing runoff in a watershed (Ponce and Hawkins 1996). On the other hand, the Storm Water Management Model (SWMM), which implements a PP model, is one of the most popular among researchers due to the diversity of hydrologic and hydraulic computation methods (Kaykhosravi, Sahereh, Khan, Usman T, and Jadidi, Amaneh 2018). For instance, the four examples mentioned previously that compared scenarios with and without PP, selected the CN method to control runoff for those subcatchments without PP and the PP model from SWMM to control runoff from PP scenarios. All four compare computed runoff in both subcatchments in order to reach some more general

conclusions. However, there is not an obvious link between both models, and hence the comparison cannot be validated.

Consequently, this study explores, on a theoretical basis, the relation between the runoff computed by those two models, the SCS-CN and PP models defined in SWMM, in order to establish, if possible, an equivalency between them, which would be beneficial to derive more consistent outcomes in broader analysis related to the hydraulic benefits of PPs. As SCS-CN relies on one parameter, an equivalent parameter has been selected for the PP model based on a previous sensitivity analysis performed by the authors (Madrazo-Uribeetxebarria et al. 2021): *pavement permeability*. This parameter plays an equivalent role. It is a superficial parameter that controls inflow to the layers below and is also easy to relate and compare against rainfall intensity. More specifically, and from a practical point of view, urban planners, practitioners, and researchers will be able to compare PP implementation runoff scenarios computed on the same model, especially pervious/impervious, by just considering one single parameter, *pavement permeability*, as this parameter can be linked to a certain CN.

Accordingly, the specific objectives of the article are as follows: (a) explore, on a theoretical basis, the relation between CN and pavement permeability, in order to obtain equivalent runoff hydrographs; (b) analyse the influence of storm depth, pavement slope, catchment shape, and PP type on that relation; and (c) set the conditions in which PP can be used to model runoff equivalent to that modelled by a certain CN.

3.2 Materials and Methods

This section describes the methodology used in the steps followed during the research process: (1) define the general experimental design, (2) describe the CN method used as a baseline scenario, (3) describe the infiltration provided by both the CN method and the PP module in SWMM, (4) define the model used to obtain the data during the experimental design, and (5) define criteria to compare obtained hydrographs along with the calibration procedure to obtain pavement permeability values.

3.2.1 Experimental Design

As the objective of this study was to compare runoff created with two different models by linking one parameter from each model, namely, pavement permeability and CN, the study was designed to compute the hydrograph for a certain CN, used as a baseline, and, based on that hydrograph, calibrate the pavement permeability from the PP model. Hence, both models were linked by means of those two parameters: pavement permeability from the PP model and CN from the SCS-CN model. The selected tool to compare both models was SWMM. The model definitions and SWMM implementations are given in Sections 3.2.2 and 4.2.6, while model setup used to compare both methods is given in Section 3.2.4. The study was also designed to explore how storm depth, pavement slope, catchment shape, and PP type influence that relation.

In order to study the effect of the storm depth, a single design storm was selected, as it is common to rely on them for drainage infrastructure design purposes. Selected return periods were 2, 10, and 100 years, all three with a duration of 6 h (Watt and Marsalek 2013). The selected method to define such a storm was the alternating block method (Chow 2010), based on previously defined IDF curves. Details of the selected IDF curves and defined storm depths are given in Section 3.2.4.

To study the effect of pavement type, three typical permeable cross-sections were selected (see Figure 3.1): Permeable Concrete (PC), Permeable Asphalt (PA), and Permeable Interlocking Pavers (PIP). Although layer thickness may vary greatly depending on project conditions such as traffic loadings or subgrade bearing capacity, a common layout for urban conditions was defined based on a Spanish standard (MOPU 1986), where 10 cm of asphalt was defined over 40 cm of aggregate. In addition,typical pavement and soil layer thicknesses were selected from the SUDS manual (Woods Ballard et al. 2015). With this approach, and based on the layout definition provided by SWMM (see Figure 3.1a), a storage layer of 400 mm depth was defined for all three sections. All but PC were considered with a soil layer of 50 mm. Pavement layer was defined 100 mm thick for PC and PA, but 80 mm for PIP.

To analyse the slope effect, three slopes were selected from the typical range of PPs (CALTRANS 2013; CASQA 2003): 1%, 2%, and 6%. As SUDS units are relatively small, the proposed area for the study was 100 m^2. However, three types of catchment were defined to check the effect of the catchment shape: *narrow*, *squared*, and *wide* catchments. As the defined area was 100 m^2, shape defining widths were 1 m for the *narrow* shape, 10 m for the *squared* shape, and 100 m for the *wide* shape.

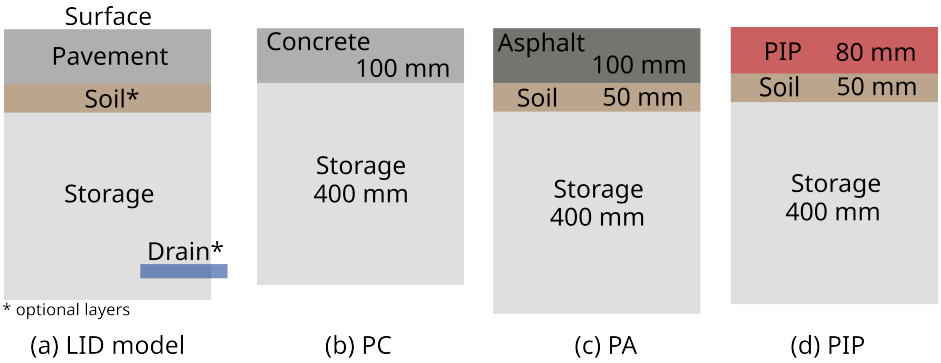

Figure 3.1: PP layouts for (a) general SWMM model, and tested (b) PC, (c) PA, and (d) PIP.

To study the CN effect's variation, a total of 12 CNs were selected between 40 and 100 for each previously mentioned case. In fact, 12 intervals were selected for that range, and to avoid overlapping points, each of the previous cases was given a random CN from that interval. Considering the three storm depths, three PP types, 3 shapes, 3 slopes, and 12 CNs, for a total of 972 points or relations between CN and pavement permeability, were obtained.

Based on those experimental variables, baseline runoff hydrographs with the SCS-CN method were generated, and their runoff hydrographs were computed. Afterwards, the PP hydrographs were calibrated and, thus, pavement permeability values were obtained. The correlation, obtained for a single event, will later be tested for a continuous event, using continuous 1-year data series.

Data analysis in this study was made with R (R Core Team 2023), an open source programming language. Data communication between R and SWMM was carried out with the *swmmr* package (Leutnant, Döring, and Uhl 2019). For model calibration, DE algorithm was used, implemented in the DEoptim package (Ardia et al. 2020).

3.2.2 Curve Number Method

The CN method from the Soil Conservation Service (SCS), currently the NRCS-CN method, was developed as a method of runoff computation designed for small agricultural watersheds. The method is included in Section 4 of the National Engineering Handbook (NEH-4) published by the SCS, U.S. Department of Agriculture (SCS 1956). At first, CN was developed from many experimental watersheds and is now extensively used to calculate direct runoff created by a precipitation event. In spite of being originally intended for agricultural sites, its applicability has also been extended to the urban environment (Balbastre-Soldevila, García-Bartual, and Andrés-Doménech 2019).

The SCS-CN method is based on two fundamental hypotheses and the water balance equation, $P = I_a + F + R$, where P is total rainfall, I_a is initial abstraction, F is actual infiltration, and R is the amount of direct surface runoff. The first hypothesis assumes proportional equalities between direct runoff and potential runoff, $R/(P - I_a)$, and actual infiltration and maximum retention, F/S_{max}. The term $P - I_a$ represents the effective rainfall or P_e, and S_{max} is the maximum potential losses to runoff in mm or maximum potential difference between effective rainfall and runoff. If that hypothesis and water balance equation are combined, the widely used Equation (3.1) for runoff (R) computation is obtained, which is dimensionally homogeneous:

$$R = \frac{(P - I_a)^2}{(P - I_a) + S_{max}} \tag{3.1}$$

The second hypothesis assumes there is some initial abstraction in the beginning of the rainfall, I_a, and it is related to potential maximum retention, S_{max}, by the factor λ. Thus, $I_a = \lambda \cdot S$. Despite the controversy around the value of λ, the original method gives a median of 0.2 for λ, as given in Equation (3.2):

$$I_a = \lambda \cdot S_{max} = 0.2 \cdot S_{max} \qquad [\text{mm}] \tag{3.2}$$

The value of S_{max} is transformed to CN by an identity, see Equation (3.3), in order to have a soils/land/cover coefficient with a direct positive relationship to calculated R. The underlying difference between S_{max} and CN is that the former is a dimensional quantity [L], whereas the latter is a non-dimensional quantity and varies conveniently from 0 to 100. Although CN theoretically varies from 0 to 100, values between 40 and 98 are practical design values validated by experience (Ponce and Hawkins 1996). The original expression

gave S_{max} in inches; thus, in metric units, the formula for CN differs from the original (Hawkins et al. 2009):

$$S_{max} = 254 \cdot \left(\frac{100}{CN} - 1 \right) \qquad [\text{mm}] \tag{3.3}$$

Using the method requires selecting a CN from tables or experience, based on soils land use, hydrologic condition, and initial moisture status. The U.S. Forest Service developed CNs for forested lands, and SCS elaborated woodland runoff CNs. Moreover, CNs for urban lands were built by weighting representative CNs for impervious land types and open spaces in good condition. Current editions of NEH-4 contain a variety of CN tables and charts for an array of additional soils and land uses (Hawkins et al. 2009).

3.2.3 Storm Water Management Model

SWMM is a dynamic rainfall–runoff simulation model used for single-event or long-term (continuous) simulation of runoff quantity and quality from primarily urban areas (Rossman and Huber 2015). Being a distributed model, SWMM divides a urban plot into several subcatchments. As urban areas usually contain a mix of land surfaces, subcatchments can be partitioned into two primary categories: pervious surfaces, allowing infiltration into the soil, and impervious surfaces, over which no infiltration occurs.

A third category can also be added, that corresponding to a SUDS, named Low-Impact Development (LID) control in SWMM, which can be globally defined in the model and, later, included into any subcatchment. It is also possible that the entire subcatchment is occupied by the LID control; in that case, there will not be any pervious or impervious surfaces. This article will just consider two types of surfaces: a pervious area and an LID area completely occupied by PP.

The runoff created in a subcatchment by a rainfall is estimated with a nonlinear reservoir model in SWMM, as shown in Figure 3.2. Subcatchment inflows are runoff (q_0) from other subcatchments and precipitation (i), but the first will not be considered here. Outflows are evaporation (e), infiltration (f), runoff (q), and drain outflow ($q3$). In Figure 3.2, d or d_1 are water level elevations over the infiltration surface; they account for reservoir volume, and d_s or D_1 indicate the minimum water level to produce runoff or outflow from the reservoir, respectively.

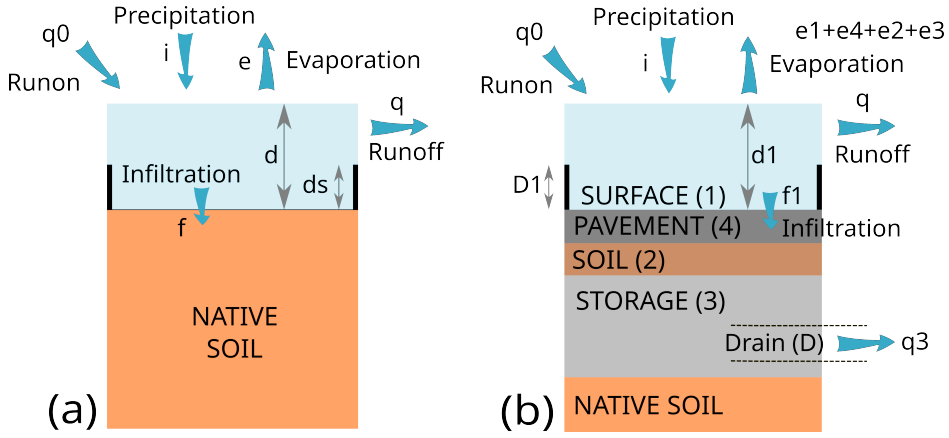

Figure 3.2: Non-linear reservoir models for (a) a pervious area and (b) an LID area.

In order to compute runoff with the SCS-CN method, a standard pervious area was selected, as shown in Figure 3.2a. The CN method is new to SWMM5 as an alternative to computing infiltration. The model implemented it because most practitioners were familiar with it, but also because there are several tabulated CNs available for numerous soil groups and land uses. The original CN method is a lumped loss method that combines interception, depression storage, and infiltration losses. The method calculates, for a rainfall event, the total rainfall excess. More details about its implementation in SWMM can be found in the hydrology manual (Rossman and Huber 2015).

In order to compute runoff with the PP model, an area completely occupied by PP was selected, as shown in Figure 3.2b. Conceptually, SWMM represents a generic LID unit via multiple horizontal layers, which later are integrated in order to create several LID control types (Rossman 2010). Specifically, PP is created by combining the following layers (Figure 3.2): Surface, Pavement, Soil, Storage, and Drain. Two of those layers are optional, Soil and Drain. The model solves a simple mass balance equation for each layer in order to compute hydrological processes into the LID control. Those balances yield the water volume increase or decrease over time by computing the difference between the inflow water flux rate and outflow flux rate (Rossman 2010). More details about LID units in SWMM can be found in the user's manual (Rossman 2015).

As shown in Figure 3.2, the LID model has some differences with a standard subcatchment in SWMM. As mentioned previously, a nonlinear reservoir model

is also applied to the LID area, but with some differences. Firstly, we need to consider that inflows (precipitation) are equal in both subcatchments. Secondly, potential evaporation rates are computed in the climatological module of SWMM, and thus, it is equal to both. However, evaporation rates differ because LID areas usually have more water available, as layers below the surface are considered. Hence, the main difference between the two models lies in the infiltration, which is computed differently. That makes computed runoff differ in both areas, even if the evaporation rate remains equal.

The above shows how different computation in a LID area is compared to a pervious area. In the LID area, runoff generation potential relies not just on the native soil properties, but also on the PP layers and their characteristics. For this article, *pavement permeability* was the selected as the parameter to calibrate runoff, as it is a property of the upper layer and its values are easy to link to an inflow.

3.2.4 Model Setup

The model setup was designed to compare the performance, in terms of runoff creation capacity, of two different models: the SCS-CN model and the LID model for PPs. To measure and compare runoff hydrographs from two models, two equivalent catchments were created, as shown in Figure 3.3. The SCS-CN catchment was defined with the general SWMM model and infiltration was calculated with the CN method. The LID catchment was defined as entirely occupied by PP.

SCS-CN catchment characteristics were defined in the catchment properties, while LID properties were set to zero, as they are overwritten by LID properties when modelled as an entirely LID occupied catchment. The used parameters are given in Table 3.1. The Manning value for SCS-CN subcatchment was set to zero to avoid any delay in the runoff (Rossman and Huber 2015). Initial abstraction depth was fixed at 1 mm, based on previous studies for urban areas, taking the value for traditional pavements (Rammal and Berthier 2020).

Although a unique LID control type, PP, was studied, three typical cross-sections were analysed (see Figure 3.1) to explore if there was any difference in the obtained permeability value. All three types were considered without any drain. Layer properties were identical for all three types, see Table 3.2, but impervious surface fraction was 0.90 for PIP (Mullaney and Lucke 2014). For all parameters, standard values were used, taken from the SWMM manual (Rossman and Huber 2016).

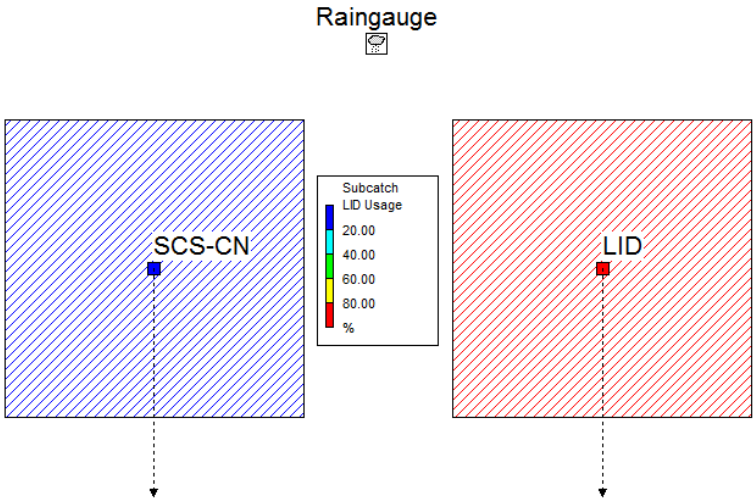

Figure 3.3: Defined catchments: completely pervious (blue) and 100% LID occupied (red).

Table 3.1: SWMM parameters for subcatchment.

Property	*Units*	*SCS-CN value*	*LID value*
Area	ha	0.01	0.01
Width	m	1-10-100	-(1)
Slope	%	1-2-6	-(2)
% Imperv	%	0	0
N-Perv	Manning n	0[3]	-(4)
Dstore-Perv	mm	1	-(5)

(1): defined in the Width for the LID implementation.

(2): defined in the Slope for the LID properties.

(3): to activate SCS-CN subroutine and prevent runoff delay.

(4): defined in the Roughness for the LID properties.

(5): defined in the Berm Height for the LID properties.

All three PP types were implemented identically into the LID subcatchment, as shown in Table 3.3.

Table 3.2: SWMM parameters for Permeable Pavement type LID controls.

LAYER/Factor	Symbol	Units	PC Value	PP Value	PIP Value
SURFACE					
Berm Height	D_1	mm	1	1	1
Vegetation Volume Fraction	$1-\phi_1$	-	0	0	0
Roughness	n	Manning n	0.02	0.02	0.02
Slope	S	%	1-2-6	1-2-6	1-2-6
PAVEMENT					
Thickness	D_4	mm	100	100	80
Void Ratio	$\phi_4/(1-\phi_4)$	Voids/Solids	0.25	0.25	0.25
Imperviouss Surf. Frac.	F_4	-	0	0	0.9
Permeability	K_4	mm/h	*	*	*
SOIL					
Thickness	D_2	mm	0	50	50
Porosity	ϕ_2	vol. frac.	-	0.45	0.45
Field Capacity	θ_{FC}	vol. frac.	-	0.1	0.1
Wilting Point	θ_{WP}	vol. frac.	-	0.05	0.05
Conductivity	K_{2S}	mm/h	-	100	100
Conductivity Slope	HCO	-	-	50	50
Suction Head	ψ_2	mm	-	50	50
STORAGE					
Thickness	D_3	mm	400	400	400
Void Ratio	$\phi_3/(1-\phi_3)$	Voids/Solids	0.7	0.7	0.7
Seepage Rate	K_{3S}	mm/h	10	10	10
DRAIN					
Flow Coefficient	C_{3D}	-	0	0	0

*: this value is the calibrated parameter.

Table 3.3: SWMM parameters for LID implementation into the LID subcatchment.

Property	Units	LID Value
Area of each unit	m^2	100
Number of Units	-	1
Surface Width per Unit	m	1-10-100
% Initially Saturated	%	0
% of Subcatchment Occupied	%	100

Climatological data for this study were gathered from the Igeldo weather station (43°19'0" N, 2°0'0" W) and Miramon weather station (43°17'20" N, 1°58'16" W), both placed in Donostia/San Sebastián (Spain), which is located in the Bay of Biscay.

The first station was chosen because of its large historical data. In order to study the hydraulic response of the PP, a single event of a 6-hour duration was selected, with a volume of 90.7 mm for a 100-year return period (named 6hT100), 61.4 mm for a 10-year return period (named 6hT10), and 43.7 mm for a 2-year return period (named 6hT2). Those events were obtained from IDF curves created based on Igeldo station data, used to generate a design storm with the alternating block method and considering 15 min time steps.

The second weather station, Miramon, was selected because it had 10 min interval temperature and precipitation data, best suited to perform a continuous or long-term analysis. Thus, in order to test results obtained with the previous single event, data from 2019 were gathered. Annual precipitation is 1593.6 mm, with 206 dry days (minimum measured values was 0.1 mm). The average temperature for 2019 was 14.2 °C. The Hargreaves method (Hargreaves and Samani 1985) was used to compute evaporation rates based on daily max–min temperatures and the latitude.

For the continuous event, computed time steps were 2:00 min for Wet Weather and 10:00 min for Dry Weather; the reporting time step was 10:00 min. For the single event, the time step for both cases was 1:00 min and the same as the reporting time step.

3.2.5 Hydrograph Performance and Calibration

Calibration performance was checked by evaluating the Nash–Sutcliffe adimensional coefficient or NSE (Nash and Sutcliffe 1970), given by Equation (3.4) below. Usually, observed and modelled data are compared but, as this research calibrated the parameters for LID to simulate the flows produced by SCS-CN and, therefore, both are modelled, the hydrograph from the SCS-CN area was considered as a *baseline scenario* and the hydrograph from the LID area as the scenario to be compared. Hence, R is the observed runoff in SCS-CN area, $\overline{R}$ is its average, and L_i is LID area runoff. NSE values range from $-\infty$ to 1, where a value equal to 1 indicates a perfect fit.

$$NSE = 1 - \frac{\sum_{i=1}^{N}(R_i - L_i)^2}{\sum_{i=1}^{N}(R_i - \overline{R}_i)^2} \tag{3.4}$$

On the other hand, once the calibration parameter was fixed, the resulting runoff hydrographs from both areas were also compared to obtain more information. As it is common to study peak flow and volume for single events

(Dietz 2007), percent error in peak (PEP) and percent error in volume (PEV) were analysed, as shown in Equations (3.5) and (3.6), the R values being from the SCS-CN subcatchment and the L values from the LID subcatchment:

$$PEP = \frac{L^{peak} - R^{peak}}{R^{peak}} \tag{3.5}$$

$$PEV = \frac{L^{volume} - R^{volume}}{R^{volume}} \tag{3.6}$$

The calibrated parameter in this study was Pavement Permeability from the Pavement layer of the LID control. The objective function selected for calibration was the NSE defined in Equation (3.4). For minima searching of the objective function, the Differential Evolution (DE) algorithm was applied, which is one type of meta-heuristic optimization technique based on function evaluation, successfully implemented in multiple areas, as it has prove to be a useful tool for global optimization (Bilal et al. 2020). In addition, DE is particularly well-suited to find the global optimum of a real-valued function of real-valued parameters, and does not require that the function be either continuous or differentiable (Mullen et al. 2011). In this study, lower and upper bounds of the parameter to be optimized were (0, 200), and the selected maximum number of iterations (population generation) was 20. These values were validated with a previous test.

3.3 Results and Discussion

This section presents, firstly, (1) the data obtained after single event calibration: (a) the relation between CN and pavement permeability is presented, which was the main objective of the study; (b) the influence of the selected variables is discussed; and (c) the performance of the calibrated hydrographs is discussed. Secondly, (2) results for a continuous test event are discussed.

3.3.1 Relation for CN and Pavement Permeability

General Analysis

Obtained pavement permeability values after calibration process for each CN are given in Figure 3.4. As mentioned in the previous section, those points correspond to three different storm depths, three pavement layouts, three pave-

ment slopes, and three catchment shapes, with 12 CNs for each case; thus, there are 972 points.

The figure shows a clear correlation between both variables linking the two models. As may be expected, the greater the CN, the lower the pavement permeability that generates an equivalent runoff hydrograph. However, the pattern is clearly different for low and high CNs. A visual evaluation reveals that data dispersion is much greater for low CNs than for high CNs. Based on that visual analysis, the authors propose a linear regression differenced by regions, but only the one for high CNs will be considered, given by Equation (3.7):

$$permeability \quad [\text{mm/h}] \quad = 57 - 0.57 \cdot CN \qquad for \qquad 88 \leq CN \leq 100 \quad (3.7)$$

Although the figure does not show how values are influenced for the four considered variables (storm, slope, shape, and type), they are relevant. The influence of those variables will be discussed in the next section. Those variables, along with differences in how the model computes infiltration, vary the response of the PP model.

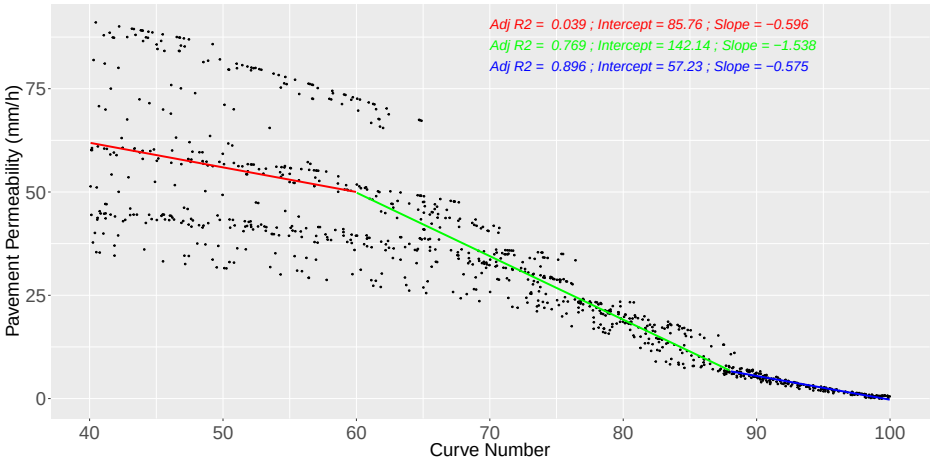

Figure 3.4: Pavement permeability values for fitted hydrographs in each selected CN and considered regression curves, with different colours for each proposed interval.

With regard to the infiltration, the basic difference is how the different methods compute infiltration (see Section 4.2.6). The infiltration capacity for SCS-CN is not constant: it increases for lower CNs, decreases as storm depth increases,

and is higher for narrow catchments. On the other hand, the infiltration capacity of PP relies mainly on the pavement permeability, with a constant value.

It is also important to consider that the SCS-CN method, although varying the infiltration capacity, computes runoff for a wider range of rain intensities if compared to the PP model, which creates runoff for rain intensities higher than pavement permeability. The SCS-CN method computes the partial infiltration of the rain, while the PP model computes runoff over a certain intensity threshold. The rain pattern also plays a role in that infiltration, as intensity varies during storm. Further details will be given in the next two sections.

Influence of Selected Variables

As mentioned before, not all variables have the same influence on pavement permeability. For performing that analysis, Figure 3.5 has been created, plotting the same figure given in Figure 3.4 but once for each analysed variable: catchment shape, storm depth, pavement slope, and PP layout.

In regard to catchment shape, characterised by the catchment width, the plot clearly shows that narrow catchments (where the width is equal to 1 m) behave quite differently from the other two catchment types, since the obtained pavement permeability values are lower than for the other two shapes. This is mainly because the time of concentration in the long catchment is considerably higher than the times given by the two other shapes. Hence, water has more time to infiltrate, and thus the equivalent hydrographs in the PP model can be modelled with a lower value of pavement permeability. In addition, pavement permeability values obtained for other considered catchment types are very similar, indicating that only long catchments provide a lower pavement permeability value.

If the storm depth variable is considered, related to the return period, the plot also shows a strong influence on the pavement permeability value. The higher the storm depth, the higher the pavement permeability value that computes an equivalent runoff hydrograph. This pattern may rely on how each model calculates infiltration. In the SCS-CN model, the infiltration increases when precipitation depth increases, while in the PP model, the infiltration capacity is mainly controlled by pavement permeability. That is why pavement permeability has to increase when precipitation depth increases, so that it can increase the infiltration capacity of the PP.

On the contrary, Figure 3.5 shows how PP layout and pavement slope have no influence on the CN and pavement permeability relation, as those points do not show any pattern. Hence, the following analyses will not consider either one or the other.

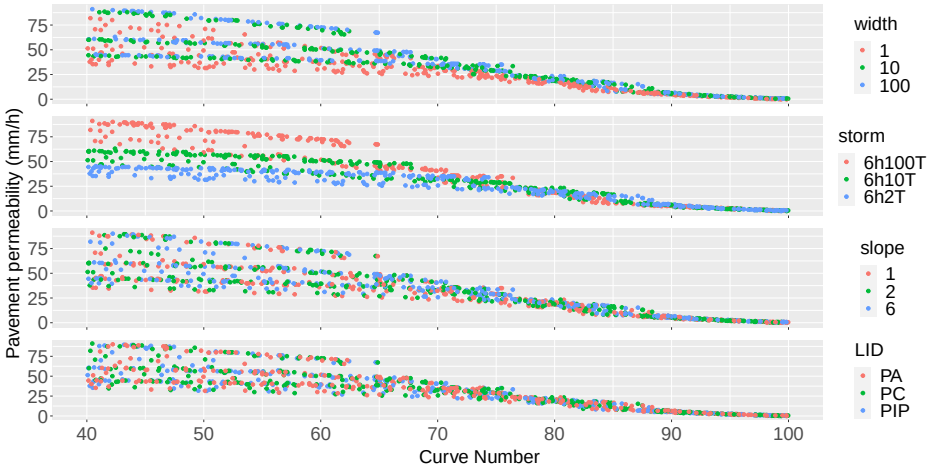

Figure 3.5: Pavement permeability values for fitted hydrographs with different colors for considered catchment shapes (first row), precipitation depth (second row), pavement slope (third row), and LID layout (fourth row).

Performance of the Equivalent Hydrographs

This section analyses PP runoff hydrographs as compared to the SCS-CN baseline hydrographs. Firstly, some example hydrographs are given in order to better visualize the obtained NSE values. Secondly, the obtained NSE values are presented, as that was the selected criteria to fit the pavement permeability value. Finally, volume and peak performance, PEV and PEP values, are discussed.

Hence, in order to show the relation between SCS-CN baseline hydrographs and calibrated ones, nine hydrogaph pairs are plotted in Figure 3.6. The first three pairs are given in the first row, and the selected hydrographs are chosen for the same storm and width case, but selecting one with a low CN, one with a medium CN, and another one with a high CN. The second row shows another three pairs of hydrographs, but in this case, the width is constant and similar CNs were selected. The third row has the same storm and similar CNs,

varying the width. The effect of those variables will be analysed along with the NSE variable.

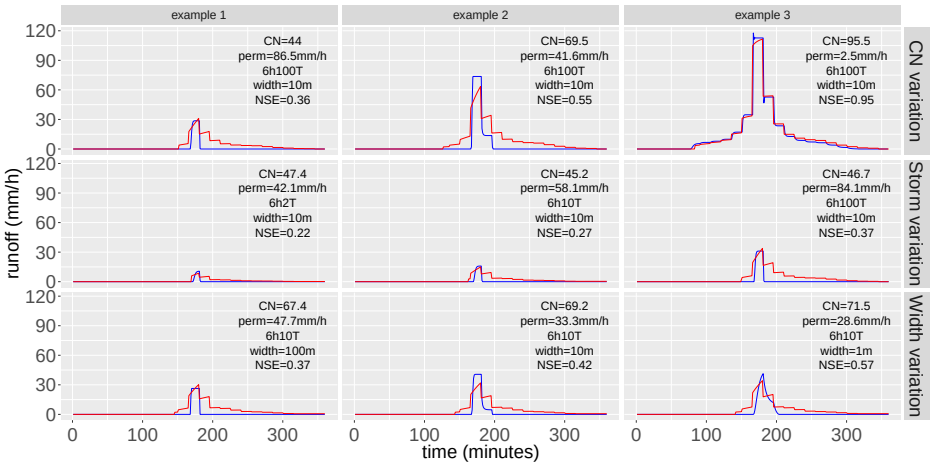

Figure 3.6: Nine examples of SCS-CN hydrographs, used as a baseline (red), and fitted LID hydrographs (blue). For each pair, baseline CN, calibrated pavement permeability, storm, width, and NSE are given.

Therefore, to check the obtained NSE values after each calibration process, Figure 3.7 gives 972 NSE values, just grouping the effect for two variables that affect the result, which were previously identified: catchment shape and precipitation depth. Several patterns can be identified from that figure: an improvement in NSE values for higher CNs and also an improvement in those values for higher storm depths and narrower catchments.

Thus, the first thing that Figure 3.6 clearly shows is that there is an improvement in NSE values while the CN value is increased (see first row of examples in Figure 3.6). For lower CNs, with high infiltration capacity, the PP can create runoff for the hydrograph peak, but as the infiltration capacity of PP will be higher than other rain intensities, no runoff is created for the rest of the storm. On the contrary, for high CNs, there is almost no infiltration, and thus there is a pavement permeability value that can simulate the baseline hydrograph. This pavement permeability, although constant, will allow similar infiltration to the SCS-CN method.

In that sense, it can be noticed in Figure 3.7 that the improvement rate is better from a certain CN, different for each combination of storm and shape. That CN is approximately 72 for the *6h2T.100* case (100-year return period and

100 m width or wide catchment). The improvement starts when the infiltration capacity is small enough that the PP can control infiltration with a constant value for a wider range of rain intensities. This depends not only on the considered CN, but also on the selected storm depth and width case.

Something similar happens with the storm depth (see second row of examples in Figure 3.6). In this case, as the infiltration capacity of the SCS-CN is reduced when storm depth increases, the PP model can accommodate the baseline hydrograph better with just one value of pavement permeability.

With regard to catchment width, the figure also shows that narrow catchments perform differently from square and wide ones (see third row of examples in Figure 3.6). This is related to the infiltration increase produced by the narrow catchment, where residence time is considerably higher than for wide or squared catchments. For the SCS-CN model, the infiltration increase is smaller in a narrow catchment than the infiltration computed by the PP model in the same type of catchment. As the infiltration capacity is partial in the first and constant in the latter, the increase in infiltration is greater in the PP model for narrow catchments.

It also can be noticed that NSE worsens for some cases, in particular for high CNs and narrow catchments. This is probably due to the same reason mentioned above but, in this case, the increase in the PP model's infiltration capacity means that the model cannot create as much runoff as the SCS-CN model.

With regard to the peak and volume performance of calibrated hydrographs given in Figure 3.8, it is clear that there is an improvement for higher CNs, which is related to the obtained NSE values. Overall, the peak values are higher for PP than for the baseline SCS-CN, while volumes are lower for the PP. The obtained peak values are better than the obtained volumes, although both improve considerably for CN values higher than 80. As mentioned before, the PP model is capable of accommodating only the peak value for low and medium CNs. Hence, PEP remains quite constant for all CNs. On the contrary, the PP model cannot accommodate the rest of flow values and, hence, PEV values are worse and only improve when flow rates are fitted not just for the peak, but for a wider range of rain intensities.

Considering both obtained pavement permeabilities and the performance of the calibrated hydrographs, the authors consider that the previously mentioned Equation (3.7) would give a reasonable equivalent response with the PP model to that obtained with the SCS-CN model. This relation, although not for all

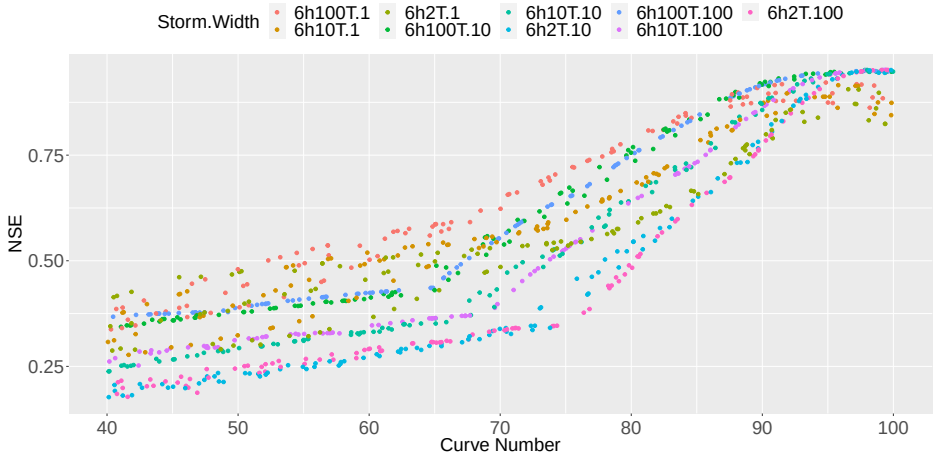

Figure 3.7: Computed NSE values after calibration. Different colours are used for each combination of storm depth and catchment shape.

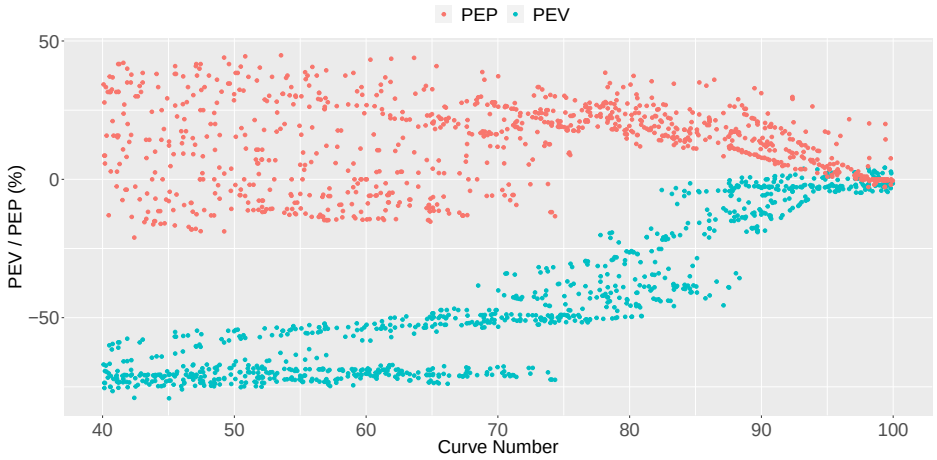

Figure 3.8: Computed PEV and PEP values for fitted hydrographs for each selected CN.

CN ranges, would be useful for a wide range of urban covers, mostly impervious (total or partial). However, if that relation is used, it is important to keep in mind that there are some limitations in its performance, as the PP model yields higher peak values and lower volume values.

3.3.2 Test Case with Continuous Event

This section analyses how pavement permeability values defined using Equation (3.7) perform when the analysed storm is not a single event but a continuous event. Performance of the PP model is only checked for CN values higher than 88, that is, the range of values which were found to be adequate for considering an equivalent hydrograph with a single event.

The first analysed variable is the NSE, characterising the hydrograph's performance. The obtained values are given in Figure 3.9, which shows how CN values are considerably worse than those obtained for a single event. That is, again, due to the differences in model definition. As mentioned in the single event analysis, the infiltration capacity of the PP model is controlled by pavement permeability. If the infiltration capacity obtained by the SCS-CN model was difficult to simulate in a single event, as shown in previous section, it is even more difficult to create an equivalent hydrograph with one unique value if the storm depths are varying, as in the continuous event. Hence, the ability of the PP model to simulate equivalent hydrographs worsens.

The figure also shows that the NSE value improves for high CNs, but this pattern is equivalent to the one obtained for a single event, and the causes are those explained in the preceding section. However, if 0.6 is considered a satisfactory threshold for NSE value, good agreement would be obtained for CNs higher than 96.

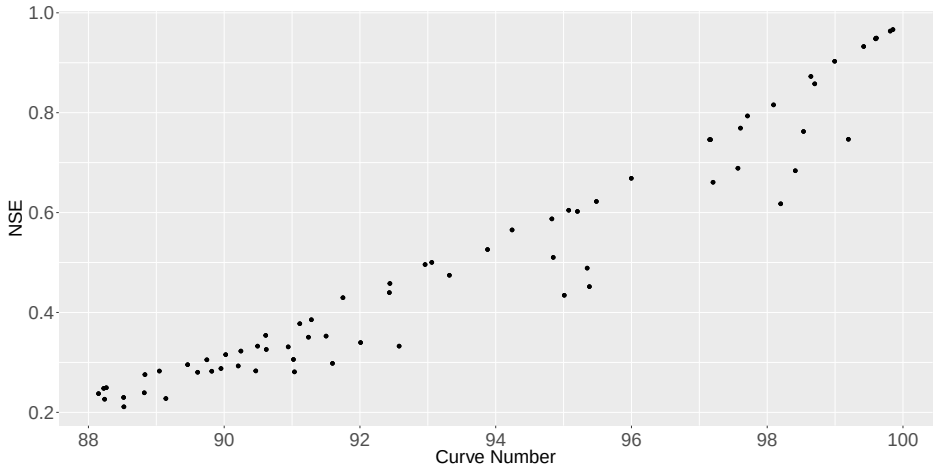

Figure 3.9: Computed NSE values for a continuous event.

If we compare results in terms of volume and peak performance, see Figure 3.10, we can see that PEP/PEV values also worsen if compared to a single event, although not as much as the NSE. In this continuous event, PEP/PEV values with an error lower than ±50% appear only for CN values higher than 98, while for the single event, that threshold value was around CN 90. This is also explained by the rain pattern and the infiltration method provided by both models. Same as in the single event, peak values perform better than volumes in the continuous event.

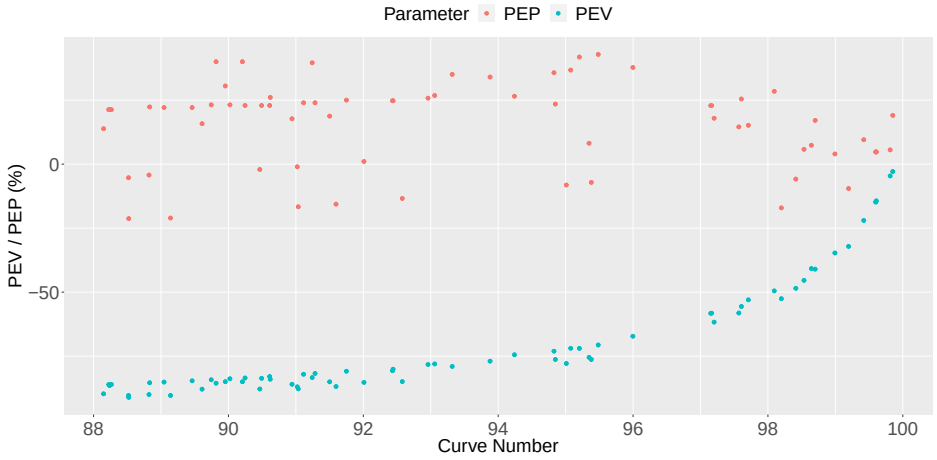

Figure 3.10: Computed PEP (red) and PEV (blue) values for a continuous event.

Hence, this continuous test case shows that permeability values obtained with Equation (3.7) are only acceptable for very impervious surfaces or very high CNs, over 96 if we consider obtained NSE values. However, if peak and volume performance are considered, the relation would only be valid for impervious surfaces, that is, for CNs higher than 99.

3.4 Conclusions

This study compares the hydraulic performance of the PP model given in SWMM and the widespread CN model by linking one parameter from each model: pavement permeability from the first and CN from the latter. The comparison has been performed with SWMM, analysing the influence of several variables involved in the PP's design: storm depth, pavement layout, catchment shape, and pavement slope. However, it should be noted that the research

was not designed to test or compare the performance of any of the mentioned models separately; the aim of the research was to link both models numerically, based on a theoretical comparison.

The article explores how different the models are and, thus, how the runoff modelled in each case differs from the other, as infiltration computations varies. Because of that disparity, the article demonstrates that we cannot consider an equivalence between the runoff hydrographs for pervious surfaces or low CNs. In addition,the article shows that catchment width and storm depth considerably influence the infiltration process, and thus the equivalency between models is significantly influenced by these variables. The article also shows that pavement slope and PP layout do not have impact on that equivalency.

However, this study shows that it is possible to generate runoff hydrographs with the PP model given in SWMM equivalent to those created with the SCS-CN method in some cases. In fact, the article gives a relation between a certain CN and the pavement permeability that creates an equivalent runoff hydrograph: $permeability$ [mm/h] $= 57 - 0.57 \cdot CN$. This relation would be valid for single events when CNs are higher than 88 and would not be influenced by the PP layout, catchment shape, storm depth, nor the pavement slope. Equivalent hydrographs would have an NSE higher than 0.60, and peak/volume performances would be in the range of $\pm 50\%$.

This was the primary goal of the article: to find an equivalency for both methods. That relation can be useful, when modelling, to compare runoff created in a certain catchment with and without PP, that is, to analyse the influence of a particular PP design based on runoff data gathered with the same model, providing more robust conclusions in broader studies. Although the conducted analysis makes the relation valid just for the PP model definition given in SWMM, it may be useful for any other PP model, or even SUDS, where infiltration is controlled by a similar surface parameter equivalent to pavement permeability; however, further studies are required.

From a purely practical perspective, it would not be necessary to change the model to check those two scenarios, as PP could also serve as an impervious surface. In addition, PP layouts are defined once in SWMM and can be implemented in several catchments. Thus, it would be enough to change one unique parameter, namely pavement permeability, just once to change the catchment response: for example, from a completely impervious surface type to a catchment with a PP, no matter how many PPs are implemented in the model.

The article also shows that the mentioned equivalency is not valid if a continuous event is modelled. In that case, the PP is much worse at obtaining a hydrograph similar to that created by the SCS-CN. Hence, a continuous event shall not be modelled using the mentioned equivalency if it does not have a CN higher than 98. In this case, the selected test event yields NSE values higher than 0.60, peak errors lower than 25%, and volume errors higher than -50%. However, the above-mentioned benefits remain valid: the same model can be used to test PP implementation.

Further research is recommended for other LID types, where the permeable pavement parameter does not exist and surface permeability is controlled by other parameters. Thus, it would be interesting to further study what the relation would look like for other types of SUDS, as those are also studied when implementing SUDS in urban environments. It also would be interesting to investigate if LID control implementation in SWMM may become simpler, as many parameters need to be changed in order to modify a catchment completely occupied by an LID to another one with a different infiltration model. Further studies are also recommended to check the links between SUDS and other models, such as the Rational one, which is also common among practitioners.

In summary, the article compares two widespread models used in urban environments that simulate runoff hydrographs and specifies under which conditions equivalent hydrographs can be obtained. Consequently, the article is expected to be useful for practitioners analysing how the implementation of certain PPs affects the runoff created in one or several areas.

Chapter 4

Experimental analysis

This chapter first analyses the hydraulic performance of several new permeable pavement systems based on 189 experimental hydrographs exploring the influence of rain intensity, slope, and, as a novelty, individual layers. Analysed variables were outflow peak, time to peak, and time to specific cumulative discharges. Secondly, based on the experimental hydrographs, the performance of the permeable pavement module defined in SWMM is explored in two steps. First, single-layer outflows were used to calibrate physically unmeasured values. Later, complete layout hydrographs were tested without calibration. Results show that the superficial permeable interlocking paver layer provides a notably higher retention capacity than the porous asphalt mixture. Individual modelling results show that the soil layer definition is inappropriate for gravel-type layers, even with a geotextile. Despite this, complete section performance is quite good without calibration if the soil layer is not selected on the model. These results are expected to reduce modelling uncertainty, especially when no calibration data is available.

Original article 3

Madrazo-Uribeetxebarria, E., Garmendia Antín, M., Alberro Eguilegor, G., & Andrés-Doménech, I. (2023). Analysis of the hydraulic performance of permeable pavements on a layer-by-layer basis. Construction and Building Materials, 387, 131587. https://doi.org/10.1016/j.conbuildmat.2023.131587

4.1 Introduction

Green infrastructure, which mimics the natural hydrological cycle, has proven to be an efficient solution to be implemented in urban environments to improve the sustainability of surface water management (Charlesworth and Wade 2014), but also as a mechanism for enhancing resilience to climate change and flooding. Sustainable Urban Drainage System (SUDS) is a more specific term used for designating certain technologies and techniques, which aim to manage stormwater in a more sustainable manner than conventional solutions (Fletcher et al. 2015), reducing the soil-sealing effect of urbanisation. One such technique is Permeable Pavement (PP) systems, which, unlike other SUDS techniques, provide a transitable hard surface while managing surface stormwater (Kuruppu, Rahman, and Rahman 2019), making it a very advantageous solution for highly urbanised areas. In addition, PP also offers several environmental benefits, such as (Xie, Akin, and Shi 2019): runoff volume and peak reduction, enhanced stormwater infiltration into the native soil, water quality improvement, heat-island effect mitigation, and traffic noise reduction.

Compared to traditional pavements, created by laying several granular materials and sealed with an impervious surface, PP systems are created with highly porous base and subbase to enable water infiltration and storage (Mullaney and Lucke 2014). That porous base is crowned by a transitable surface, also highly porous, which can be monolithic or modular, being the most researched surface materials (Tziampou et al. 2020): Permeable Concrete (PC), Permeable Asphalt mixture (PA), and Permeable Interlocking Paver (PIP).

The hydraulic properties of PP systems are fundamental for their performance as SUDS. Moreover, hydraulic processes are influenced by several sub-surface characteristics, such as layer thickness, pore size, pore distribution, and pore geometry (Tziampou et al. 2020). In that sense, the volume reduction provided by PP systems is highly influenced by surface properties, such as permeability, being the volume reduction higher for PA than for PIP (Støvring et al. 2018). In the case of newly built PIPs, infiltration capacity is higher than 90% for slopes up to 10%, being higher for lower slopes (Sañudo-Fontaneda et al. 2013). The retention capacity of PP systems is also reduced by the creation of preferential paths by PIPs (Rodriguez-Hernandez et al. 2016). In that regard, a larger aggregate size used in PP systems tends to reduce horizontal hydraulic conductivity compared to common soils considerably (Kamali, Delkash, and Tajrishy 2017).

On the other hand, PP system outflow varies in response to rainfall duration and pavement initial wetting conditions. Alsubih et al. (2017) tested the im-

pact of these latter two and found that the outflow duration for all rainfall events and tested conditions was significantly longer than the rainfall duration. Liu and Chui (2017) studied how several factors influenced runoff from PP systems, concluding that from the five checked design parameters, storage depth was the most influential factor, followed by the conductivity of the subgrade soil.

However, it is essential to integrate SUDS into the existing stormwater network (Xu et al. 2019a). For this purpose, mathematical models are a fundamental tool since they facilitate the decision-making process when implementing this type of solution in the urban environment. Nevertheless, further research is needed to improve modelling techniques and properly evaluate SUDS performance (Eckart, McPhee, and Bolisetti 2017).

There are several modelling approaches to SUDS; a detailed review can be found in Eckart, McPhee, and Bolisetti (2017). By extension, various models are also available. However, the Storm Water Management Model (SWMM) is one of the most popular among researchers, thanks to the rich selection of hydrologic and hydraulic computation methods and the free access to the model (Kaykhosravi, Sahereh, Khan, Usman T, and Jadidi, Amaneh 2018). Initially, SWMM was developed to assist practitioners in sizing stormwater and grey wastewater infrastructure (Platz, Simon, and Tryby 2020). However, it has implemented several SUDS models, named Low Impact Development Control (LIDC), including PP.

Being relatively new elements in a widely used model, these LIDC models are still being tested and their performance evaluated. Zhang and Guo (2015) tested the PP module in SWMM, comparing it with results from a standard catchment, and concluded that the infiltration rate provided by PP was incomplete, as it should take into account drainage capacity and subbase storage capacity. Randall et al. (2020) investigated the long-term performance of three experimental stalls located on a parking site and found that SWMM overestimated evaporation rates on PP. Platz, Simon, and Tryby (2020) tested the SWMM LIDCs for empirical data from specific PP monitoring and found that SWMM satisfactorily modelled the PP. However, the average predicted peak was 35% lower than the measured one, and modelled average volume was 5% lower. Madrazo-Uribeetxebarria et al. (2019) also attempted to check single-event modelling performance on SWMM for PIPs and PA surfaces, finding that peak and volume differences were less than 10%.

Even so, further research is still required. As a preliminary step to deepen the model performance, the authors conducted a sensitivity analysis of the PP

model given in SWMM. One of the most relevant conclusions obtained from the analysis was that some parameters could be neglected when the outflow from the PP is modelled. The analysis also pointed out that some parameters are more influential than others, giving an order of priority for parameters according to their influence in the outflow control (Madrazo-Uribeetxebarria et al. 2021).

Nevertheless, more than one sensitivity analysis is required to reduce modelling uncertainty. Other factors, such as the modeller's limitations in describing the physical reality, also contribute to modelling uncertainty (Radwan, Willems, and Berlamont 2004). In that regard, and bearing in mind that the PP model in SWMM is defined on a layer basis, real-life applications usually have a different layer structure than the model. Sometimes because layout includes elements not considered in the model, such as the geotextile between the base layer and the subbase layer, or because the practitioner is not sure if a specific element, the soil layer in SWMM, for example, has to be selected or how to apply it.

In that regard, Bateni et al. (2020) studied the potential of new a type of PP with micro-detention storage by setting hydrological parameters experimentally and, after calibration, testing the potential of SWMM to model the performance of the new pavement. Gülbaz and Kazezyılmaz-Alhan (2017) also compared SWMM modelling capabilities for bioretention systems based on experimental data obtained in the laboratory with constant rainfalls of 15-min duration. Instead, Turco et al. (2017) tested the HYDRUS-2D model based on laboratory data and calibrating some parameters. However, no previous study is analysing SWMM on a layer basis.

The global objective of this study is twofold. Firstly, it explores the hydraulic response of new PPs, where clogging has yet to start, in the short term under specific controlled conditions. For that purpose, a novel approach is proposed by testing the PP system layer-by-layer, not just with the complete cross-section. Secondly, the study confronts experimental data with the PP model provided by SWMM, as no previous study is known to validate the capability of SWMM's LIDC module for representing the hydrological performance of a PP system in the short term based on experimental data. The analysis is also carried out layer-by-layer to gain new insight into the model. Although clogging is another factor to be taken into account in the long term, we underline the interest in the initial behaviour of the pavement. Hence, the specific objectives set for the study are: (1) to check how outflow hydrographs are influenced, for complete cross-sections and each layer, by slope, rain, and pavement type, and (2) to test sub-surface hydrograph prediction performance for the model.

For that purpose, the processes are set up as follows: (a) measure drain outflow hydrographs for several PP setups under specific laboratory conditions; (b) set the parameters for modelling, measuring physical parameters, and calibrating, on a layer basis, parameters that can not be physically measured; (c) compute modelling hydrographs equivalent to those measured under laboratory conditions with previous parameters without calibration; and (d) characterise the modelling performance of SWMM by comparing experimental and modelling results.

Thereby, the article presents, firstly, the materials and methodology used during this study in Section 4.2. Later, obtained results are presented in Section 4.3 and discussed in Section 4.4. All three sections were divided into two, one related to experimental data and another related to modelling data. Finally, conclusions are given in Section 4.5.

4.2 Materials and methods

In order to measure outflow hydrographs from several cross-sections under different rain intensities and slopes, 40-minute laboratory experiments were conducted. This section describes (4.2.1) the selected precipitation regime, (4.2.2) the equipment used to perform mentioned experiments, (4.2.3) analysed materials and layouts, (4.2.4) the experimental procedure, (4.2.5) the selected criteria to analyse experimental hydrographs, and (4.2.6) how modelling data were obtained and compared. The methodology described in this section is summarised in Figure 4.1.

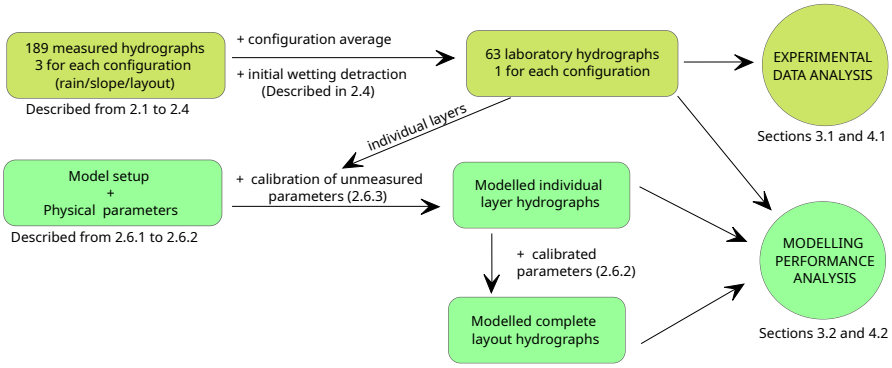

Figure 4.1: Flowchart describing the methodology followed to obtain experimental and derived modelling results.

4.2.1 Climatological data

The study was undertaken with data gathered in Donostia/San Sebastián (Spain), facing the Bay of Biscay in an Atlantic climate. Climatological data was gathered from Igeldo weather station (43°19′0″N, 2°0′0″W), with extensive historical data and average annual rainfall of 1500 mm. Based on IDF curves for the period 1927-2016 (DHI 2018), 35/70/140 mm/h intensities were selected, named *low*/*high*/*extreme*, correspondent to a 2/10/500 return period rainfalls of 15 minutes duration, which corresponds, for urban watersheds, to the range of the most frequent time of concentrations values until the network inlet (Freire Diogo and Antunes do Carmo 2019). Hence, applied precipitation volumes were 8.75 mm, 17.5 mm, and 35 mm.

4.2.2 Equipment

Experimental tests were carried out on a GUNT HM-164 hydrological bench. The original bench had a circuit to create artificial rain but was modified to better control flows, create uniform raindrops, and measure outflows. An image of the bench and a diagram of the modified circuit are shown in Figure 4.2.

The precipitation regime was simulated by a grid of evenly spaced mesh of 81 drippers located in the upper part of the hydrological bank, at a distance of 40 cm to 60 cm, depending on the tested layer. The mesh was kept horizontal during the experiments to ensure uniform dripper discharge. The selected flow was controlled with two rotameters; the first one, rotameter A, had a flow range of 15 to 160 l/h, and the second one, rotameter B, had a range of 5 to 50 l/h. Rotameter A set *high* and *extreme* precipitation regimes, while rotameter B set *low* precipitation. The applied flow was measured by a 15 mm iPerl flowmeter with a graphic display of 1 l/h precision. Flow was controlled by several valves placed along the circuit.

The bench had a platform to lay the material, and a specific slope could be selected. Materials were laid out in half of the test bench, resulting in all analysed cross sections having a surface area of 1.0 m x 1.0 m. All tested materials were laid over an impermeable, smooth surface of waterproofing high-density polyethylene geomembrane laid over the bench platform. Water was drained over the membrane to an outflow pipe, discharging the hydrograph buckets. Thus, outflow from the test bench was collected in 15 identical buckets which an individual capacity of 5700 ml. The collected volume was measured by registering the water level using a ruler placed on the side of the bucket. The water levels were deduced from horizontal pictures, with an accuracy

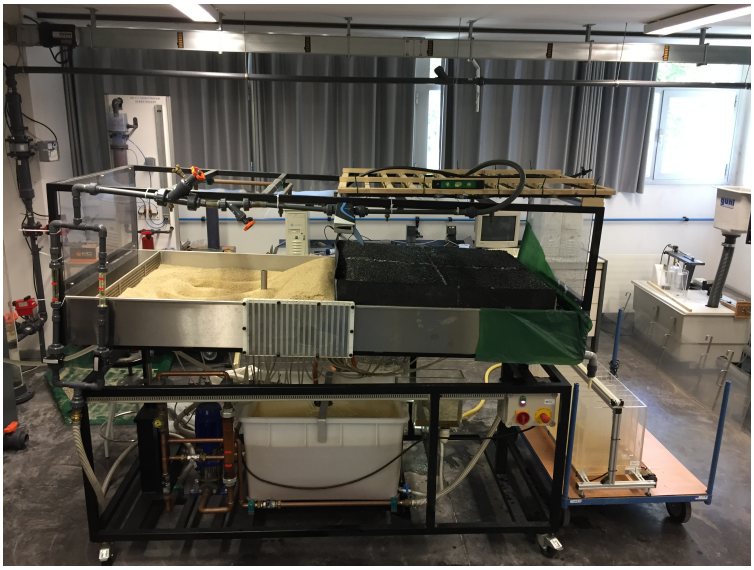

(a) Experimental bank.

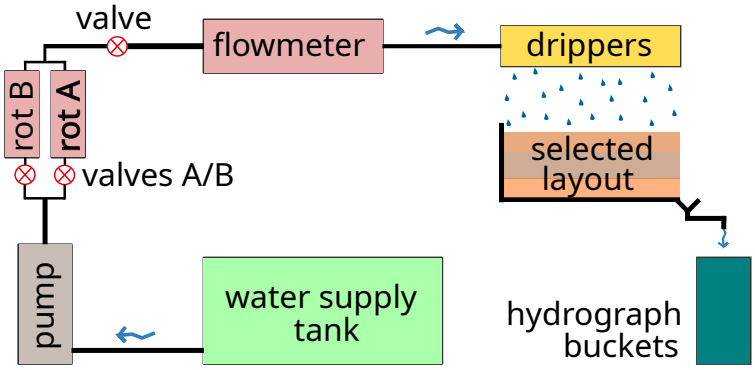

(b) Schematic representation of the experimental bank.

Figure 4.2: (a) Experimental bank and (b) a diagram with the key components.

of ±0.25 mm. Hence, the volume measuring error was 4.45 ml, which is, for volumes measured in one minute, 0.20% of extreme flow, 0.40% of high flow, and 0.80% of low flow.

4.2.3 Materials

This study explores the hydraulic performance of two types of PPs: PA and PIP, two of the most used pavements (Palla et al. 2014). Both were laid out over a base layer of small gravel (also named soil), with a geotextile below, laid over a subbase layer of big gravel (also named storage or STOR). Materials were first tested individually, and those layouts were named *PAind*, *PIPind*, *SOIL*, and *STOR70/140*. The individual layer analysis required additional materials, such as plastic cells (named cells), as a base for top layer materials, and a mosquito mesh (named mesh) to avoid material loss from PIPs. All layouts were placed over the waterproof membrane (named membrane), which provided flow parallel to the bench inclination. Complete layouts were named *PAcom* and *PIPcom*. All tested layouts and materials are given in Figure 4.3.

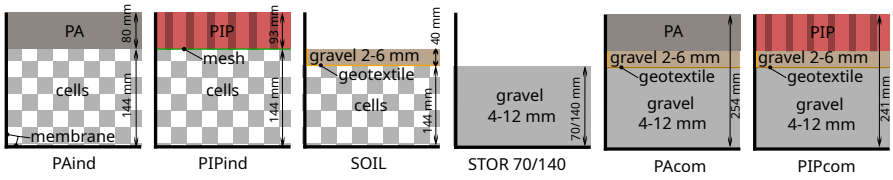

Figure 4.3: Tested cross-sections, the first four for individual layers (PAind, PIPind, SOIL and STOR70/140), and the last two for complete layouts (PAcom and PIPcom).

A local supplier, Asfaltia, laid the PA on top of an existing concrete surface and compacted it with a roller. Later, it was cut into square pieces of 0.50 m x 0.50 m to be joined together in the test bench. The joints between pieces were filled with standard silicone to avoid infiltration. PA was laid in two layers. The first layer, the one below and named PA16, was 5 cm thick, with a maximum aggregate size of 16 mm. The one above, PA11, was 4 cm thick, with a maximum aggregate size of 11 mm. The percent of binder by mass in the mixture was 4.3 % for PA16 and 4.4 % for PA11. The binder in both cases was polymer-modified bitumen, with a softening point of 70 °C and penetration values at 25 °C of 45/80, in 0.1 mm. The porosity was 20% (void ratio of 25%) for both layers. The hydraulic permeability was 250 000 mm/h for the complete section, measured using a constant head permeameter.

PIPs were AQUATA clay paving blocks from Wienerberger. PIP's dimensions were 80 mm thick, 200 mm long, and 63 mm wide. The PIPs had protrusions

that left a void space between them and allowed water to infiltrate; those protrusions were 6 mm x 6 mm. Thus, the surface block had an empty volume of 9.84%, filled with the same small gravel used as a base material (Mullaney and Lucke 2014), described below. Considering the latter value and the void ratio of the filling material without being compacted, the PIP's void ratio was 0.05. The hydraulic permeability of PIPs was measured with the same permeameter used for PA, but the measured permeability was 90 000 mm/h.

The bedding or soil layer was 40 mm thick, formed with small limestone gravel, sizes between 2 and 6 mm. The gravel was compacted in the experimental bench after being laid. The porosity of the gravel was experimentally determined in a 100 ml plastic beaker, filling the pores with water and weighing additional water, replicating the measure three times. Measured mean values were 0.45 (void ratio of 0.82) for compacted gravel and 0.49 (void ratio of 0.97) for uncompacted one. Additionally, non-woven polyester geotextile, Danofelt PY 200 from Danosa, was placed below the bedding layer. The water permeability perpendicular to the unloaded plane for geotextile is at least 18 000 mm/h, according to the manufacturer specifications complying with UNE EN ISO 11058 standard.

Storage gravel was limestone gravel, with sizes between 4 mm and 12 mm (Woods Ballard et al. 2015). The layer was tested with two thicknesses as an individual layer, 70 and 140 mm. Both thicknesses were selected considering depth limitations on the test bench. The first was the highest possible depth for the complete layout, and the second was selected considering the minimum recommended depth for pedestrian areas (Weiss et al. 2019; Woods Ballard et al. 2015; Smith and Hein 2013). Those layers were named *STOR70* and *STOR140*. Gravel was compacted in place by hand. Void ratios were measured the same way as smaller gravel but using a 500 ml bucket instead. The measured porosities were equal to the ones obtained for the small gravel.

In addition to the examined material, plastic cells and a mosquito mesh were used in the individual layer configuration. The plastic cells, provided by Atlantis, were 52 mm thick and had a porosity of 90%. The cells were placed on cross-sections *PAind* and *PIPind*, as well as on the SOIL layout, as shown in Figure 4.3. The mosquito mesh was located on the *PIPind* configuration, below the pavers, and above the plastic cells. The cells allowed fast water flow and minimized the influence on the outflow. The mesh prevented material loss from the PIP joints to the cell holes below.

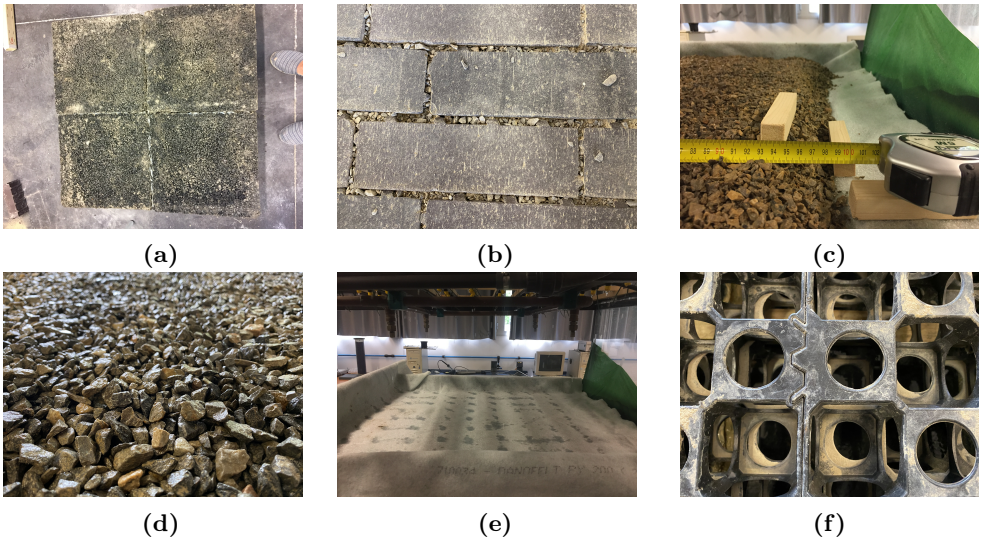

Figure 4.4: Tested materials (a) PA, (b) PIPs with filled voids, (c) gravel 2/6 mm, (d) gravel 4/12 mm, (e) geotextile, and (f) plastic cells.

4.2.4 Experimental procedure

The experimental procedure consisted of applying three precipitation regimes for 15 minutes to the selected cross-sections given in Figure 4.3 under three defined slopes (Hou et al. 2019; Woods Ballard et al. 2015; Alonso López 2010): 1%, 2%, and 6%. Those three slopes are pavement and cross-section slopes simultaneously, as layout depth is constant. Under those configurations, outflow from the cross-sections was measured for 30 minutes. The experiments were replicated three times for each configuration. As each layout had nine configurations, a total of 189 hydrographs were measured.

The outflow was measured in the buckets at the circuit's end. In order to correctly capture the beginning and end of the hydrographs, considered time intervals were not constant. Thus, these are interval ending points: 1:00, 1:30, 2:00, 2:30, 3:00, 3:30, 4:00, 4:30, 5:00, 5:30, 6:00, 7:00, 8:00, 9:00, 11:00, 13:00, 15:00, 15:30, 16:00, 16:30, 17:00, 17:30, 18:00, 19:00, 20:00, 22:00, 25:00, and 30:00. Hence, the considered flows will be the average flow of those intervals, referred to mid-point of the interval. Consequently, measured hydrographs had 28 flow points. Previously calibrated rotameters were used to control inflow visually and set it to the theoretical *low/high/extreme* value. Applied real

inflow in each experiment was calculated with the display value given by the flowmeter, which was, once placed on the test bench, also previously calibrated.

A standard systematic wetting process was designed for all experiments. The process involved a steady rain for 5 minutes followed by a dry interval of 5 minutes. After those initial 10 minutes, the principal experiment was conducted. The process has been graphically described in Figure 4.5, setting the beginning of the experimental hydrograph as the initial time.

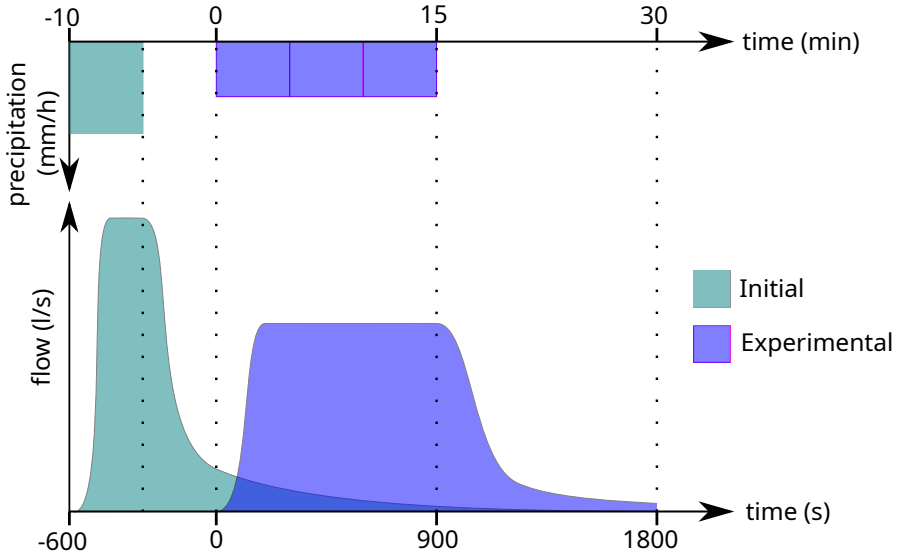

Figure 4.5: A diagram with the experimental procedure, with analysed experimental precipitation/hydrograph in blue and initial wetting rain/hydrograph in green.

The recession curve of the wetting process was first deduced to discriminate the effect of the initial wetting process on the experimental hydrograph (Tallaksen 1995), depicted as the overlapping hydrograph surfaces in Figure 4.5. The exponential method was selected for that purpose (Sujono, Shikasho, and Hiramatsu 2004), and Equation (4.1) was used to define the recession curve, where Q_0 is the flow at the beginning of the recession curve, α is a constant related to section characteristics, and t is the time from the beginning of the recession curve. The higher the α, the faster the outflow from the section.

$$Q_t = Q_0 \cdot e^{-\alpha \cdot t} \tag{4.1}$$

The selected rain intensity for the wetting process was 140 mm/h, as it provided the highest flow value for the recession curve and, consequently, the lowest error, which increased with decreasing flows. Therefore, the recession curve of the wetting process was calculated based on linear regression with Equation 4.1. Then, laboratory data were calculated as the difference between the measured hydrographs and wetting process hydrographs.

This procedure accepts that the grains are not completely dry initially. Given the number of planned tests and their duration, the time required to ensure a completely dry section would be unaffordable. On the contrary, the created wetting condition aims to ensure an equivalent initial condition for all tests. The wetting process's impact on the results will be discussed later.

4.2.5 Experimental hydrograph characterisation

Several parameters were calculated to characterise the hydraulic performance of studied cross sections, defined below (Rodriguez-Hernandez et al. 2016; Palla et al. 2014). The first two are typical parameters used to characterise the hydrologic performance of PPs. The late two provide additional information regarding retention capacity.

(a) Outflow Peak (OP), as the maximum outflow peak measured at the outlet;

(b) Time to Peak (TP), as the time elapsed from the beginning of rainfall to outflow peak;

(c) Timing Indexes (T_{50} and T_{80}), the time to a certain cumulative discharge, as percent, of inflow or precipitation.

4.2.6 Modelling data

This section will describe, firstly, (4.2.6) the model used to simulate the hydrographs obtained in the laboratory, (4.2.6) how that model has been set up to create artificial hydrographs, and, last, (4.2.6) selected criteria to analyse model performance and perform the calibration process. The methodology followed to simulate, calibrate and compare modelling data is summarised in Figure 4.6.

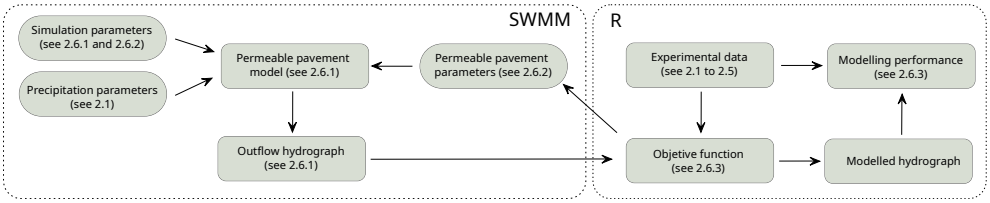

Figure 4.6: Flowchart describing the methodology followed to obtain modelling results. On the left data managed with SWMM and, on the right, data managed with R.

Storm Water Management Model

SWMM is a dynamic rainfall-runoff simulation model used for a single event or long-term (continuous) simulation of runoff quantity and quality from primarily urban areas (Rossman and Huber 2015). Since its origin, SWMM has implemented several SUDS, named LID controls in the model, the permeable pavement being one of them. PP is defined as a combination of several layers: Surface, Pavement, Soil, Storage, and Drain. Two of those layers are optional, Soil and Drain layer.

During the selected simulation time and applying the specified time steps, SWMM performs a moisture balance between layers. It keeps track of water transfers and determines how PP transforms inflow hydrographs into a runoff, sub-surface storage, sub-surface drainage, or infiltration into the native soil. Details about the used equations are given in Rossman and Huber (2016). In addition, Madrazo-Uribeetxebarria et al. (2022) and Madrazo-Uribeetxebarria et al. (2021) provide a more detailed description of the PP modelling process.

Defined PP may have two inflows, precipitation, and inflow from another area, which can be another subcatchment of another area from the subcatchment where PP is implemented. This study will just consider precipitation inflow. On the other hand, there may be three outflows from the layout: runoff, infiltration to native soil (seepage), or outflow from the drain. This study places the layout over an impermeable membrane, so infiltration to native soil will not be considered. Also, as initial tests confirmed, no runoff was created. Thus, the runoff will not be considered. Although evaporation is an outflow from the system, being a short-term analysis, it will not be considered either.

The PP can be implemented into a subcatchment, but there is another option, a subcatchment can be fully occupied by the LID control. For this study, a subcatchment fully occupied by PP has been considered. The 28 input parameters used by the model to perform the moisture balance are given in

Table 4.1. As mentioned in the introduction, pavement clogging and drain control parameters were not considered.

Model setup

Six LID controls were defined in the model to simulate the hydrographs obtained in the laboratory, matching the ones shown in Figure 4.3: four to check an individual layer and two with the complete cross-section. All LID controls were of the PP type. The parameters used to define each one are shown in Table 4.1.

The table parameters were given a known value when it was physically measured. When the values were not quantified, a calibration process was carried out, which will be detailed later. Those calibrated values are shown with the symbol * in the table. For calibration purposes, individual layers were used, and obtained values were applied to the complete cross-sections.

The LID controls had all a surface of 1 m^2 and were considered a subcatchment entirely occupied by a LID control of PP type. The outfall from the subcatchment was directed to a couple of nodes. The first one, *Runoff*, collected surface runoff, and the second one, *Drain*, collected outfall infiltrated from the permeable surface that percolated through the section. There are two additional nodes, *Junction* and *Outfall*, which were only created to provide an outlet for the water collected by the other two nodes. The *RainGauge* object provided the precipitation for the *PPsurface* subcatchment.

The selected time step for computing purposes was 1 second for both Wet Weather and Dry Weather. All the hydrograph values used to analyse the model performance were collected from the *Drain* element, where inflows to that element were stored. In order to compare experimental data with modelling data, gathered hydrographs were transformed into a 28-point hydrograph, with measuring points equal to that measured in the laboratory, and described in Section 4.2.4.

Model performance and calibration

The Nash-Sutcliffe adimensional coefficient (NSE) was selected to compare modelled hydrographs with experimental ones (Nash and Sutcliffe 1970). The NSE values are given in Equation (4.2), where O_i and $\overline{O}_i$ are experimental values and M_i are modelled ones. NSE values range from $-\infty$ to 1, where a value equal to 1 indicates a perfect fit.

Table 4.1: SWMM parameters for the PP type of LID control.

		INDIVIDUAL				COMPLETE	
LAYER / Parameter	*Units*	*STOR70/140*	*SOIL*	*PAind*	*PIPind*	*PAcom*	*PIPcom*
SURFACE							
Berm Height , D_1	mm	0	0	0	0	0	0
Veget. Vol. Frac. , $1-\phi_1$	-	0	0	0	0	0	0
Roughness , n	$s \cdot m^{-1/3}$	0.02	0.02	0.017*	0.016*	0.017	0.016
Slope , S	%	1-2-6	1-2-6	1-2-6	1-2-6	1-2-6	1-2-6
PAVEMENT							
Thickness , D_4	mm	0.01	0.01	93	80	93	80
Void Ratio , $\phi_4/(1-\phi_4)$	Voids/Solids	0.99	0.99	0.25	0.97	0.25	0.97
Imperv. Surf. Frac. , F_4	-	0	0	0	0.9	0	0.9
Permeability , K_4	mm/h	100000	100000	250000	90000	250000	90000
Clogging Factor , -	-	0	0	0	0	0	0
Regen. Interval , -	days	0	0	0	0	0	0
Regen. Fraction , -	-	0	0	0	0	0	0
SOIL							
Thickness , D_2	mm	0	38	0	0	0	0
Porosity , ϕ_2	vol. frac.	-	0.44	-	-	-	-
Field Capacity , θ_{fc}	vol. frac.	-	0.09*	-	-	-	-
Wilting Point , θ_{wp}	vol. frac.	-	0.03	-	-	-	-
Conductivity , K_{2S}	mm/h	-	100000*	-	-	-	-
Cond. Slope , HCO	-	-	40	-	-	-	-
Suction Head , ψ_2	mm	-	80	-	-	-	-
STORAGE							
Thickness , D_3	mm	77-159	144	144	144	85	85
Void Ratio , $\phi_3/(1-\phi_3)$	Voids/Solids	0.82	0.99	0.99	0.99	0.82	0.82
Seepage Rate , K_{3S}	mm/h	0	0	0	0	0	0
Clogging Factor , -	-	0	0	0	0	0	0
DRAIN							
Flow Coefficient , C_{3D}	-	8* - 7*	600*	18*	4*	7.5	7.5
Flow Exponent , K_{3D}	-	1.6*-1.6*	0.2*	1.6*	1.5*	1.6	1.6
Offset , D_{3D}	mm	0	0	0	0	0	0
Open Level , -	mm	-	-	-	-	-	-
Closed Level , -	mm	-	-	-	-	-	-
Control Curve , -	-	-	-	-	-	-	-

*: values obtained after calibration process.

Table 4.2: Maximum, minimum and initial parameter values for calibration purposes.

Parameter	Units	minimum	maximum	initial value
Roughness (n)	$s \cdot m^{-1/3}$	0.01	0.02	0.015
Field Capacity (θ_{fc})	vol. frac.	0.06	0.2	0.1
Conductivity (K_{2S})	mm/h	0	100 000	500
Flow Coefficient (C_{3D})	-	0	1000	5
Flow Exponent (K_{3D})	-	0	100	1

$$NSE = 1 - \frac{\sum_{i=1}^{N}(O_i - M_i)^2}{\sum_{i=1}^{N}(O_i - \overline{O}_i)^2} \tag{4.2}$$

As part of the model parameters were physically measured, individual cross sections were considered a source for unmeasured data (see Table 4.1). A calibration process was carried out to set those unmeasured parameters. Once individual layer calibration was conducted, those values were introduced in the complete cross-sections to check the model performance.

However, as the soil layer had several unmeasured parameters which should be calibrated, just conductivity and field capacity were allowed to vary during calibration. The remaining unmeasured soil parameters, wilting point, conductivity slope, and suction head, were fixed to a value obtained from the SWMM manual based on a previously conducted sensitivity analysis (Madrazo-Uribeetxebarria et al. 2021). Considered parameter ranges for the calibration process are given in Table 4.2.

Differential Evolution Algorithm (DEA) was used for calibration purposes, which is particularly convenient for finding the global optimum of a real-valued function of a real-valued parameter and not requiring a continuous or differentiable function (Mullen et al. 2011). Calibrated values were obtained with the differential evolution algorithm provided by the *DEoptim* package for the *R* programming language (R Core Team 2023). The selected objective function for calibration purposes was previously defined in Equation (4.2). Calibration for all hydrographs of the same layout was conducted once. Thus, the objective function was $\sum_{i=1}^{i=9} NSE_i$.

In order to compare modelled results with laboratory tests, both Peak and Volume errors were also analysed (Huang et al. 2016), named Pe and Ve:

$$error \quad (\%) = \frac{X_{model} - X_{experimental}}{X_{experimental}} \cdot 100 \tag{4.3}$$

4.3 Results

To provide an analysis of the experimental hydrographs and compare them with the ones provided by the model, experimental hydrographs are presented first (Section 4.3.1), and model performance later (Section 4.3.2).

4.3.1 Experimental data

No runoff was observed at any experimental setup or layout. Nevertheless, slight water losses were observed due to raindrop splashes, which went out of the bench after contacting the surface. This phenomenon has mainly been observed with PIPs.

Recession curve

Calculated recession curves were 21, all for the 140 mm/h rainfall used in the initial wetting process, one for each cross-section and slope. Measured curve (MEA), used as a baseline, and extrapolated recession curves (REC), using Equation (4.1), are given in Figure 4.7. Note that the time axis starts at 1200 seconds in that figure, as explained by the procedure detailed in Figure 4.5. Data shows that, generally, the recession curve tends to be lower than measured at the beginning of the extrapolation.

Outflow hydrographs (laboratory or LAB) were calculated based on deduced curves, detracting recession values (REC) from measured ones (MEA). Deduced LAB curves, to be used from now on, together with measured and recession curves, are shown in Figure 4.8. Only hydrographs related to PAcom layout are shown to simplify the image. Initial flow values are close to zero in all cases.

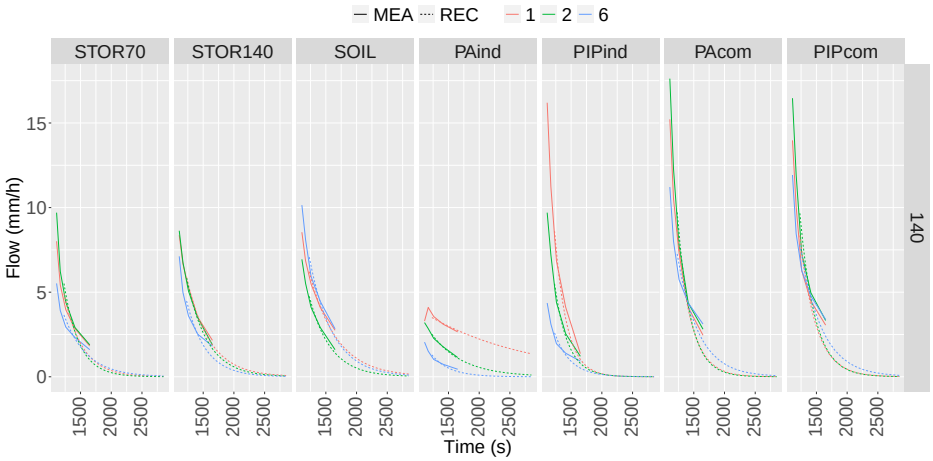

Figure 4.7: Recession curve baselines (continuous line, named MEA) and extrapolated ones (dotted lines, named REC) for 140 rain, different colours are shown for each slope.

Laboratory hydrographs

Regarding laboratory hydrographs, the ones being analysed hereafter, Figure 4.9 shows differences between layouts. Only PIP-related hydrographs were plotted in this case. Visual analysis shows that the peak is reached earlier for thinner layers. It also can be noticed that the storage layer reaches the peak slower than the other two single layers, soil and PIPind. In addition, the delay of the peak results in higher outflows during the last half of the experiment.

Figure 4.10 is provided for detailed peak analysis, showing all considered cases. Higher rain intensities create higher peaks. Also, thicker layouts create higher peaks, in general. It is not the case for the soil layer, which shows similar peaks in the thinnest storage layer. Although higher slopes provide greater peaks as a general rule, there are some cases where the highest peak does not correspond to the highest slope. On the surface layer, results also show a higher peak for PIPind than for PAind.

Detailed time-to-peak values are given in Figure 4.11. It can be observed that the thicker the section, the higher the time to the peak. However, PAind indices are clearly lower than soil ones. Also, higher rains result in faster peaks. For complete layouts and small rains, the maximum peaks are around 900 seconds, close to the end of the rainfall. It also can be noted that higher slopes yield a

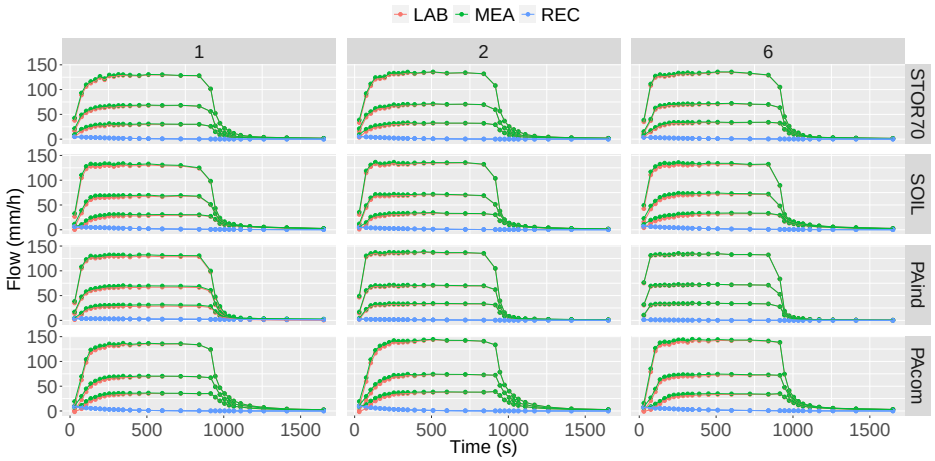

Figure 4.8: Measured hydrographs (green), recession curves (blue), and laboratory hydrographs (red) deduced from the first two. Only PA related layouts are shown, separated for different slopes (columns) and layouts (rows).

lower time to peak, in general, although complete layouts do not follow that pattern.

Concerning the time indices obtained, given in Figure 4.12, lower precipitation intensities result in higher time indices. On the contrary, the slope influence on time indexes needs to be clarified. The case with a different pattern is the soil layer, where 6% time indexes are higher than 2%. A thicker section yields a higher time index for analysed cross-sections, but some exceptions exist. PAind and PIPind are superficial layers, but both time indices differ, as PIPind shows higher indices than PAind. Also, although the soil layer is the thinnest, its time indices are higher than PIPind or PAind, even higher than the STOR140 layout for low rains.

4.3.2 Model performance

Individual layers are presented separately, as their hydrographs were used to calibrate unmeasured parameters from the model. Hence, complete layouts will be presented later using calibrated parameters obtained in the first section.

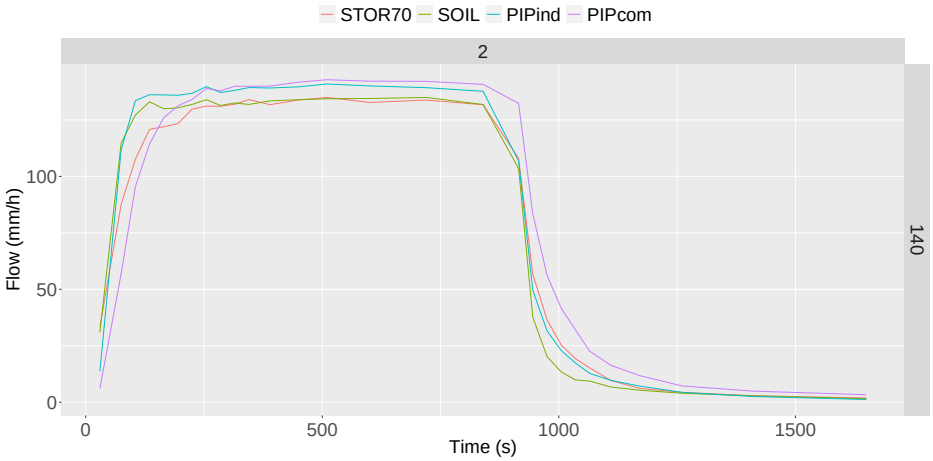

Figure 4.9: Outflow from PIP related layouts for 140 rain and 2% slope, with different colours for each layout.

Table 4.3: NSE values for a layer-by-layer calibration.

Layer	STOR70/140	Soil	PAind	PIPind
Minimum NSE	0.832	−2.130	0.845	0.867
Average NSE	0.968	−0.851	0.959	0.954
Maximum NSE	0.993	0.153	0.991	0.988

Hydrographs by layer

The parameter values obtained from individual layer hydrographs after calibration are given in Table 4.1, together with the physically measured parameter values used during calibration. The NSE values corresponding to the calibration process are given in Table 4.3. Analysed by layer, the soil layer values are notably worse than other individual layers.

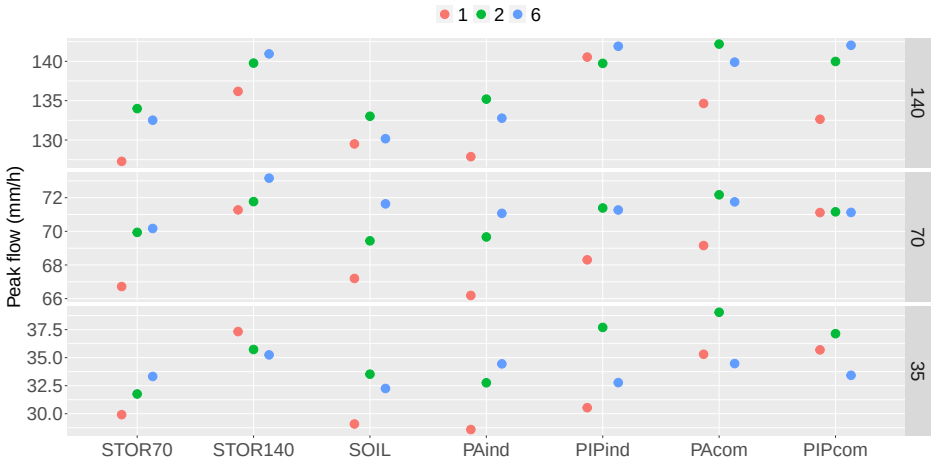

Figure 4.10: Peak values from experimental cross-sections. Different colours and shapes are given for rain and slope cases.

Hydrographs for complete layouts

Complete hydrographs were calculated using the parameter values calibrated in the previous section (see Table 4.1). The hydrographs were calculated without considering any soil layer in the model, as individual layer results showed an unsatisfactory output. NSE results comparing laboratory and modelled hydrographs are given in Figure 4.13. The minimum value is 0.74, which can be considered good. PAcom yields slightly better results than the PIPcom layout.

Calculated Peak and Volume errors for modelled hydrographs are given in Figure 4.14. Almost all errors are positive; thus, modelled hydrographs overestimate the volume and peak. Errors are higher for lower slopes. Average Pe and Ve are 3.2 % and 2.8 %. Both maximums are smaller than 8 %, and both minimums are close to 0 %.

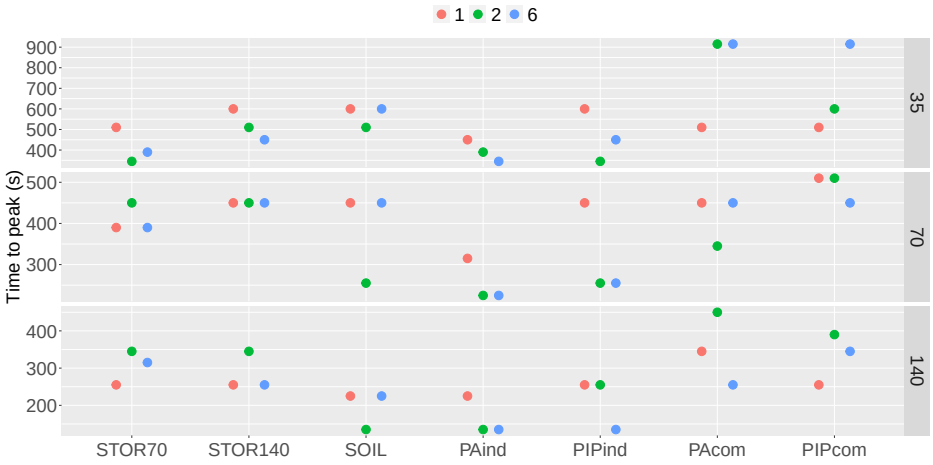

Figure 4.11: Time to peak values from experimental cross-sections. Different colours and shapes are given for rain and slope cases.

4.4 Discussion

4.4.1 Experimental data

The lack of runoff is consistent with other laboratory studies for PPs (Palla et al. 2014) but is also in line with previous site experiments performed with PP systems (Støvring et al. 2018; Bean, Hunt, and Bidelspach 2007; Brattebo and Booth 2003). This shows how effectively the new PP reduces runoff, especially for short individual events.

Higher raindrop splashes on PIPs are due to their horizontal surface. As PA and gravel provide irregular surfaces, they tend to split the raindrop, and the observed water loss was minimal. This phenomenon shall directly affect the level of comfort perceived by users if PIPs and PA are compared. In any case, losses have been considered negligible compared to measured water flows and volumes.

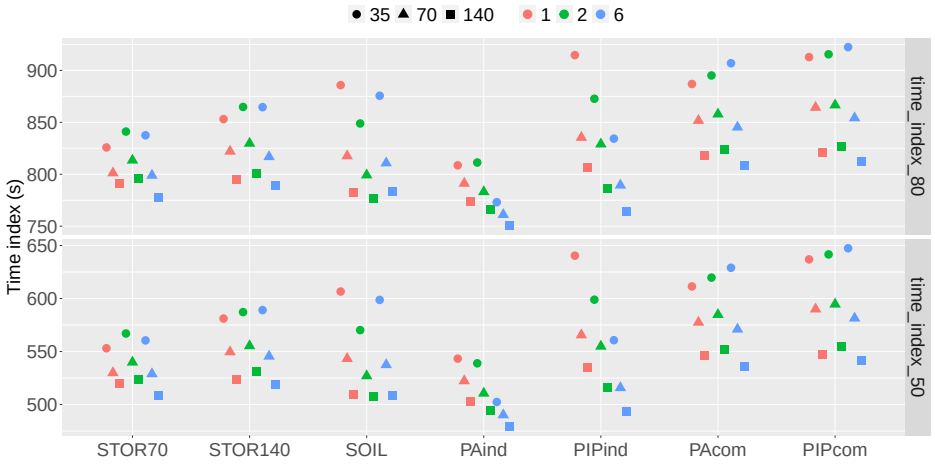

Figure 4.12: Calculated time index values, T_{50} and T_{80}, for outflow hydrographs on experimental cross-sections. Different shapes are given for rain cases and different colours for slope cases.

Recession curve

The visual analysis of Figure 4.7 clearly shows that extrapolation considers lower flow rates than measured data in most cases. Nevertheless, obtained values were considered acceptable for calculating the impact of the initial wetting process during the last 1200 seconds of the experiment, as those recession flows were considerably lower than measured flows.

Although constant rain was applied during the experiment, and a constant outflow may be expected, a slightly decreasing flow tendency was noticed once the peak value was reached. However, that decreasing tendency was corrected after the recession curve values were detracted from measured ones. In particular, the obtained initial flow values were close to zero once recession values were detracted, showing that the flow measured during the first minute for those cases was mainly due to the initial wetting process. It also shows that the impact of the wetting process on the outflow was minimal.

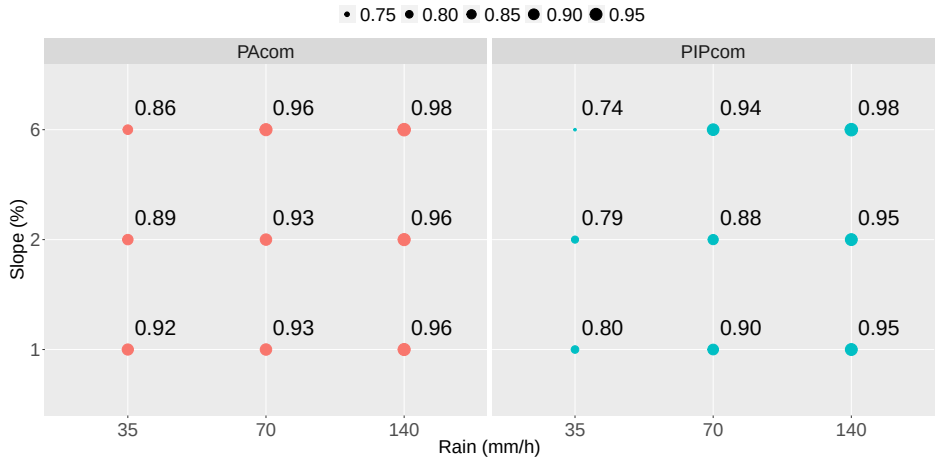

Figure 4.13: Obtained NSE values given as point size for complete layouts, PAcom (red) and PIPcom (blue), with separated values for different rain and slope combination.

Laboratory hydrographs

The first visual analysis from Figure 4.9 may be considered consistent, as increasing layer thickness increases water retention. In that case, the time to peak and outflow are higher once the rain has stopped, which makes sense from a water balance perspective.

According to peak values shown in Figure 4.10, higher slopes provide greater peaks than lower ones because the detention process is less significant in steeper slopes, as water is easier drained by gravity. Regarding the impact of depth, showing greater peaks for thicker layers differ from what initially may be expected. This effect is noticeable for two storage layers with different depths (STOR70 and STOR140). It may be expected that thicker layers delay outflow and reduce peak flow. An explanation may be that water can travel a longer path for thicker layers and, hence, more interstitial particle surface contributes to the outflow. Therefore, the peak is delayed but with a higher value. In addition, depths are not high enough to delay the beginning of the peak over rain duration, which contributes to the mentioned behaviour.

If time to peak is analysed, see Figure 4.11, thicker cross-sections yield higher times to the peak, as may be expected. Thus, more time is needed for water to flow through the entire layout. However, individual superficial layers and individual storage layers respond differently. As storage layers are on the bottom,

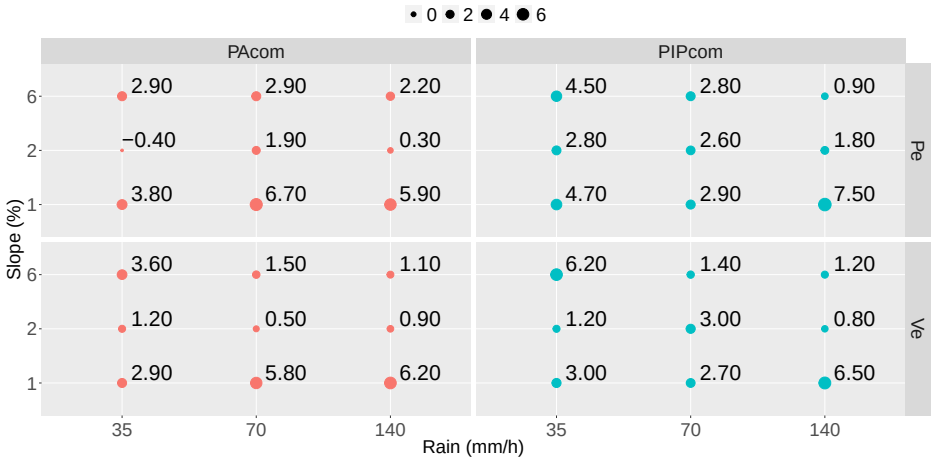

Figure 4.14: Peak (Pe) and Volume (Ve) error for modelled hydrographs with complete layouts, PAcom (left) and PIPcom (right), size is proportional to error value.

water flow is parallel to it and travels through the gravel section horizontally. Therefore, water needs more time to reach the exit; that is, the time to peak is greater. As complete layers also have the gravel layer beneath, they perform similarly. On the contrary, water flows freely over the membrane for superficial layers tested individually. Regarding the impact of rain intensity, higher rains result in faster peaks, probably because the section saturates faster and, thus, drains water out of the layout faster.

For complete layouts and small rains, the maximum peaks are around 900 seconds, close to the end of the rainfall, suggesting that the layout may still reach saturation. However, plotted hydrographs, such as the ones in Figure 4.9, show that hydrograph slopes tend to be horizontal around 900 seconds, confirming layout has almost saturated completely.

About the time indices given in Figure 4.12, it is clear that higher time indices for lower precipitation intensities suggest that the retention capacity of the pavement decreases as precipitation increases, as higher intensities indicate a higher precipitation volume. Concerning the slope influence on time indices, one might initially assume that the higher the slope, the lower the time index, as water is drained faster and the detention capacity of the section is reduced. That pattern is apparent for superficial PAind and PIPind layers. However, there is a discrepancy with the 1% slope in many other cases, as the time index is lower than that for higher slopes. That is the case for storage layers and

most of the complete section values. A possible explanation for the soil layer behaviour, with a different pattern, may rely on the geotextile. The horizontal permeability of the geotextile may be altered for sloping positions. Also, a capillary barrier effect could affect differently for different section slopes to the vertical permeability of the geotextile.

In superficial layers, PIPind shows higher indexes than PAind, which the porosity-related properties of the sections may explain. Regarding the porosity distribution, PA has a uniform porosity, facilitating water infiltration as it reaches the surface. On the contrary, water over PIPs has to reach joints to infiltrate. On the other hand, PA's overall porosity is higher than the porosity of the PIP. These two porosity-related characteristics may well explain the difference. Also, although the soil layer is the thinnest, its time indices are higher than PIPind or PAind, even higher than the 140 mm storage layer for low rains. This discordance may be due to the geotextile layer below the soil, which may influence the detention capacity of all the layers. In any case, the retention capacity performance is opposed to that found by Støvring et al. (2018).

It should be noted that the experimental procedure may reduce the peak time compared to a dry layout, as first water does not adhere to material grains. The procedure may also reduce obtained time indexes compared to a completely dry section. Nevertheless, the procedure should not impact the peak value reached after the section is saturated. The values obtained here may be valid, as natural sections may often be wet in an Atlantic climate where rain is 180 days per year.

4.4.2 Model performance

Hydrographs by layer

Overall, average NSE values for individual layers show, see Table 4.3, that the model gives a very good response if physical parameters of the pavement are introduced and some unmeasured parameters are calibrated. Those unmeasured parameters were drain coefficient, exponent, and Manning n for pavements. This last parameter value obtained by calibration was close to those given by bibliographic references. On the contrary, drain parameters could not be obtained from bibliographic sources, as they have no physical meaning.

Except for the soil layer, the minimum NSE value is over 0.80, which can be considered a good prediction. However, the soil layer values are significantly

poorer. For this layer, both experimental and modelled hydrographs are given in Figure 4.15. It can be appreciated that it is difficult to capture the experimental hydrograph's initial flow for all analysed slopes and rain intensities. The model cannot reproduce initial outflow, although the performance improves for higher rain intensities.

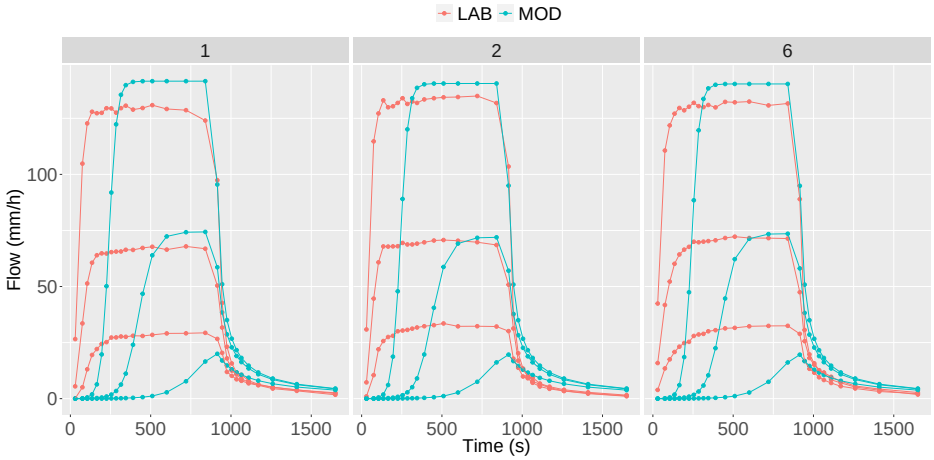

Figure 4.15: Experimentally measured hydrographs (red) and modelled ones (blue) for individual soil layer. Different slopes are given in columns. Average NSE is −0.851.

The above may be related to the fact that the soil layer was conceived as engineered for bio-retention cells, where infiltration from the upper pavement layer is modelled based on the Green-Ampt equation (Rossman and Huber 2016). As open-graded aggregates tend to drain more water by gravity than soils with smaller particles (Støvring et al. 2018), this approach is not the most suitable for modelling gravel-type layers, even with a geotextile beneath. In that sense, the soil layer may be expected to represent the geotextile effect on the flow, but the results show the opposite.

Hydrographs for complete layouts

All modelled hydrographs showed good agreement, with an average NSE of 0.907, higher for PAcom (0.931) than for PIPcom (0.882). However, PIPcom under 35 rain and 6% slope present a minimum value of 0.74. All hydrographs are given in Figure 4.16. The average value is higher than the one obtained by Platz, Simon, and Tryby (2020) after calibrating and validating on-site data; the average NSE was 0.74. Hydrographs predicted by a single controlled event

may be expected to fit better with measured ones and get better predictions. However, Platz, Simon, and Tryby (2020) calibrated all parameters, and this study did not.

Overall, the model predicts a higher flow than the measured one. That discrepancy is more significant at the hydrographs' beginning and end, although it can also be observed at the peak values. The difference is higher for lower rain intensities and low slopes. That difference causes an advance in drained volume. It seems related to the drain coefficient and exponent used for modelling. As those two parameters do not have an actual physical meaning in the experiment, calibrated parameters for a single storage layer were used. Hence, as the single-layer outflow is faster than the complete-layer outflow (see Figure 4.9), drain parameters advance outflow for the complete layout, which may be reduced if those two parameters were calibrated for a complete layout.

However, modelled hydrographs also show a flow value during the first measured minute, while laboratory hydrographs have almost no flow during the first minute. A faster experimental outflow may be expected due to the initial wetting process, but the results show the contrary. That model behaviour probably does not consider the initial water that covers material grains, delaying initial flow. Moreover, the first initial wetting process may forward experimental flow.

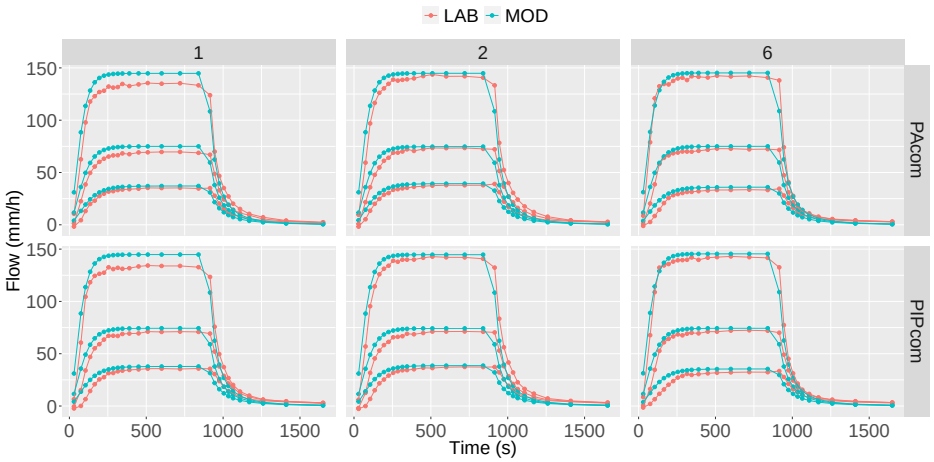

Figure 4.16: Experimental (red) and modelled (blue) hydrographs for complete layouts. Different sections are given in rows and slopes in columns.

Modelling hydrographs overestimating experimental ones, given in Figure 4.14, is probably related to the two reasons mentioned above, higher drain coefficient and exponent, and a faster flow, leading to overestimating the volume and the peak. However, errors may be considered reasonably low.

4.4.3 Research limitations and uncertainty

Although the authors consider that the results here presented are interesting and potentially useful for practitioners involved in the hydrologic design of PPs, the methodology proposed in this research presents certain limitations to be considered related to (a) the test bench dimensions, which are much smaller than real applications; (b) the materials selected for the surface, which are limited to new unclogged pavements; (c) the material selected for the base layer; (d) the methodological aspect, such as applied uniform rain or selected wetting process; (e) the systematic errors generated during the measurement process, as flow starting/stopping time; (f) the human errors made during the experimental process; and, (g) the assumptions made during the research process, such as neglecting water losses that took place during experiments.

4.5 Conclusion

The main contribution of this study is to explore the deficiencies of a highly used conceptual model by detailing how each of the individual layers contributes to the complete layout performance, which is a novel contribution to the literature. Based on layer-by-layer experimental data, the research first analysed how rain intensity and slope influenced the outflow from two types of permeable pavements: PIPs and PA. Later, it analyses the hydrological performance of those pavements when modelled with one of the most popular urban drainage models, the Storm Water Management Model.

Experimental results confirm, in line with previous studies, that PP systems are an excellent option to delay runoff response in urban environments, as they provide a higher detention capacity than traditional pavements. Results also reveal that the detention capacity of the superficial PIPind layer is notably higher than that provided by PAind, which is probably related to its pore distribution, although peak values are higher for the PIPind layer. Also, it was found that detention capacity increases for low rain volumes and lower slopes. However, the influence of a sloping geotextile remains uncertain, and further research is recommended.

On the other hand, modelling results show that the model performance is generally quite good without considering the base and subbase layers as one, with a geotextile between them. However, the model forwards the flow if compared to the experimental one. Besides, drain outflow modelling based on orifice parameters makes it difficult to set drainage coefficient and exponent for cases that do not match mentioned physical orifice-type drains. The latter induces a faster initial outflow for modelled hydrographs. The study also found that calibrated Manning values were close to those given by bibliographic references. In any case, further study of the drainage outflow model is advisable to understand how its parameters can condition the outflow. It also would be interesting to deepen the study of long-term performance under laboratory conditions.

Another interesting finding in the modelling part relates to the optional soil layer given in the model. That layer definition was not valid for gravel-type base layers. Its hydraulic behaviour does not match a soil-type layer defined using the Green-Ampt equation, even with a geotextile below. Thus, those layers, including the geotextile, shall be modelled along with the storage layer. For a better understanding of the model, it would be interesting to study how sandy soils may perform, on the one hand, and how the geotextile layer may be modelled in order to capture its hydraulic properties better.

In summary, the two main contributions of this article are to explain in detail the performance of each layer contained in a PP system and the validation of modelling results for the complete layout without calibration. The first one shall be useful for researchers and practitioners to understand each layer's influence better, both for design and modelling purposes. The second one shall increment designers' confidence in the modelling results when the complete layout can not be calibrated. In short, the results obtained in this study are expected to increase practitioners' confidence while integrating a PP model into an urban subcatchment based on physical parameters that can be easily measured or predicted, but also where it is unfeasible to calibrate the PP model.

Chapter 5

Discussion

This chapter discusses the results obtained in the previous three chapters: model sensitivity analysis, model comparison, and experimental analysis. The chapter also integrates some preliminary results from the experimental plot in Txominenea. These preliminary results, presented at several congresses, were mentioned in the initial Research Outputs section and Figure 1.2, and are provided as appendices at the end of the document.

5.1 Model analysis with numerical experiments

The main objective of the numerical experiments was to facilitate the model implementation deepening its understanding. Designed experiments, sensitivity analysis, and a comparison with a well-known model proved to be a practical methodology for exploring the model. The first was valuable in detecting the most critical parameters to focus on, and the second was effective as a baseline to compare the results provided by the PP model.

Results showed how effective PPs are for reducing runoff from urban surfaces to the stormwater network. In particular, sensitivity analysis, with 164 000 simulations over different setups, only produced runoff in 0.9% of the cases. The lack of runoff is mainly due to the high pavement permeability, higher

than the precipitation intensity for most simulated cases, representing realistic conditions over a wide range of precipitation.

Although the number of parameters present in the PP model from the Storm Water Management Model (SWMM) is relatively high, a total of 20, Sensitivity Analysis (SA) provided a clearer vision of how those parameters influence the outflow from a PP section. The analysis showed that roughness, a parameter from the superficial layer, has little influence on the outflow. This finding may be helpful during the PP model definition, as roughness is challenging to estimate.

On the second layer defined by the model, pavement, no negligible parameter was identified by the SA. Although pavement permeability was not the most influential parameter, the analysis showed that it could be considered the critical parameter to link the PP model from SWMM with the Curve Number (CN) model, as it is easily comparable with rain intensity. That was the reason for selecting it.

In that regard, the comparison of the model with the CN method shows that pavement permeabilities higher than 80 mm/h correspond to CNs lower than 40, which are in line with those for pervious areas or greenfield sites. Hence, PPs may be considered a very effective technique to reduce surface runoff in urban areas since pavement permeability values are considerably higher than 80 mm/h, even for partially clogged pavements.

The model comparison also showed that runoff created with the PP model is very different from the one created with the CN model, at least when the pavement permeability parameter controls the runoff from the PP model. Infiltration capacity is identified as the most significant difference. For the PP model, infiltration capacity corresponds to all precipitation volume for those cases when the rain intensity is lower than pavement permeability. This evidence confirms, again, PP's effectiveness.

The third layer of the PP model, soil, is probably the most unknown layer for practitioners, as its definition or parameters are related to soils and are not easy to measure. In addition, it is the layer containing the most significant number of parameters, a total of seven. The SA showed that this layer contains one of the most influential parameters, soil thickness, although three other parameters may be neglected.

According to the SA, the seepage rate was the most influential parameter in the storage layer. In particular, the seepage rate is a source of significant uncertainty in PPs, as its value often approximates existing conditions, which may

vary along the site. This evidence conditioned the design of the experimental site, as it was waterproofed to avoid any seepage into the natural soil.

A comparison of complete layouts with the CN method also shows that inflow to the complete section can be controlled by pavement permeability. When those permeability values are below 10 mm/h, pavement performance is over that characterised by the $CN = 86$. This value shows how vital PP maintenance is to keep PP's initial performance, as clogged PPs' performance will be close to impervious surfaces.

Finally, the relation between PP and CN models showed that it is possible to create equivalent runoff hydrographs with the PP model to those created with the CN model, but that equivalency is only acceptable for high CN values or impervious surfaces. Although that equivalency may be seen as unpractical for being only valid for high CN values, it is, in fact, a precious reference for comparing several scenarios with the same model in SWMM, actually the PP model. Those scenarios are settings with and without PP. If that link were undetermined, it would be challenging to establish an impervious scenario with the PP model and even more to relate its runoff with any known reference.

5.2 PP performance with experimental results

The experimental tests' main objective was to better understand the hydraulic performance of PPs and their materials. Not only globally but also on a layer basis, as that is the base for the conceptual SWMM model here analysed. The tested materials correspond to those implemented in the experimental Txominenea plot, facilitating the interpretation of the experimental site still to come.

The experimental part, with several layer configurations, produced no visible runoff, which is consistent with data reported in the literature. Hence, experimental results also confirmed the effectiveness of PPs for reducing runoff, especially for short individual events.

Although not intended to explore, raindrop splashes were detected during the experimental part, lower in asphalt than pavers. This side effect is probably explained by the irregular surfaces on the asphalt, which tends to split the raindrop and minimise the water splash. This phenomenon shall directly affect the level of comfort perceived by users if pavers and asphalt are compared.

Many findings related to the experimental part are related to the water retention capacity of PPs, an essential factor regarding SUDS performance. As may be expected, lower slopes provide lower peaks than higher ones because the detention process is more significant in gentle slopes, as water is harder drained by gravity. On the contrary, thicker layers provide greater peaks, which differs from what initially may be expected. An explanation may be that water can travel a longer path for thicker layers and, hence, more interstitial particle surface contributes to the outflow. Higher time indices for lower precipitation intensities also suggest that the retention capacity of the pavement decreases as precipitation increases.

On the other hand, experiments facilitated the identification of different layer responses to rain. Individual superficial and storage layers respond differently if the time to peak is analysed. As storage layers are on the bottom, water flow is parallel to it and travels through the gravel section horizontally. Therefore, water needs more time to reach the exit; that is, the time to peak is greater. This performance also affects complete layouts, as gravel is located below on the water path. Experimental results were also valuable in finding that the retention capacity of pavers as a superficial layer is better than asphalt.

It was also found that there is a discrepancy in the retention capacity for some cases, as the time index is lower than that for higher slopes. A possible explanation may rely on the geotextile. The horizontal permeability of the geotextile may be altered for sloping positions. Also, a capillary barrier effect could act differently on the vertical permeability of the geotextile depending on the slope.

Concerning the preliminary results for the subsurface cells, experimental results detected too much difference in the outflow if layouts with and without cells were compared for small slopes. Results suggest that the geotextile could be the main reason for this difference. It could be that, in some way, the geotextile creates a barrier to water.

5.3 Model analysis with experimental results

In this case, the main objective of the designed experiments was to test the model against pavement performance under controlled conditions. Given that the PP model is defined on a layer basis, experimental configuration on a layer basis and conducted SA configuration, also considering optional layers, was found to be quite valuable, as it allowed to identify much easier the role of

each layer in the outflow from the PP. In conjunction, both provided valuable insight into model performance for outflow calculation.

If model performance is analysed for complete sections and compared to experimental data, results are slightly better for permeable asphalt than for pavers, although it was confirmed that the cross-section type had no influence when runoff from the layout was compared with the CN model. However, it can be observed that simulated hydrographs are similar to those experimental ones, with Nash–Sutcliffe Efficiency (NSE) coefficient values higher than 0.74, although the average is 0.91. The high NSE results may indicate that good outflow values may be obtained with the model by defining it with physical parameters, easily measurable, considering previously mentioned roughness and drain exceptions.

Also, results show that modelled peaks are higher than measured ones, with an increasing difference for small slopes and rains, in line with obtained NSE values. Both peak and volume errors are minor, with an average of 3%. Results show those model predictions are better for high slopes and intensities, which may be helpful when modelling PPs, as it may point to which cases model prediction may be more or less reliable.

However, the experimental data analysis found that the model does not correctly simulate the soil or base layer, which includes a geotextile when the layer is created with small clean gravel. Even calibrating several parameters, the outflow from the model is much slower than the outflow from the experimental layout. Simulation results considerably improve if the soil layer is considered part of the storage layer. These results, in conjunction with the SA, may indicate that the soil layer shall be included in the model only if a *soil type* base layer is laid under the pavement, which is not considered a common practice for PPs. Thus, it is not recommended to use the soil layer for modelling the PPs, unless a filter layer is included between the pavement and the storage layer.

The model calibration with experimental data also showed that drain outflow parameters are difficult to define, as they do not have a physical meaning, making it difficult to set those parameters for a particular layout, even calibrated, increasing outflow uncertainty. In addition, roughness values obtained by calibration with experimental data were in line with expected theoretical values, showing that technical references can be an acceptable source for fixing surface roughness. The parameters defined in the model are not difficult to measure on the pavement layer, and modelling of the experimental data showed that obtained results are reasonably good if physical values are used.

5.4 PP performance from monitored site

The main objective of the experimental plot at a 1:1 scale was to gather data on the PP hydraulic performance in a particular climate. There were several new challenges in the design of the new plot, evidencing the lack of reliable information regarding PPs and their performance.

The first one was the design of the experimental site itself. However, this is inherent to any new construction site, as each has specifications and particularities. Nevertheless, the site design originated in too small areas to be controlled. Hence, as PPs enhance water retention and reduce peak flows, outflows from the experimental sites were too small to be measured with a standard triangular weir initially foreseen, losing precision. Therefore, rectangular thin weirs had to be tested and calibrated to measure outflows from the plot.

The second challenges was designing a reliable data collection system, as the site intended to be a long-term data source. Hence, a new data collection system had to be designed to be controlled from the university, where data could be stored and visualized live. Another issue related to the monitored site was the optimal data collection time interval, as too long intervals may drain batteries too fast. These new challenges evidenced the difficulties of monitoring stormwater sites with accurate data.

Regarding preliminary results, there is a notable difference between the runoff peak and volumes collected in the PPs areas, where those values are notably lower than standard pavement sites. These results align with the numerical and experimental data collected for now.

5.5 General discussion

As mentioned previously, designed experiments seem appropriate for this dissertation's general objective. A step-by-step process from model analysis, individual and comparative, to material analysis, at reduced and 1:1 scales, allows the design of a PP model that supports decisions related to its implementation at a city level.

The experimental design also showed how practical was the selected order for each step. First, the sensitivity analysis of the model. Second, the comparison based on that sensitivity analysis. Later, the experimentation with the materials, but having in mind the model configuration. Following, the experimental

data was tested against the model to check the performance. Further on, 1:1 site data will be used to test and calibrate the pavement model, which will finally be used to design the performance of new pavements.

Chapter 6

Conclusions

6.1 Final remarks

This dissertation analyses the hydraulic response of permeable pavements (PP) using numerical and experimental data. First, the document explores the Storm Water Management Model (SWMM) by providing a detailed global sensitivity analysis (SA). Secondly, the dissertation explores an application of the model in a broader context, comparing its runoff with the one created by the widespread curve number (CN) model. Finally, the document provides a deeper insight into the model by comparing it with experimental data obtained under controlled conditions in the laboratory.

The first stage of this study has shown that although several inputs are defined in the PP model, there are few parameters that really influence the outflow. Identifying those parameters shall help practitioners implement PPs in a broader model, focusing on specific parameters instead of all the model provides. Classifying them by layers shall also be helpful, as the influence of the model is defined on a layer basis, with some optional layers.

The second stage of this study found a relationship between the pavement permeability of the PP model and the widespread CN model to understand the PP model better. The research intended to fill a gap for broader analysis,

when several scenarios are analysed, with and without SUDS, a widespread practice, as several steps are required to switch scenarios in large models. From a practical point of model application, this research suggests that implementing the PP into the catchment model shall be simplified to simplify the scenario analysis.

As a third stage of the study, laboratory results were compared with modelling ones. PPs can be considered an excellent option to delay runoff, which is more significant for low storms and lower slopes. Results also showed that the model performance is quite acceptable under experimental conditions, which should reduce uncertainty when practitioners apply the model, even without calibration, using physical values. The analysis confirmed that roughness could be fixed using values given by the bibliography, but drain values are difficult to link with a particular physical meaning.

These three steps were proven to be an efficient combination to explore the PP model in SWMM, and all three are expected to be helpful for practitioners while designing new PP sites or researchers when studying PPs and their effects.

Hence, the dissertation is a tiny step into the broad goals set in the very early steps of this study. It still needs to get a reliable model to explore the influence of SUDS at a city scale. Despite this, research provides a solid background to continue exploring the influence of PPs in stormwater networks. Results will not only be valid at the municipal level, but they will also have a global impact, as it may be helpful to worldwide practitioners to analyse the influence of PPs in the broader network.

6.2 Future research

Experimental results showed that although geotextile was included, its influence on the outflow shall be further analysed. The model needs to account for the geotextile, and even the soil layer could not be satisfactorily modelled. Both need further research. Also, modelling the outflow showed that it is challenging to match drainage parameters to the physical characteristics, as they are based on an orifice flow. Hence, it is advisable to continue developing the drainage model. Long-term analysis under laboratory conditions is recommended.

The study has mainly focused on the hydrologic and hydraulic design of PPs, but we shall remember that quality performance is an essential aspect of SUDS

as an active element of the stormwater management network, which may be an important future research line.

The study has also analysed mainly the influence of rain intensity, PP type, and slope, but the influence of other factors shall be explored. The study has analysed new unclogged PPs, but further studies are necessary to set how pavement aging affects its hydraulic performance during its service life. The study has also focused on three main types of PPs (asphalt, concrete, and pavers), but it is recommended to expand the research to other types of PPs. Although the study has focused on PPs, it is interesting to continue exploring other SUDS models, considering that each technique has a different maturity level.

References

Ahiablame, Laurent M. and Ranish Shakya (2016). "Modeling flood reduction effects of low impact development at a watershed scale". In: *Journal of Environmental Management* 171, pp. 81–91. ISSN: 10958630. DOI: 10.1016/j.jenvman.2016.01.036 (cit. on p. 32).

Ajmal, Muhammad et al. (2015). "Improved runoff estimation using event-based rainfall-runoff models". In: *Water Resources Management* 29.6, pp. 1995–2010. ISSN: 1573-1650. DOI: 10.1007/s11269-015-0924-z (cit. on p. 34).

Alonso López, F. (2010). *Accesibilidad en los espacios públicos urbanizados*. Ministerio de Vivienda, Gobierno de España (cit. on pp. 20, 66).

Alsubih, Majed et al. (2017). "Experimental study on the hydrological performance of a permeable pavement". In: *Urban Water Journal* 14.4, pp. 427–434. DOI: 10.1080/1573062X.2016.1176221 (cit. on p. 58).

Andres-Domenech, Ignacio et al. (2018). "Hydrological performance of green roofs at building and city scales under Mediterranean conditions". In: *Sustainability* 10.9. DOI: 10.3390/su10093105 (cit. on p. 10).

Andrés-Doménech, Ignacio et al. (2021). "Sustainable urban drainage systems in Spain: A diagnosis". In: *Sustainability* 13.5. DOI: 10.3390/su13052791 (cit. on p. 2).

Archer, GEB, Andrea Saltelli, and IM Sobol (1997). "Sensitivity measures, ANOVA-like techniques and the use of bootstrap". In: *Journal of Statistical Computation and Simulation* 58.2, pp. 99–120 (cit. on p. 14).

Ardia, David et al. (2020). *DEoptim: Differential Evolution in R*. version 2.2-5 (cit. on p. 37).

Arnone, Elisa et al. (2018). "The role of urban growth, climate change, and their interplay in altering runoff extremes". In: *Hydrological Processes* 32.12, pp. 1755–1770. ISSN: 0885-6087. DOI: 10.1002/hyp.13141 (cit. on p. 1).

Bach, Peter M. et al. (Apr. 2014). "A critical review of integrated urban water modelling – Urban drainage and beyond". In: 54. ISSN: 1364-8152. DOI: 10.1016/j.envsoft.2013.12.018 (cit. on p. 33).

Baiamonte Giorgio (Oct. 2019). "SCS Curve Number and Green-Ampt infiltration models". In: *Journal of Hydrologic Engineering* 24.10, p. 04019034. DOI: 10.1061/(ASCE)HE.1943-5584.0001838 (cit. on p. 34).

Balbastre-Soldevila, Rosario, Rafael García-Bartual, and Ignacio Andrés-Doménech (2019). "A comparison of design storms for urban drainage system applications". In: *Water* 11.4. DOI: 10.3390/w11040757 (cit. on p. 38).

Bateni, Norazlina et al. (Dec. 2020). "Hydrological impact assessment on permeable road pavement with subsurface precast micro-detention pond". In: *Water and Environment Journal* 34.S1, pp. 960–969. ISSN: 1747-6585. DOI: 10.1111/wej.12613 (cit. on p. 60).

Bean, Eban Zachary, William Frederick Hunt, and David Alan Bidelspach (2007). "Evaluation of four permeable pavement sites in eastern North Carolina for runoff reduction and water quality impacts". In: *Journal of Irrigation and Drainage Engineering* 133.6, pp. 583–592. ISSN: 0733-9437. DOI: 10.1061/(ASCE)0733-9437(2007)133:6(583) (cit. on p. 78).

Bilal et al. (2020). "Differential Evolution: A review of more than two decades of research". In: *Engineering Applications of Artificial Intelligence* 90, p. 103479. ISSN: 0952-1976. DOI: 10.1016/j.engappai.2020.103479 (cit. on p. 45).

Biswas, Aindrila (2020). "A nexus between environmental literacy, environmental attitude and healthy living". In: *Environmental Science and Pollution Research* 27.6, pp. 5922–5931. ISSN: 0944-1344. DOI: 10.1007/s11356-019-07290-5 (cit. on p. 10).

Brattebo, Benjamin O and Derek B Booth (2003). "Long-term stormwater quantity and quality performance of permeable pavement systems". In: *Water Research* 37.18, pp. 4369–4376. ISSN: 0043-1354. DOI: 10.1016/S0043-1354(03)00410-X (cit. on p. 78).

Brown, R R and M A Farrelly (2009). "Delivering sustainable urban water management: a review of the hurdles we face". In: *Water Science and Technology* 59.5, pp. 839–846. ISSN: 0273-1223. DOI: 10.2166/wst.2009.028 (cit. on p. 2).

Brunetti, Giuseppe, Jiří Šimůnek, and Patrizia Piro (2016). "A comprehensive numerical analysis of the hydraulic behavior of a permeable pavement". In: *Journal of Hydrology* 540, pp. 1146–1161. ISSN: 00221694. DOI: 10.1016/j.jhydrol.2016.07.030 (cit. on p. 11).

Brunetti, Giuseppe et al. (2018). "On the use of global sensitivity analysis for the numerical analysis of permeable pavements". In: *Urban Water Journal* 15.3, pp. 269–275. ISSN: 1573-062X. DOI: 10.1080/1573062X.2018.1439975 (cit. on p. 11).

CALTRANS (2013). *Pervious pavement design guidance* (cit. on p. 36).

CASQA (2003). *Stormwater best management practice handbook* (cit. on p. 36).

Chalom, Andre and Paulo Inacio Knegt Lopez de Prado (2017). *Parameter space exploration with Latin Hypercubes*. R package version 0.4.7 (cit. on p. 22).

Chandrappa, Anush K. and Krishna Prapoorna Biligiri (2016). "Pervious concrete as a sustainable pavement material – Research findings and future prospects: A State-of-the-art review". In: *Construction and Building Materials* 111, pp. 262–274. ISSN: 09500618. DOI: 10.1016/j.conbuildmat.2016.02.054 (cit. on p. 33).

Charlesworth, Sue and Rebecca Wade (2014). "Multiple benefits from surface water management – SUDS". In: *CLEAN – Soil, Air, Water* 42.2, pp. 109–110. DOI: 10.1002/clen.201470014 (cit. on pp. 2, 58).

Charlesworth, Sue M (2010). "A review of the adaptation and mitigation of global climate change using sustainable drainage in cities". In: *Journal of Water and Climate Change* 1.3, pp. 165–180. DOI: 10.2166/wcc.2010.035 (cit. on p. 32).

Chow, Ven Te (1959). *Open-Channel Hydraulics*. New York, McGraw-Hill (cit. on p. 19).

— (2010). *Applied hydrology*. Tata McGraw-Hill Education (cit. on pp. 18, 36).

Ciriminna, Diego et al. (2022). "Numerical comparison of the hydrological response of different permeable pavements in urban area". In: *Sustainability* 14.9. ISSN: 2071-1050. DOI: 10.3390/su14095704 (cit. on p. 32).

Costa, Ialy Rayane de Aguiar et al. (2020). "Sensitivity of hydrodynamic parameters in the simulation of water transfer processes in a permeable pavement". In: *RBRH* 25 (cit. on p. 11).

Davison, Anthony Christopher and David Victor Hinkley (1997). *Bootstrap methods and their application*. 1. Cambridge university press (cit. on p. 14).

DHI (2018). *Estudio de actualización del análisis de las precipitaciones intensas y recomendaciones de cálculo de caudales de avenidas en pequeñas cuencas del territorio histórico de Gipuzkoa*. Tech. rep. Gipuzkoako Foru Aldundia (cit. on p. 62).

Dietz, Michael E (2007). "Low impact development practices: A review of current research and recommendations for future directions". In: *Water, air, and soil pollution* 186.1, pp. 351–363. DOI: doi.org/10.1007/s11270-007-9484-z (cit. on p. 45).

Eckart, K, Z McPhee, and T Bolisetti (2017). "Performance and implementation of low impact development - A Review". In: *Science of the Total En-*

vironment 607, pp. 413–432. ISSN: 18791026. DOI: 10.1016/j.scitotenv.2017.06.254 (cit. on pp. 32, 59).

Efron, Bradley (1979). "Computers and the theory of statistics: thinking the unthinkable". In: *SIAM review* 21.4, pp. 460–480 (cit. on p. 14).

Elliott, A. H. and S. A. Trowsdale (2007). "A Review of models for low impact urban stormwater drainage". In: *Environmental Modelling and Software* 22.3, pp. 394–405. ISSN: 13648152. DOI: 10.1016/j.envsoft.2005.12.005 (cit. on p. 33).

Fletcher, T D, H Andrieu, and P Hamel (2013). "Understanding, management and modelling of urban hydrology and its consequences for receiving waters: A state of the art". In: *Advances in Water Resources* 51, pp. 261–279. ISSN: 0309-1708. DOI: https://doi.org/10.1016/j.advwatres.2012.09.001 (cit. on p. 32).

Fletcher, Tim D. et al. (2015). "SUDS, LID, BMPs, WSUD and more – The evolution and application of terminology surrounding urban drainage". In: *Urban Water Journal* 12.7, pp. 525–542. ISSN: 17449006. DOI: 10.1080/1573062X.2014.916314 (cit. on pp. 2, 32, 58).

Freire Diogo, António and José Antunes do Carmo (2019). "Peak flows and stormwater networks design—current and future management of urban surface watersheds". In: *Water* 11.4. DOI: 10.3390/w11040759 (cit. on p. 62).

Geyler, Stefan, Norman Bedtke, and Erik Gawel (2019). "Sustainable stormwater management in existing settlements-municipal strategies and current governance trends in Germany". In: *Sustainability* 11.19. DOI: 10.3390/su11195510 (cit. on p. 10).

Gülbaz, Sezar and Cevza Melek Kazezyılmaz-Alhan (Dec. 2017). "An evaluation of hydrologic modeling performance of EPA SWMM for Bioretention". In: *Water Science and Technology* 76.11, pp. 3035–3043. ISSN: 0273-1223, 1996-9732. DOI: 10.2166/wst.2017.464 (cit. on p. 60).

Gupta, Hoshin V. and Saman Razavi (2018). "Revisiting the basis of sensitivity analysis for dynamical earth system models". In: *Water Resources Research*

54.11, pp. 8692–8717. ISSN: 0043-1397. DOI: 10.1029/2018WR022668 (cit. on p. 11).

Hargreaves, George H and Zohrab A Samani (1985). "Reference crop evapotranspiration from temperature". In: *Applied engineering in agriculture* 1.2, pp. 96–99 (cit. on pp. 18, 44).

Hawkins, Richard H et al. (2009). *Curve Number hydrology: State of the practice*. Tech. rep. Environmental and Water Resources Institute (EWRI) of the American Society of Civil Engineers. DOI: 10.1061/9780784410042 (cit. on p. 39).

Hou, Jingming et al. (2019). "Experimental study for effects of terrain features and rainfall intensity on infiltration rate of modelled permeable pavement". In: *Journal of Environmental Management* 243, pp. 177–186. ISSN: 0301-4797. DOI: 10.1016/j.jenvman.2019.04.096 (cit. on p. 66).

Hu, Chen et al. (2021). "A new urban hydrological model considering various land covers for flood simulation". In: *Journal of Hydrology* 603, p. 126833. ISSN: 0022-1694. DOI: 10.1016/j.jhydrol.2021.126833 (cit. on p. 34).

Huang, Chien-Lin et al. (Sept. 2018). "Optimization of low impact development layout designs for megacity flood mitigation". In: *Journal of Hydrology* 564, pp. 542–558. ISSN: 0022-1694. DOI: 10.1016/j.jhydrol.2018.07.044 (cit. on p. 32).

Huang, Jian et al. (2016). "Temporal evolution modeling of hydraulic and water quality performance of permeable pavements". In: *Journal of Hydrology* 533, pp. 15–27. ISSN: 00221694. DOI: 10.1016/j.jhydrol.2015.11.042 (cit. on p. 72).

Iooss, Bertrand and Paul Lemaître (2015). "A review on global sensitivity analysis methods". In: *Uncertainty management in simulation-optimization of complex systems*. Springer, pp. 101–122. DOI: 10.1007/978-1-4899-7547-8_5 (cit. on p. 11).

Iooss, Bertrand et al. (2020). *Global sensitivity analysis of model outputs*. R package version 1.21.0 (cit. on p. 22).

Jato-Espino, Daniel et al. (2016). "Rainfall-runoff simulations to assess the potential of SUDS for mitigating flooding in highly urbanized catchments". In: *International Journal of Environmental Research and Public Health* 13.1. ISSN: 16604601. DOI: 10.3390/ijerph13010149 (cit. on p. 33).

Kamali, Meysam, Madjid Delkash, and Massoud Tajrishy (2017). "Evaluation of permeable pavement responses to urban surface runoff". In: *Journal of Environmental Management* 187, pp. 43–53. ISSN: 0301-4797. DOI: 10.1016/j.jenvman.2016.11.027 (cit. on p. 58).

Kayhanian, Masoud et al. (2019). "Application of permeable pavements in highways for stormwater runoff management and pollution prevention: California research experiences". In: *International Journal of Transportation Science and Technology* 8.4, pp. 358–372. DOI: 10.1016/j.ijtst.2019.01.001 (cit. on p. 19).

Kaykhosravi, Sahereh, Khan, Usman T, and Jadidi, Amaneh (2018). "A comprehensive review of low impact development models for research, conceptual, preliminary and detailed design applications". In: *Water* 10.11. DOI: 10.3390/w10111541 (cit. on pp. 2, 10, 32, 34, 59).

Krebs, Gerald et al. (2016). "Simulation of green roof test bed runoff". In: *Hydrological Processes* 30.2, pp. 250–262. ISSN: 0885-6087. DOI: 10.1002/hyp.10605 (cit. on p. 11).

Kuruppu, Upeka, Ataur Rahman, and M Azizur Rahman (2019). "Permeable pavement as a stormwater best management practice: a review and discussion". In: *Environmental Earth Sciences* 78.10. ISSN: 1866-6280. DOI: 10.1007/s12665-019-8312-2 (cit. on pp. 3, 10, 33, 58).

Lee, Seungwook et al. (2022). "Runoff reduction effects at installation of LID Facilities under different climate change scenarios". In: *Water* 14.8. ISSN: 2073-4441. DOI: 10.3390/w14081301 (cit. on p. 33).

Leimgruber, Johannes et al. (2018). "Sensitivity of model-based water balance to low impact development parameters". In: *Water* 10.12. ISSN: 2073-4441. DOI: 10.3390/w10121838 (cit. on p. 11).

Leutnant, Dominik, Anneke Döring, and Mathias Uhl (2019). "swmmr - an R package to interface SWMM". In: *Urban Water Journal* 16.1, pp. 68–76.

ISSN: 1573-062X. DOI: 10.1080/1573062X.2019.1611889 (cit. on pp. 22, 37).

Li, Hui, Masoud Kayhanian, and John T. Harvey (2013). "Comparative field permeability measurement of permeable pavements using ASTM C1701 and NCAT permeameter methods". In: *Journal of Environmental Management* 118. ISBN: 0301-4797, pp. 144–152. ISSN: 03014797. DOI: 10.1016/j.jenvman.2013.01.016 (cit. on p. 33).

Liao, Xianghua et al. (2018). "Approach for evaluating LID measure layout scenarios based on random forest: Case of Guangzhou-China". In: *Water* 10.7. DOI: 10.3390/w10070894 (cit. on p. 10).

Liu, Chun Yan and Ting Fong May Chui (2017). "Factors influencing stormwater mitigation in permeable pavement". In: *Water* 9.12, p. 988. ISSN: 2073-4441. DOI: 10.3390/w9120988 (cit. on p. 59).

Liu, Tianqi et al. (2021). "Low impact development (LID) practices: A review on recent developments, dhallenges and prospects". In: *Water, Air, & Soil Pollution* 232.9, p. 344. ISSN: 1573-2932. DOI: 10.1007/s11270-021-05262-5 (cit. on p. 32).

Luo, Pingping et al. (Oct. 2022). "Urban flood numerical simulation: research, methods and future perspectives". In: *Environmental Modelling & Software* 156, p. 105478. ISSN: 1364-8152. DOI: 10.1016/j.envsoft.2022.105478 (cit. on p. 32).

Madrazo-Uribeetxebarria, Eneko et al. (2019). "Hydraulic performance of permeable asphalt and PICP in SWMM, validated by laboratory data". In: *WIT Transactions on Ecology and the Environment*. Vol. 238. WitPress, pp. 569–579. DOI: 10.2495/SC190491 (cit. on p. 59).

Madrazo-Uribeetxebarria, Eneko et al. (2021). "Sensitivity analysis of permeable pavement hydrological modelling in the Storm Water Management Model". In: *Journal of Hydrology* 600, p. 126525. ISSN: 00221694. DOI: 10.1016/j.jhydrol.2021.126525 (cit. on pp. 35, 60, 69, 72).

Madrazo-Uribeetxebarria, Eneko et al. (Dec. 2022). "Modelling runoff from permeable pavements: A link to the Curve Number method". In: *Water* 15.1, p. 160. ISSN: 2073-4441. DOI: 10.3390/w15010160 (cit. on p. 69).

McKay, Michael D and Richard J Beckman (1979). "A comparison of three methods for selecting values of input variables in the analysis of output from a computer code". In: *Technometrics* 21, pp. 239–244 (cit. on p. 14).

MOPU (1986). *Norma 6.1-IC-Secciones de firme*. Tech. rep. Ministerio de Obras Públicas y Urbanismo (MOPU) (cit. on p. 36).

Mullaney, Jennifer and Terry Lucke (2014). "Practical review of pervious pavement designs". In: *Clean - Soil, Air, Water* 42.2, pp. 111–124. ISSN: 18630650. DOI: 10.1002/clen.201300118 (cit. on pp. 10, 41, 58, 65).

Mullen, Katharine et al. (2011). "DEoptim: An R package for global optimization by Differential Evolution". In: *Journal of Statistical Software* 40.6, pp. 1–26. DOI: 10.18637/jss.v040.i06 (cit. on pp. 45, 72).

Nash, J Eamonn and Jonh V Sutcliffe (1970). "River flow forecasting through conceptual models part I—A discussion of principles". In: *Journal of hydrology* 10.3, pp. 282–290. DOI: 10.1016/0022-1694(70)90255-6 (cit. on pp. 44, 70).

Niazi, Mehran et al. (2017). "Storm Water Management Model: performance review and gap analysis". In: *Journal of Sustainable Water in the Built Environment* 3.2, p. 04017002. DOI: 10.1061/JSWBAY.0000817 (cit. on p. 11).

Palla, A. et al. (2014). "Influence of stratigraphy and slope on the drainage capacity of permeable pavements: laboratory results". In: *Urban Water Journal* 12.5, pp. 394–403. DOI: 10.1080/1573062X.2014.900091 (cit. on pp. 64, 68, 78).

Palla, Anna and Ilaria Gnecco (2015). "Hydrologic modeling of low impact development systems at the urban catchment scale". In: *Journal of Hydrology* 528, pp. 361–368. ISSN: 00221694. DOI: 10.1016/j.jhydrol.2015.06.050 (cit. on pp. 10, 33).

Panos, Chelsea L., Jordyn M. Wolfand, and Terri S. Hogue (2020). "SWMM sensitivity to LID siting and routing parameters: Implications for stormwater regulatory compliance". In: *JAWRA Journal of the American Water Resources Association* 56.5, pp. 790–809. DOI: https://doi.org/10.1111/1752-1688.12867 (cit. on p. 11).

Pappalardo, Viviana and Daniele La Rosa (2020). "Policies for sustainable drainage systems in urban contexts within performance-based planning approaches". In: *Sustainable Cities and Society* 52, p. 101830. ISSN: 2210-6707. DOI: 10.1016/j.scs.2019.101830 (cit. on p. 1).

Pardossi, Alberto et al. (2009). "Root zone sensors for irrigation management in intensive agriculture". In: *Sensors* 9.4, pp. 2809–2835. DOI: 10.3390/s90402809 (cit. on p. 20).

Peng, Zhangjie and Virginia Stovin (2017). "Independent validation of the SWMM green roof module". In: *Journal of Hydrologic Engineering* 22.9, p. 04017037. DOI: 10.1061/(ASCE)HE.1943-5584.0001558 (cit. on p. 11).

Platz, Michelle, Michelle Simon, and Michael Tryby (2020). "Testing of the Storm Water Management Model low impact development modules". In: *JAWRA Journal of the American Water Resources Association* 56.20, pp. 283–296. DOI: 10.1111/1752-1688.12832 (cit. on pp. 59, 83, 84).

Ponce, Victor M and Richard H Hawkins (1996). "Runoff Curve Number: Has it reached maturity?" In: *Journal of hydrologic engineering* 1.1, pp. 11–19. DOI: 10.1061/(ASCE)1084-0699(1996)1:1(11) (cit. on pp. 34, 38).

Pujol, Gilles (2009). "Simplex-based screening designs for estimating metamodels". In: *Reliability Engineering & System Safety* 94.7, pp. 1156–1160. ISSN: 0951-8320. DOI: 10.1016/j.ress.2008.08.002 (cit. on p. 11).

Qi, Wenchao et al. (Aug. 2021). "A review on applications of urban flood models in flood mitigation strategies". In: *Natural Hazards* 108.1, pp. 31–62. ISSN: 1573-0840. DOI: 10.1007/s11069-021-04715-8 (cit. on p. 32).

Qin, Hua-peng, Zhuo-xi Li, and Guangtao Fu (2013). "The effects of low impact development on urban flooding under different rainfall characteristics". In: *Journal of Environmental Management* 129, pp. 577–585. ISSN: 0301-4797. DOI: 10.1016/j.jenvman.2013.08.026 (cit. on p. 10).

R Core Team (2023). *R: a language and environment for statistical computing*. R Foundation for Statistical Computing. Vienna, Austria (cit. on pp. 22, 37, 72).

Radwan, Mona, Patrick Willems, and Jean Berlamont (2004). "Sensitivity and uncertainty analysis for river quality modelling". In: *Journal of Hydroinformatics* 6.2, pp. 83–99. ISSN: 1464-7141. DOI: 10.2166/hydro.2004.0008 (cit. on pp. 2, 60).

Rammal, Mohamad and Emmanuel Berthier (2020). "Runoff losses on urban surfaces during frequent rainfall events: A review of observations and modeling attempts". In: *Water* 12.10. ISSN: 2073-4441. DOI: 10.3390/w12102777 (cit. on p. 41).

Randall, Mark et al. (2020). "Comparison of SWMM evaporation and discharge to in-field observations from lined permeable pavements". In: *Urban Water Journal*, pp. 1–12. ISSN: 1573-062X. DOI: 10.1080/1573062X.2020.1776737 (cit. on pp. 12, 19, 28, 59).

Ratto, M et al. (2007). "Uncertainty, sensitivity analysis and the role of data based mechanistic modeling in hydrology". In: *Hydrology and Earth System Sciences* 11.4, pp. 1249–1266. DOI: 10.5194/hess-11-1249-2007 (cit. on p. 13).

Rodriguez-Hernandez, Jorge et al. (2016). "Laboratory study on the stormwater retention and runoff attenuation capacity of four permeable pavements". In: *Journal of Environmental Engineering* 142.2, p. 04015068. DOI: 10.1061/(ASCE)EE.1943-7870.0001033 (cit. on pp. 58, 68).

Rodríguez-Rojas, M. I. et al. (2020). "Middle-term evolution of efficiency in permeable pavements: a real case study in a Mediterranean climate". In: *International Journal of Environmental Research and Public Health* 17.21. ISSN: 1660-4601. DOI: 10.3390/ijerph17217774 (cit. on p. 10).

Rossman, L (2015). *Storm Water Management Model user's manual Version 5.1*. EPA/600/R-14/413b. US EPA Office of Research and Development, Washington, DC (cit. on pp. 3, 12, 19, 22, 40).

Rossman, Lewis A (2010). "Modeling low impact development alternatives with SWMM". In: *Journal of Water Management Modeling*. DOI: 10.14796/JWMM.R236-11 (cit. on pp. 15, 40).

Rossman, Lewis A. and Wayne C. Huber (2015). *Storm Water Management Model reference manual Volume I, Hydrology*. EPA/600/R-15/162A. US

EPA Office of Research and Development, Washington, DC (cit. on pp. 15, 39–41, 69).

Rossman, Lewis A. and Wayne C. Huber (2016). *Storm Water Management Model reference manual Volume III – Water Quality*. EPA/600/R-16/093. U.S. EPA Office of Research and Development, Washington, DC (cit. on pp. 17, 19, 41, 69, 83).

Saltelli, A (2002). "Making best use of model evaluations to compute sensitivity indices". In: *Computer Physics Communications* 145.2, pp. 280–297. ISSN: 0010-4655. DOI: 10.1016/S0010-4655(02)00280-1 (cit. on p. 14).

Saltelli, Andrea et al. (2008). *Global sensitivity analysis. The Primer*. John Wiley & Sons, Ltd. ISBN: 9780470725184. DOI: 10.1002/9780470725184 (cit. on pp. 13, 14, 22).

Saltelli, Andrea et al. (2019). "Why so many published sensitivity analyses are false: A systematic review of sensitivity analysis practices". In: *Environmental Modelling & Software* 114, pp. 29–39. ISSN: 1364-8152. DOI: 10.1016/j.envsoft.2019.01.012 (cit. on p. 11).

Salvadore, Elga, Jan Bronders, and Okke Batelaan (2015). "Hydrological modelling of urbanized catchments: A review and future directions". In: *Journal of Hydrology* 529.P1, pp. 62–81. ISSN: 0022-1694. DOI: 10.1016/j.jhydrol.2015.06.028 (cit. on p. 32).

Sañudo-Fontaneda, Luis A. et al. (2013). "Laboratory analysis of the infiltration capacity of interlocking concrete block pavements in car parks". In: *Water Science and Technology* 67.3, 675–681. DOI: 10.2166/wst.2012.614 (cit. on p. 58).

Sarrazin, Fanny, Francesca Pianosi, and Thorsten Wagener (2016). "Global sensitivity analysis of environmental models: Convergence and validation". In: *Environmental Modelling & Software* 79, pp. 135–152. DOI: 10.1016/j.envsoft.2016.02.005 (cit. on p. 14).

Scholz, Miklas and Piotr Grabowiecki (2007). "Review of permeable pavement systems". In: *Building and Environment* 42.11, pp. 3830–3836. ISSN: 03601323. DOI: 10.1016/j.buildenv.2006.11.016 (cit. on p. 10).

SCS (1956). *Hydrology, National Engineering Handbook* (cit. on p. 38).

Shin, Mun-Ju et al. (2013). "Addressing ten questions about conceptual rainfall-runoff models with global sensitivity analyses in R". In: *Journal of Hydrology* 503, pp. 135–152. ISSN: 0022-1694. DOI: 10.1016/j.jhydrol.2013.08.047 (cit. on pp. 12, 18, 20).

Smith, David R. and David K. Hein (Nov. 2013). "Development of a national ASCE standard for permeable interlocking concrete pavement". In: *Green Streets, Highways, and Development 2013: Advancing the Practice*. American Society of Civil Engineers (ASCE), pp. 89–105. DOI: https://doi.org/10.1061/9780784413197.008 (cit. on p. 65).

Sobol', I.M. (1990). "On sensitivity estimation for nonlinear mathematical models". In: *Matematicheskoe Modelirovanie* 2.1, pp. 112–118 (cit. on p. 12).

Song, Jae Yeol and Eun-Sung Chung (2017). "A multi-Criteria decision analysis system for prioritizing sites and types of low impact development practices: Case of Korea". In: *Water* 9.4. ISSN: 2073-4441. DOI: 10.3390/w9040291 (cit. on p. 10).

Støvring, Jan et al. (2018). "Hydraulic performance of lined permeable pavement systems in the built environment". In: *Water* 10.5. ISSN: 2073-4441. DOI: 10.3390/w10050587 (cit. on pp. 58, 78, 82, 83).

Sujono, Joko, Shiomi Shikasho, and Kazuaki Hiramatsu (2004). "A comparison of techniques for hydrograph recession analysis". In: *Hydrological Processes* 18.3, pp. 403–413. ISSN: 0885-6087. DOI: 10.1002/hyp.1247 (cit. on p. 67).

Tallaksen, L M (1995). "A review of baseflow recession analysis". In: *Journal of Hydrology* 165.1, pp. 349–370. ISSN: 0022-1694. DOI: 10.1016/0022-1694(94)02540-R (cit. on p. 67).

Tennis, Paul D, Michael L Leming, and David J Akers (2004). *Pervious concrete pavements*. PCA Serial No. 2828. Portland Cement Association Skokie, IL (cit. on p. 19).

Turco, Michele et al. (2017). "Unsaturated hydraulic behaviour of a permeable pavement: Laboratory investigation and numerical analysis by using the HYDRUS-2D model". In: *Journal of Hydrology* 554, pp. 780–791. ISSN: 00221694. DOI: 10.1016/j.jhydrol.2017.10.005 (cit. on pp. 11, 60).

Tziampou, Natasa et al. (2020). "Fluid transport within permeable pavement systems: A review of evaporation processes, moisture loss measurement and the current state of knowledge". In: *Construction and Building Materials* 243, p. 118179. ISSN: 0950-0618. DOI: 10.1016/j.conbuildmat.2020.118179 (cit. on p. 58).

Watt, Ed and Jiri Marsalek (2013). "Critical review of the evolution of the design storm event concept". In: *Canadian Journal of Civil Engineering* 40.2, pp. 105–113. ISSN: 0315-1468. DOI: 10.1139/cjce-2011-0594 (cit. on p. 36).

Weiss, Peter T et al. (2019). "Permeable pavement in northern North American urban areas: research review and knowledge gaps". In: *International Journal of Pavement Engineering* 20.2, pp. 143–162. ISSN: 1029-8436. DOI: 10.1080/10298436.2017.1279482 (cit. on p. 65).

Wilcox, Bradford P. et al. (Oct. 1990). "Predicting runoff from rangeland catchments: A Comparison of two models". In: *Water Resources Research* 26.10, pp. 2401–2410. ISSN: 0043-1397. DOI: 10.1029/WR026i010p02401 (cit. on p. 34).

Woods Ballard, B et al. (2015). *The SUDS manual*. Ciria London, p. 937. ISBN: 978-0-86017-760-9 (cit. on pp. 10, 17, 20, 32, 36, 65, 66).

Xie, Ning, Michelle Akin, and Xianming Shi (2019). "Permeable concrete pavements: A review of environmental benefits and durability". In: *Journal of Cleaner Production* 210, pp. 1605–1621. ISSN: 0959-6526. DOI: 10.1016/j.jclepro.2018.11.134 (cit. on p. 58).

Xu, Changqing et al. (2019a). "Benefits of coupled green and grey infrastructure systems: Evidence based on analytic hierarchy process and life cycle costing". In: *Resources, Conservation and Recycling* 151.April, pp. 1–10. ISSN: 18790658. DOI: 10.1016/j.resconrec.2019.104478 (cit. on p. 59).

Xu, Zuxin et al. (2019b). "Runoff simulation of two typical urban green land types with the Stormwater Management Model (SWMM): sensitivity analysis and calibration of runoff parameters". In: *Environmental monitoring and assessment* 191.6, p. 343. DOI: 10.1007/s10661-019-7445-9 (cit. on p. 11).

Yazdanfar, Z and A Sharma (2015). "Urban drainage system planning and design - challenges with climate change and urbanization: a review". In: *Water Science and Technology* 72.2, pp. 165–179. ISSN: 0273-1223. DOI: 10.2166/wst.2015.207 (cit. on p. 1).

Zhang, Shouhong and Yiping Guo (2015). "SWMM simulation of the storm water volume control performance of permeable pavement systems". In: *Journal of Hydrologic Engineering* 20.8, p. 06014010. ISSN: 10840699. DOI: 10.1061/(ASCE)HE.1943-5584.0001092 (cit. on pp. 20, 34, 59).

Zhu, Yuxin et al. (2021). "Permeable pavement design framework for urban stormwater management considering multiple criteria and uncertainty". In: *Journal of Cleaner Production*, p. 126114. DOI: 10.1016/j.jclepro.2021.126114 (cit. on p. 33).

Appendix A: Cell performance

This appendix presents some preliminary findings related to the experimental part of the thesis. In particular, the findings related to the hydraulic behaviour of the subsurface cells installed below some of the permeable pavement layouts from the experimental plot of Txominenea. The reported findings were presented in the national congress entitled VI Jornadas de Ingeniería del Agua, held in Toledo in 2019.

Análisis hidráulico y modelización de geoceldas de drenaje subsuperficial en pavimentos permeables

Madrazo-Uribeetxebarria, E.[a], Garmendia-Antín, M.[b1], Almandoz-Berrondo, F. J.[b2], Andrés-Doménech, I.[c]

[a]Departamento de Ingeniería Nuclear y Mecánica de Fluidos, UPV/EHU, Escuela de Ingeniería de Bilbao, C/ Rafael Moreno "Pichici", 1, 48013 Bilbao, E-mail: eneko.madrazo@ehu.eus, [b]Departamento de Ingeniería Nuclear y Mecánica de Fluidos, UPV/EHU, Escuela de Ingeniería de Gipuzkoa, Europa plaza,1 20018 Donostia-San Sebastián, E-mail: [b1]maddi.garmendiaa@ehu.eus, [b2]jabier.almandoz@ehu.eus y [c]Instituto Universitario de Investigación de Ingeniería del Agua y Medio Ambiente (IIAMA), Universitat Politècnica de València, Camino de Vera s/n, 46022 Valencia, E-mail: igando@hma.upv.es

Línea temática | C. Agua y ciudad

RESUMEN

Los pavimentos permeables son una de las soluciones por las que se puede optar para gestionar la escorrentía en entornos urbanos, tanto en cantidad como en calidad. Los tipos de pavimento permeable son múltiples, pero todos disponen, en comparación con los tradicionales, de una capa subbase muy porosa que permite gestionar el agua de lluvia infiltrada a través de la superficie impermeable. A su vez, algunos fabricantes recomiendan instalar celdas de plástico bajo la capa de subbase, celdas que incrementan la porosidad de dicha capa, facilitando así el drenaje horizontal en el fondo de la sección. El artículo estudia, por un lado, como es la respuesta hidráulica del pavimento ejecutado con las celdas de plástico colocadas bajo la subbase, comparándola con la subbase sin celdas. Para ello, se han realizado ensayos de laboratorio a las dos subbases, una con celdas y otra sin celdas, frente a diferentes intensidades de lluvia y pendientes de fondo, midiendo los hidrogramas del agua infiltrada a la salida de la sección. Por otro lado, se ha analizado la respuesta hidráulica de ambas configuraciones con el modelo matemático SWMM ante las mismas condiciones estudiadas en el laboratorio. La modelización se ha realizado utilizando exclusivamente el módulo LID de SWMM, el cual permite modelizar pavimentos permeables. De esa forma, se ha comprobado y confirmado la validez del modelo, pudiendo extrapolar los datos a otras zonas urbanas con pavimentos permeables de similares características.

Palabras clave | SWMM, pavimentos permeables, LID, celdas drenaje subsuperficial, modelización, drenaje sostenible.

INTRODUCCIÓN

En el ciclo natural del agua parte de la precipitación escurre hasta los cursos fluviales, pero la mayoría se infiltra, se evapora o es absorbida por la vegetación. Este ciclo natural se altera considerablemente cuando el desarrollo urbano transforma una zona virgen. En las áreas urbanas se reduce la superficie que permite la infiltración, así como la vegetación que favorece la evapotranspiración, de ahí que la escorrentía superficial aumente. Consecuentemente, se intensifican los problemas de inundación, contaminación y erosión (Woods Ballard et al., 2015). En ese contexto, los Sistemas Urbanos de Drenaje Sostenible (SUDS) pretenden reducir los efectos negativos del proceso de urbanización, intentando recuperar los procesos hidrológicos mermados por la impermeabilización. Estos sistemas y las técnicas que los componen son muy variados, pero los objetivos que persiguen pretenden recuperar aquellos procesos que las superficies impermeables obstaculizan: la infiltración y la evapotranspiración.

Los pavimentos permeables son un tipo de técnica SUDS que, además, posibilita captar la escorrentía allí donde se genera. En consecuencia, son adecuados para gestionar el drenaje, ya que optimizan el uso del suelo, permiten la infiltración a las capas inferiores a través del pavimento, y proporcionan una superficie transitable para vehículos y peatones (Mullaney y Lucke, 2014). Los pavimentos permeables suelen ser, principalmente, de dos tipos: pavimentos de naturaleza porosa y pavimentos impermeables en disposición permeable, generalmente a través de la junta de los elementos impermeables tales como adoquines (Sañudo Fontaneda et al., 2012).

Al contrario que los pavimentos tradicionales, los pavimentos permeables se diseñan para facilitar el flujo vertical de agua a través del pavimento. Las secciones de dichos pavimentos, dependiendo del tipo y las condiciones hidrológicas, incluyen varios materiales porosos, así como otros materiales filtrantes tales como geotextiles (Korkealaakso et al. 2014). En general, estos pavimentos suelen constar de una capa superficial (capa de rodadura), una base de apoyo y una subbase que permite el almacenamiento de agua, toda vez que confiere al conjunto la resistencia estructural adecuada.

Como se ha mencionado, es habitual disponer geosintéticos en la construcción de los pavimentos permeables. Se suele denominar geosintético a un amplio rango de materiales manufacturados a partir de polímeros, siendo los más conocidos los geotextiles, las geomallas, las geomembranas, las georredes y los geocompuestos. En general, estos se utilizan como una parte integral de las obras, en contacto con suelos, rocas o cualquier otro material relacionado con la obra civil. Se suelen emplear con diferentes objetivos: separación, filtración, drenaje, refuerzo, contención y control de la erosión. A pesar de que el desarrollo de los geosintéticos en las cuatro últimas décadas ha posibilitado nuevas estrategias para mejorar el rendimiento de carreteras pavimentadas (Yin y Shukla, 2006), la mayor parte de las aplicaciones de los geosintéticos han sido en carreteras asfaltadas con poco tráfico (Flutcher y Wu, 2013), por ejemplo, mediante el uso de geoceldas.

Las geoceldas son estructuras tridimensionales y permeables con forma de malla o panal de abeja, que se pueden crear a partir de celdas rectangulares o triangulares ensambladas mediante geomallas y uniones especiales, o fabricar en planta a partir de tiras de poliéster cosidas o polietileno de alta densidad (Yin y Shukla, 2006). Las geoceldas no solo se utilizan en los pavimentos de césped o grava reforzados, generando una estructura de confinamiento en la capa superficial, sino que, en algunos casos, se han instalado bajo la subbase del pavimento permeable, de forma que funciona como un drenaje subsuperficial del paquete de firme. En ese sentido, algunas empresas del sector incluyen en sus catálogos detalles de instalación con celdas colocadas bajo la subbase.

Este estudio analiza el comportamiento hidráulico de las geoceldas de drenaje subsuperficial, es decir, colocadas bajo la subbase de pavimentos permeables. El análisis se realiza mediante ensayos de laboratorio a dos tipos de subbase, con y sin geoceldas. Además de medir la respuesta hidráulica ante varias intensidades de lluvia y pendientes, se analiza la respuesta hidráulica proporcionada por el modelo SWMM (Storm Water Management Model), un modelo dinámico de simulación lluvia-escorrentía que permite simular, principalmente en zonas urbanas, la cantidad de escorrentía y su calidad tanto para un evento de lluvia como para una lluvia continua (Rossman, 2015). Desde su versión 5.0, SWMM permite modelar con un alto grado de detalle técnicas SUDS incorporadas en el sistema de drenaje, a través del módulo de cálculo LID (Low Impact Development). La utilización de dichas unidades LID permite analizar con más detalle el modelo y, además, determinar con mayor precisión los parámetros significativos que más incidencia tienen en el comportamiento hidráulico resultante.

METODOLOGÍA

El análisis hidráulico se ha realizado en base a ensayos de laboratorio realizados a las capas que componen la subbase, analizándolas por separado, y midiendo la respuesta hidráulica ante diversos episodios de lluvia en varias condiciones de pendiente. Posteriormente, se ha estudiado la respuesta hidráulica del modelo SWMM para esos mismos eventos en las mismas condiciones.

Datos de laboratorio

Los datos de laboratorio se han obtenido en un banco hidrológico, HM 165 de Gunt, modificado para medir la lluvia infiltrada a través del material colocado en ella (Figura 1). Al banco hidrológico se le ha impermeabilizado la mitad de la superficie, equivalente a 1 m², mediante una geomembrana. Dicha geomembrana genera una especie de recipiente, con un lateral libre; que evitará la fuga de agua por la parte alta de la sección y los laterales, pero permitirá la salida de agua por el lateral situado en la parte baja. El agua infiltrada se emboca a un orificio y se dirige a una cubeta de hidrogramas donde se recogerá y se realizará una medición volumétrica.

Asimismo, al banco se le ha añadido una parrilla de 81 goteros en la parte superior para simular las lluvias deseadas. Los goteros se han distribuido en el metro cuadrado de forma uniforme en 9 filas con 9 goteros por fila. Los goteros se han conectado mediante tuberías de 16 mm de diámetro, rigidizadas mediante una parrilla de listones de madera. Se han utilizado unos pequeños tacos de madera para mantener horizontal la superficie de los goteros durante los cambios de pendiente aplicados a la estructura del banco hidrológico.

Debido a que los nudos de las redes de drenaje urbano que captan la escorrentía superficial recogen superficies o subcuencas pequeñas, en general, se ha adoptado una duración de lluvia de 15 minutos para determinar las intensidades máximas aplicables, similar al tiempo de concentración de las mencionadas cuencas. En base a dicha duración, se han utilizado las curvas IDF de la estación de Igeldo (Donostia/San Sebastián) para determinar intensidades correspondientes a períodos de retorno de 2 y 10 años: 35 y 70 mm/h (DFG, 2018). Con ello, se han querido considerar tanto intensidades ordinarias (2 años) como aquellas con un período de retorno habitual en el diseño de las redes de drenaje urbano (10 años). El caudal aportado a la parrilla de goteros, gobernado mediante dos válvulas de asiento, se ha controlado mediante dos rotámetros de 5-50 l/h y 15-160 l/h. Asimismo, se ha añadido un contador de agua iPerl adicional tras las válvulas.

Figura 1 | Banco hidrológico modificado: (1) rotámetros, (2) válvulas (3) contador (4) parrilla de goteros (5) recipiente para material ensayado (6) salida (7) cubeta de hidrogramas

Las secciones tipo analizadas son dos, con y sin celdas, y se muestran en la Figura 2. Únicamente se han analizado las dos subbases. Todo el material ensayado procede de una obra cercana, ejecutada en la misma ciudad de Donostia/San Sebastián. El material ensayado en la capa de almacenamiento era grava caliza de cantera, cuyo tamaño de árido están entre 4 y 12 mm, de acuerdo con las especificaciones aportadas por la cantera. El índice de huecos ($V_{huecos}/V_{sólidos}$) se midió en el laboratorio, pesando el agua almacenada en los huecos de la grava contenida en un recipiente de plástico de 500 ml. La medición del índice de huecos se realizó en dos supuestos: grava compactada y grava sin compactar. Para el primer caso, se rellenó el recipiente con grava y se compactó de forma manual, aplicándole 50 golpes con el mango de un destornillador. En total se realizaron 18 mediciones, 9 sin compactar y 9 compactados. Los resultados obtenidos para el índice de huecos fueron los siguientes: 0.78 para la grava compactada y 0.98 para la grava sin compactar.

Las celdas utilizadas eran de 52 mm de espesor, de la empresa Atlantis, con una porosidad del 90% de acuerdo a las especificaciones dadas por el fabricante. El geotextil utilizado era un geotextil no tejido de poliéster, tipo Danofelt PY 200 de la empresa Danosa, con una de permeabilidad al agua perpendicularmente al plano sin carga de 18000 mm/h como mínimo, de

acuerdo a las características indicadas por el fabricante (UNE EN ISO 11058). La geomembrana utilizada para impermeabilizar la sección era PEAD de 2 mm de espesor.

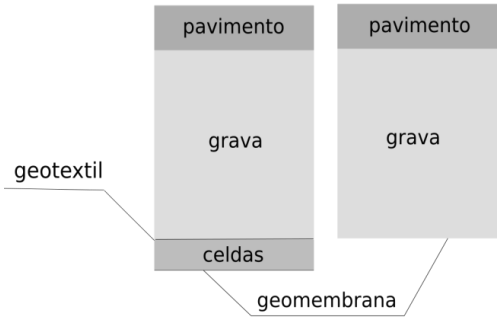

Figura 2 | Secciones tipo comparadas.

En el banco de pruebas, los dos tipos de subbase se colocaron directamente sobre la geomembrana impermeable, de acuerdo a la disposición indicada en la Figura 2. En ambas, la grava se ha compactó manualmente impactando sobre un listón de madera dispuesto sobre la grava, mediante un martillo de plástico. En ambos casos, el espesor de grava ensayada fue de 70 mm. Precisamente, la sección total fue de 70 mm en el caso de la sección sin celdas, mientras que en la sección con celdas la sección total fue de 122 mm. En el banco, la lluvia generada por la parrilla caía directamente sobre la grava de la subbase, infiltrándose en esta y generando un flujo lateral que se recogía en el orificio de salida dispuesto a tal fin. Es importante señalar que no se observó escorrentía superficial en ninguna prueba. Como resultado, no se ha instaló ningún elemento adicional de medición.

Por lo que respecta a las pendientes del pavimento, a pesar de que las diferentes normativas autonómicas de accesibilidad aplicables en zonas urbanas son dispares, los valores de la pendiente transversal mínimas son muy similares, siendo un 2% el valor más habitual, pero, además, es habitual adoptar una pendiente transversal mínima del 1% para evacuar las aguas pluviales. En cuanto a la pendiente longitudinal de los itinerarios peatonales accesibles, los valores máximos exigidos oscilan entre el 6% y el 8% (Alonso López et al., 2010). Por ello, se ensayan las dos pendientes límite: la mínima (1%) y la máxima longitudinal (6%).

En total se han realizado 4 ensayos por cada tipo de material ensayado (dos pendientes y dos lluvias), y todos los ensayos se han realizado tres veces. Los 24 ensayos se han realizado de forma aleatoria para cada tipo de material. El procedimiento aplicado ha sido el siguiente: tras ajustar la pendiente del banco de pruebas, se le ha aplicado a la sección una lluvia de 140 mm/h durante 5 minutos, en el cual se ha aprovechado el último minuto para ajustar el caudal de la lluvia. Tras esos primeros 5 minutos, se ha dejado drenar la sección otros 5 minutos, momento en el cual se ha comenzado con el ensayo. Conscientes de la importancia de la humedad inicial, también se ha medido la humedad inicial de las secciones tras los 10 minutos de preparación. Para ello, al finalizar la jornada se prepararon las secciones con el procedimiento antes descrito, pero, en ese caso, se dejó drenar toda la noche y se midió el volumen de salida. Ese volumen se consideró como el volumen de agua inicial o humedad inicial de la sección. Las mediciones realizadas indicaron que la humedad inicial era del 1.0%.

Para medir los flujos infiltrados y generar los hidrogramas de salida, se colocó una cubeta de hidrogramas a la salida del banco de pruebas. La medición del caudal de lluvia se realizó durante 30 minutos (15 minutos con lluvia y 15 minutos sin lluvia). El cubo tenía 16 contenedores con una superficie de 17800 mm^2 cada uno, y una capacidad de 6.5 litros por contenedor. De esta manera, utilizando 14 de las 16 cubetas, la duración del hidrograma se dividió en 28 intervalos no homogéneos. Como resultado, y teniendo en cuenta que había que capturar más detalles en la curva creciente y decreciente del hidrograma, los límites de los intervalos seleccionados han sido (en mm:ss): 00:00, 1:00, 1:30, 2:00, 2:30, 3:00, 3:30, 4:00, 4:30, 5:30, 6:00, 7:00, 8:00, 9:00, 11:00, 13:00, 15:00, 15:30, 16:00, 17:00, 17:30, 18:00, 19:00, 20:00, 22:00, 25:00 y 30:00.

Modelo hidrológico

El modelo hidrológico utilizado fue el correspondiente a la versión 5.1.013 del SWMM, el cual permite definir unidades LID en las subcuencas, unidades LID se corresponden con diferentes técnicas SUDS, entre las cuales está el pavimento permeable. La cuenca modelizada ha sido de 1 m^2, idéntica a las superficies probadas en el laboratorio. En el modelo, la superficie de pavimento permeable ocupa toda la subcuenca, es decir, la subcuenca contempla una unidad LID que la cubre en su totalidad. En consecuencia, de todos los parámetros generales que definen una subcuenca en SWMM, sólo se fijó la superficie (1 m^2). El resto de los parámetros generales (pendiente, anchura, rugosidad, etc.) se consideraron nulos al ser definidos en la unidad LID a través de la opción *Control LID* (*LID Control*).

Así, al activar la opción *Control LID* es necesario fijar algunos parámetros generales de la unidad LID, los cuales se muestran en el editor LID (LID editor) de la subcuenca (Tabla 2). Por un lado, la anchura de la superficie se ha fijado en 1 m, según las características del banco de pruebas. Por otro lado, el valor de la humedad inicial se ha fijado en el 1%, como se ha explicado en el apartado anterior. Además, se ha generado un nudo exterior a la cuenca, para evacuar el agua infiltrada que sale por el dren. En él se medirán los caudales, y el hidrograma generado será el utilizado para comparar los resultados del modelo con los resultados obtenidos en el laboratorio.

Tabla 1 | Parámetros de utilización de las unidades LID.

Parámetro	Unidades	Valor
Ancho de la superficie por unidad	m	1
% Inicialmente saturado	%	1,0

La unidad LID definida para caracterizar el pavimento permeable tiene varias capas: superficie, pavimento, suelo, almacenamiento y drenaje. Cada capa se caracteriza mediante los parámetros que se muestran en la Tabla 1 (no se muestran los parámetros de la capa suelo, pues no se consideró). Los valores de la capa de pavimento se han seleccionado para que esa capa no influya en la capa inferior, de forma análoga a como se ha realizado en los ensayos de laboratorio, donde se han ensayado las capas inferiores sin la capa de pavimento. Por ejemplo, para ignorar el efecto del pavimento, se definió con un espesor mínimo y un índice huecos (V_{huecos}/ $V_{sólidos}$) máximo, de forma que el agua de lluvia va directamente a la capa inferior (capa de almacenamiento).

Algunos de los parámetros se midieron en el laboratorio o fueron facilitados por el fabricante. Tal y como se ha mencionado en el apartado anterior, el espesor y el índice de huecos se midieron en el laboratorio. El índice de huecos de la subbase con celdas se calculó teniendo en cuenta sus espesores y los índices de huecos correspondientes a cada material: 0.79 para la grava y de 9.00 para las celdas, según datos del fabricante. De ese modo, el índice de huecos del conjunto se consideró de 1.77.

Otros parámetros se establecieron en función de las características del banco de pruebas, como la altura de la berma, considerada nula porque el lado de la parte inferior de la superficie estaba libre y el agua podía fluir libremente; la separación del drenaje, el cual se consideró nulo, al disponer de un lateral libre; la tasa de infiltración, que también se consideró nula al disponerse de una superficie inferior impermeable. Se consideró un valor igual a 1000 mm/h para la permeabilidad del pavimento, valor inferior a los habituales pero muy superior a la intensidad de lluvia estudiada.

Tabla 2 | Parámetros de la unidad LID.

	Parámetros		
Capa	**Nombre**	**Unidades**	**Valores**
SUPERFICIE	Altura de resguardo	mm	0
SUPERFICIE	Fracción de vegetación del volumen	-	0
SUPERFICIE	Rugosidad de la superficie	-	0.012
SUPERFICIE	Pendiente de la superficie	%	1-6
PAVIMENTO	Espesor	mm	0.0001
PAVIMENTO	Relación de vacíos	-	0.9999
PAVIMENTO	Fracción de superficie impermeable	-	0
PAVIMENTO	Permeabilidad	mm/h	1000
PAVIMENTO	Factor de colmatación	-	0
PAVIMENTO	Intervalo de regeneración	días	0
PAVIMENTO	Fracción de regeneración	-	0
ALMACENAMIENTO	Espesor	mm	70 y 122
ALMACENAMIENTO	Relación de vacíos	-	0.78 y 1.77
ALMACENAMIENTO	Tasa de infiltración	mm/h	0
ALMACENAMIENTO	Factor de colmatación	-	0
DRENAJE	Coeficiente de flujo	-	calibrado
DRENAJE	Exponente de flujo	-	calibrado
DRENAJE	Separación	mm	0
DRENAJE	Nivel de abertura	mm	0
DRENAJE	Nivel de cierre	mm	0
DRENAJE	Curva de control	-	0

Calibración del modelo

De la Tabla 1 se calibraron el coeficiente y exponente del drenaje, calibración que se realizó manualmente dado el reducido número de parámetros. Para ello se utilizaron los hidrogramas medidos en el laboratorio. La evaluación del rendimiento de los eventos modelados se realizó utilizando el coeficiente adimensional de Nash-Sutcliffe (Nash & Sutcliffe, 1970), dado por la Ecuación (1). En ella, Oi son los datos observados en laboratorio, $\bar{O}$ es la media de los valores observados, y Pi son los valores modelados. Sin embargo, dado que se dispone de datos de laboratorio para diferentes eventos y pendientes, se utilizó la del conjunto de NSE al para evaluar los parámetros calibrados.

$$NSE = 1 - \frac{\sum \left(O_i - P_i\right)^2}{\sum \left(O_i - \bar{O}_i\right)^2} \quad (1)$$

Por otra parte, como los eventos del laboratorio son eventos únicos (no continuos), y estos son habituales para estudiar el flujo máximo y el volumen (Green & Stephenson, 1986), también se analizaron el porcentaje de error en el pico (PEP) y el porcentaje de error en el volumen (PEV), tal y como se muestra en las ecuaciones (2) y (3), de forma que *P* corresponde a los valores modelados y *O* los valores observados.

$$PEP = \frac{P_{punta} - O_{punta}}{O_{punta}} \quad (2)$$

$$PEV = \frac{P_{volumen} - O_{volumen}}{O_{volumen}} \quad (3)$$

RESULTADOS Y DISCUSIÓN

En primer lugar, se presentan los resultados obtenidos en el laboratorio. A continuación, se presentan y discuten los resultados obtenidos con la calibración del modelo matemático.

Hidrogramas de laboratorio

En el laboratorio se han obtenido 8 hidrogramas de agua infiltrada, 4 para cada tipo de subbase. En las capas analizadas, los hidrogramas obtenidos con la mayor de las pendientes, 6%, muestran un pico mayor en comparación con los caudales correspondientes a las pendientes del 1% (Figura 3), tal y como inicialmente se podría esperar. En este sentido, el volumen de agua captada para la pendiente del 6% es mayor que el correspondiente a la del 1%, lo cual también parece lógico, ya que las inclinaciones mayores drenan un mayor volumen de agua para el mismo periodo de tiempo. Por lo tanto, las pendientes menores necesitan más tiempo para evacuar el mismo volumen de agua.

Además, los valores iniciales del caudal son más bajos en el caso de la pendiente más pronunciada (Figura 3). Parece sensato pensar que, después del procedimiento de preparación inicial (5 minutos de lluvia y 5 minutos de evacuación), la humedad inicial o el volumen de agua retenida es menor en el caso de la pendiente más pronunciada porque, como se mencionó anteriormente, las pendientes más pronunciadas drenan el agua infiltrada más rápidamente.

Por otro lado, si se comparan los hidrogramas generados por las dos subbases, se aprecia que ambas son similares en el caso de la pendiente mayor del 6% pero, en cambio, difieren significativamente con la pendiente del 1% (Figura 4), situación que se repite con ambas intensidades. En el segundo caso, cuando la pendiente es del 1%, se puede apreciar que hidrograma de las celdas es algo menor al inicio y tarda más tiempo en alcanzar el caudal pico. Además, la subbase de plástico, a pesar de necesitar más tiempo para alcanzar la punta con pendientes pequeñas, también tiene una punta mayor que la correspondiente a la subbase sin celdas. Además, también se puede observar que el volumen evacuado por la sección de las celdas es mayor para la subbase con celdas.

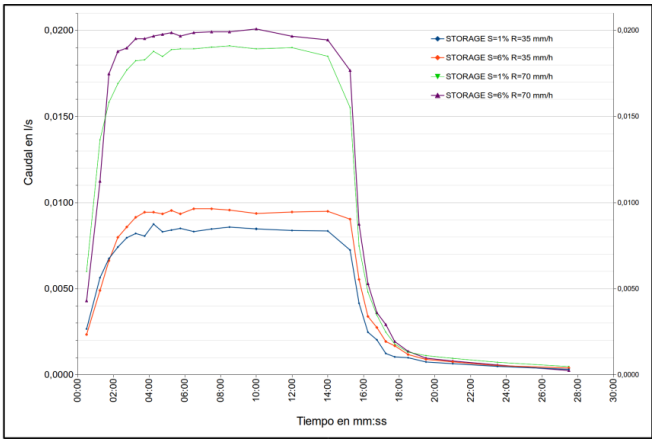

Figura 3 | Hidrogramas correspondientes a la capa base sin celdas, para las dos lluvias (R) y dos pendientes (S) analizadas

En general, los hidrogramas obtenidos son acordes a lo esperado a tenor de los materiales ensayados y sus características, pero destaca la diferencia entre hidrogramas cuando la pendiente es pequeña. En ese caso, que el caudal punta y el volumen evacuado sean mayores parece lógico, pues las celdas permiten una salida más fácil para el agua infiltrada. No así que el caudal inicial sea menor. El motivo principal para que exista esa diferencia podría residir en el geotextil. Podría ser que, de alguna forma, el geotextil genera una barrera al agua. Por otro lado, tampoco parece lógico que los hidrogramas sean muy similares cuando la pendiente es del 6%.

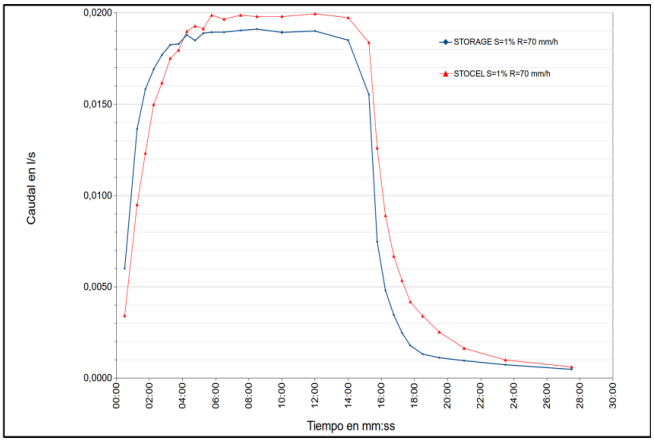

Figura 4 | Hidrogramas correspondientes a la lluvia de 70 mm/h y pendiente del 1% para las dos subbases analizadas.

Calibración

Los valores que mejor reprodujeron los hidrogramas de laboratorio fueron diferentes para ambas subbases. Para la subbase sin celdas los valores de la capa de drenaje que mejor reprodujeron los hidrogramas fueron 10 para el coeficiente y 1,8 para el exponente. Estos valores son similares a los obtenidos en la calibración de otros ensayos similares para una zanja de infiltración (Sañudo-Fontaneda, 2018). De acuerdo con el NSE calibrado, los resultados muestran un desempeño general

aceptable para la estimación del modelo, mejor para la mayor de las intensidades. Los resultados obtenidos para la subbase sin celdas se resumen en la Tabla 3.

Los datos también muestran que para pendientes pequeñas el modelo no solo sobrestima el valor del pico, sino que también genera una sobreestimación en el volumen de salida. Por otro lado, los valores de flujo máximo para las pendientes más pronunciadas, así como los volúmenes, presentan resultados aceptables que están bastante cerca de los datos obtenidos en el laboratorio.

Tabla 3 | Valores obtenidos para la capa de almacenamiento sin celdas (Coeficiente 10, Exponente 1.8)

Lluvia (mm/h)	**35**	**35**	**70**	**70**
Pendiente (%)	**1**	**6**	**1**	**6**
NSE	0.963	0.968	0.976	0.977
PEP (%)	9.1	-3.0	6.0	1.0
PEV (%)	7.3	-4.7	4.7	0.8

Los valores obtenidos al calibrar la capa de almacenamiento con celdas son similares a los obtenidos en la capa de almacenamiento sin celdas, pero se han obtenido con un exponente en la capa de drenaje algo menor, en concreto 1.5. El menor exponente se debe a la diferencia en los hidrogramas de salida. Los resultados de la calibración se muestran en la Tabla 4. En ellas se puede observar que los NSE son algo peores que los resultados sin celdas, a pesar de que el porcentaje en volumen es sensiblemente mejor.

Tabla 4 | Valores obtenidos para la capa de almacenamiento con celdas (Coeficiente 10, Exponente 1.5)

Lluvia (mm/h)	**35**	**35**	**70**	**70**
Pendiente (%)	**1**	**6**	**1**	**6**
NSE	0.853	0.948	0.946	0.982
PEP (%)	8.9	-3.2	5.9	1.0
PEV (%)	-2.3	1.9	0.3	0.6

CONCLUSIONES

Los resultados muestran que los hidrogramas generados a la salida de las subbases son similares para pendientes grandes, del 6%, pero sensiblemente diferentes para pendientes del 1%. Se debe considerar que la subbase con celdas tiene una lámina de geotextil, cuya influencia se debería de analizar con más detalle. Ese sería un aspecto a estudiar en futuras investigaciones.

Por otro lado, los hidrogramas generados mediante el modelo indican que la fiabilidad de éste es aceptable cuando se modelan subbases usando el editor LID de SWMM mediante los parámetros físicos de la subbase. Eso muestra que los parámetros definidos en el laboratorio podrían ser extrapolados a otras cuencas homogéneas de características similares, siempre y cuando se trate de eventos únicos, pues otro aspecto a estudiar sería la respuesta del modelo ante eventos continuos, cuando las características climáticas del entorno influyen en su desempeño. Ello permitiría, además, poder estudiar cómo éstas

cuencas homogéneas podrían integrarse automáticamente en un modelo automático mediante Sistema de Información Geográfica.

Cabe destacar que los parámetros correspondientes a la capa de almacenamiento del modelo para SWMM están concebidos para modelar bases granulares, normalmente grava, no así para modelar celdas o incluir el efecto de geotextiles. Por ello, el valor máximo que se puede introducir para el índice de huecos es de 1.00. En el supuesto de que la capa de almacenamiento contenga algún tipo de celda con una porosidad muy elevada, el valor del índice de huecos es considerablemente mayor, pues el volumen de huecos es mayor que el volumen de sólidos. Ello ha impedido que en este estudio se haya podido utilizar el parámetro físico correspondiente, y sería un aspecto a tener en cuenta al utilizar el modelo SWMM.

Por otro lado, los parámetros de la capa de drenaje tienen una enorme influencia en el flujo de salida de la sección. En esta investigación se calibraron el coeficiente y el exponente de la capa de drenaje para un banco de pruebas específico, con un lado completamente libre, pero estos parámetros, al no tener un significado físico concreto, deben de ajustarse a las características de la subcuenca correspondiente.

Asimismo, de cara a futuras investigaciones, sería interesante analizar el comportamiento de las subbases frente a la colmatación de los poros, así como la influencia de un terreno permeable en el comportamiento hidráulico e, incluso, analizar el desempeño específico de otros tipos de LID.

AGRADECIMIENTOS

Agradecemos sinceramente al Ayuntamiento de Donostia/San Sebastián el material utilizado en los ensayos de laboratorio, sin el cual no ser podría haber realizado el presente estudio.

REFERENCIAS

Alonso López, F., Cruz Mera, A. de la, de Souza, E., Reyes Torres, R., Viéitez Vivas, A. M., Peinado Margalef, N., … Corredor Sierra, B. (2010). Accesibilidad en los espacios públicos urbanizados.

DFG (2018). Estudio de actualización del análisis de las precipitaciones intensas y recomendaciones de cálculo de caudales de avenidas en pequeñas cuencas del territorio histórico de Gipuzkoa (2017/03-BH-ZN). Informe de la Diputación Foral de Gipuzkoa, España.

Flutcher, S., & Wu, J. T. H. (2013). A state-of-the-art review on geosynthetics in low-volume asphalt roadway pavements. International Journal of Geotechnical Engineering, 7(4), 411–419.

Green, I. R. A., & Stephenson, D. (1986). Criteria for comparison of single event models. Hydrological Sciences Journal, 31(3), 395–411. https://doi.org/10.1080/02626668609491056.

Korkealaakso, J., Kuosa, H., Niemeläinen, E., & Tikanmäki, M. (2014). Review of pervious pavement dimensioning, hydrological models and their parameter needs . State-of-the-Art. Climate Adaptative Surface CLASS.

Mullaney, J., & Lucke, T. (2014). Practical review of pervious pavement designs. Clean - Soil, Air, Water, 42(2), 111–124

Nash, J. E., & Sutcliffe, J. V. (1970). River flow forecasting through conceptual models part I — A discussion of principles. Journal of Hydrology, 10(3), 282–290. https://doi.org/https://doi.org/10.1016/0022-1694(70)90255-6.

Sañudo Fontaneda, L. Á., Rodríguez Hernández, J., Castro Fresno, D. (2012). Diseño y Construcción de Sistemas Urbanos de Drenaje Sostenible (SUDS). E.T.S. de Ingenieros de Caminos, Canales y Puertos.

Sañudo-Fontaneda, L. A., Jato-Espino, D., Lashford, C., & Coupe, S. J. (2018). Simulation of the hydraulic performance of highway filter drains through laboratory models and stormwater management tools. Environmental Science and Pollution Research, 25(20), 19228–19237. https://doi.org/10.1007/s11356-017-9170-7

Rossman, L. A. (2015). Storm water management model user's manual, version 5.1. US Environmental Protection Agency: Cincinnati, OH, USA.

Woods Ballard, B., Wilson, S., Udale-Clarke, H., Illman, S., Ashley, R., & Kellagher, R. (2015). The SUDS manual. CIRIA, London, UK.

Yin, J. H., & Shukla, S. K. (2006). Fundamentals of Geosynthetic Engineering. Taylor & Francis Group. London, UK

Appendix B: Field monitoring

This appendix presents some preliminary findings related to the monitoring configuration for the experimental Txominenea plot. In particular, the findings related to data collection from a rain gauge and several outflows from the permeable pavement systems. The reported findings were presented at the international conference entitled International Congress on Energy Efficiency and Sustainability in Architecture and Urbanism in Donostia in 2022.

13th International Conference on Energy Efficiency and Sustainability in Architecture and Urbanism (EESAP 13)

13º Congreso Internacional sobre Eficiencia Energética y Sostenibilidad en Arquitectura y Urbanismo (EESAP 13)

Universidad del País Vasco/Euskal Herriko Unibertsitatea
Donostia-San Sebastián, Spain
28-29 september 2022
www.eesap.eu

Please complete this template and email as an attachment to papers@eesap.eu

Progress towards sustainable stormwater management: Field monitoring of permeable pavements

Hacia una gestión sostenible de las aguas pluviales: Monitorización in situ de pavimentos permeables

[1]**Maddi Garmendia Antin**, [2]Eneko Madrazo-Uribeetxebarria, [3]Alexander Martín-Garín and [1]Jose Antonio Millán

[1]University of the Basque Country UPV/EHU
Faculty of Engineering of Gipuzkoa, San Sebastian
[2]University of the Basque Country UPV/EHU
Faculty of Engineering of Bilbao, Bilbao
[3]University of the Basque Country UPV/EHU
Faculty of Architecture, San Sebastian
943017270; maddi.garmendiaa@ehu.eus

Key Words: (SUDS, monitoring, urban drainage, rainfall-runoff modeling. | SUDS, monitorización, drenaje urbano, modelización precipitación-escorrentía

Abstract: The use of sustainable urban drainage systems (SUDS) in cities is becoming increasingly widespread. Partly, because of concerns about climate change and the associated flood risks and partly, because of increasingly strict requirements regarding the quality of discharges and the insufficient capacity of our wastewater treatment plant systems. However, there is still much uncertainty in their design and implementation: costs, life cycle, modelling, etc.

One of the most widely used tools in the management of urban drainage networks is hydrological-hydraulic modelling. Almost all water utilities have models that allow them to understand the operation of the network,

prioritize investments and estimate the impact of changes in the network. However, these models can only be realistic (and useful) if we provide real data for their calibration. In this sense, very little information is available to integrate sustainable urban drainage systems into the models.

This research consists of the field monitoring of both rainfall events and SUDS behaviour. Specifically, the SUDS technique analyzed are permeable pavements. For this, the first step is the construction of a 1-1 scale model, integrated in the urbanization of the city. Then, a monitoring system is designed to collect data continuously. Obtained data shows not only the effectiveness of the monitoring site for gathering SUDS data, but also the ability of SUDS to control precipitation.

Also, collected data allows evaluating the behaviour of the permeable pavement under real operating conditions and will be used later to carry out the calibration of the model. This calibration is fundamental to properly apply rainfall-runoff models and, therefore, to better understand SUDS performance and adequately plan the future implementation of new SUDS.

1. INTRODUCTION

The traditional urbanization process has a negative impact on the urban hydrological cycle: it increases surface runoff, increases runoff velocity, decreases the concentration time, and reduces water quality (Dietz, 2007). Sustainable Urban Drainage Systems (SUDS) replicate the natural hydrologic cycle (infiltration, filtration, storage, lamination, evapotranspiration) and thus reduce the flood risk and pollution risk (Woods Ballard et al., 2015).

Most SUDS have layers prepared to collect rainwater runoff that falls on them or on nearby areas. Depending on the characteristics of the ground, rainwater can be infiltrated (recharging aquifers), reused, or simply retained in order to be discharged into the underground drainage network. Specifically, permeable pavements can reduce runoff by 50-90% on average (Shafique and Reeho, 2015). Moreover, it has been found that for small intensities, permeable pavements can achieve up to 95% reduction in peak flow and up to 90% reduction in runoff volume (Liu et al., 2017).

Some of the research conducted with permeable pavements place great value on hydraulic-hydrologic models, where such modeling can only represent the actual runoff once calibrated (Andrés-Doménech et al., 2018). While computational models show high accuracy in replicating laboratory data, they overestimate hydrograph discharge and their accuracy decreases with rainfall intensity (Sañudo-Fontaneda et al., 2018). Therefore, although the benefits of SUDS in general, and permeable pavements in particular, are evident, there is still some uncertainty surrounding the parameters that define such hydraulic-hydrologic models, as well as their calibration and validation."

The objective of this work is to continue this line of research, and specifically, to establish a methodology for monitoring SUDS in relation to the hydraulic response of permeable pavements. To this end, the first step is the construction of a 1-1 model integrated in the urbanization of the city and the design of a monitoring system that allows continuous data collection.

1. INTRODUCCIÓN

El proceso de urbanización tradicional afecta negativamente al ciclo hidrológico urbano: aumenta la escorrentía superficial, incrementa la velocidad de la misma, disminuye el tiempo de concentración, y reduce la calidad del agua (Dietz, 2007). Los Sistemas Urbanos de Drenaje Sostenible (SUDS) reproducen el ciclo hidrológico natural (infiltración, filtración, almacenamiento, laminación, evapotranspiración) y, por tanto, reducen el riesgo de inundación y el de contaminación (Woods Ballard et al., 2015).

La mayoría de los SUDS disponen de capas preparadas para almacenar el agua de lluvia que cae sobre ellos o sobre áreas cercanas. Según las características del terreno, el agua de lluvia puede infiltrarse (recargando los acuíferos), reutilizarse o, simplemente, puede retenerse para posteriormente descargarla hacia la red de drenaje soterrada. En concreto, los pavimentos permeables pueden reducir la escorrentía un 50-90% de media (Shafique and Reeho, 2015). Más aún, se ha comprobado que para intensidades pequeñas los pavimentos permeables pueden llegar a reducir hasta un 95% la punta de caudal y hasta un 90% el volumen de escorrentía (Liu et al., 2017).

Algunas de las investigaciones llevadas a cabo con pavimentos permeables ponen en valor los modelos hidráulico-hidrológicos, donde dicha modelación únicamente puede representar la escorrentía real una vez calibrada (Andrés-Doménech et al., 2018). Si bien los modelos computacionales muestran una gran precisión para replicar los datos de laboratorio, éstos sobrestiman la descarga de los hidrogramas y su precisión decrece con la intensidad de lluvia (Sañudo-Fontaneda et al., 2018). Por tanto, aunque los beneficios de los SUDS en general, y los pavimentos permeables en particular, son evidentes, aún existe cierta incertidumbre en torno a los parámetros que definen dichos modelos hidráulico-hidrológicos, así como su calibración y validación".

El objetivo de este trabajo es continuar con esta línea de investigación, y concretamente, establecer una metodología para la monitorización de los SUDS en relación a la respuesta hidráulica de los pavimentos permeables. Para ello, el primer paso es la construcción a escala 1-1 de un modelo integrado en la urbanización de la ciudad y el diseño de un sistema de monitorización que permita recoger los datos de forma continua.

2. BACKGROUND

Natural hydrological processes, such as infiltration and surface runoff, are altered in urban environments, as the urbanization process modifies the physical environment and, therefore, water dynamics. The lack of knowledge of these new, more complex urban hydrological processes is the main reason that has prevented the standardization of these hydrological models adapted to the urban environment. Today, one of the main problems making the development of such models difficult is the lack of data (Salvadore et al., 2015). Therefore, the collection of full-scale data that improve the understanding of hydrological processes related to SUDS is crucial.

Despite the fact that the SUDS concept is not new, there is still resistance to adopt them as a common solution, being the lack of monitored projects one of those reasons (Rodríguez-Rojas, 2020). At the state level, the first project related to permeable pavements dates back to 2003 (Castro-Fresno et al., 2013), a project that has been joined during these years by other projects where field data were monitored (Andrés-Doménech et al.,

2021). Even so, there are few permeable pavements where data on their hydraulic response or quality performance are collected. As an added difficulty, the great climatic variability existing at state level makes it difficult to apply such data in areas with a completely different pluviometric regime (Abellán García et al, 2021).

In recent years, several SUDS have been built in different municipalities of the Basque Country. However, in most cases, these SUDS have been built in isolation and without measurement elements that could yield data on the actual performance of the SUDS in terms of peak flow reduction, time delay of peak flow or runoff pollution reduction.

In this research, a permeable pavement pilot plant has been designed where different modules of permeable pavement and conventional pavement (used as a control environment) have been built specifically for the purpose of the research, as well as a series of manholes to collect and monitor filtered and runoff rainwater. In this way, the aim is to characterize the hydraulic behavior of permeable pavements on a real scale and under real conditions. These data will allow the calibration of a hydraulic-hydrological model, which is essential to adequately plan the future implementation of new SUDS.

2. ANTECEDENTES

Los procesos hidrológicos naturales, tales como la infiltración y la escorrentía superficial, se ven alterados en los entornos urbanos, dado que el proceso de urbanización modifica el entorno físico y, por tanto, la dinámica del agua. El desconocimiento de estos nuevos procesos hidrológicos urbanos, más complejos, es el principal motivo que ha dificultado la estandarización de los dichos modelos hidrológicos adaptados al entorno urbano. Hoy en día, uno de los problemas principales que dificultan el desarrollo de dichos modelos es la falta de datos (Salvadore et al., 2015). Por ello, es importante la toma de datos a escala real que mejoren la comprensión de los procesos hidrológicos relacionados con los SUDS.

A pesar de que el concepto SUDS no es nuevo, existen aún resistencias de cara a adoptarlos como una solución habitual, siendo la falta de proyectos monitorizados una de esas razones (Rodríguez-Rojas, 2020). A nivel estatal, el primer proyecto relacionado con los pavimentos permeables data de 2003 (Castro-Fresno et al., 2013), proyecto al cual se han sumado durante estos años otros proyectos donde se monitorizaban datos de campo (Andrés-Doménech et al., 2021). Aún así, son pocos los pavimentos permeables donde se recolectan datos sobre su respuesta hidráulica o rendimiento de calidad. Como dificultad añadida, la gran variabilidad climática existente a nivel estatal dificulta la aplicación de dichos datos en ámbitos con un régimen pluviométrico completamente diferente (Abellán García et al, 2021).

En los últimos años, son varios los SUDS que se han ido construyendo en distintos municipios del País Vasco. Sin embargo, en la mayor parte de los casos, estos SUDS se han construido de forma aislada y sin elementos de medición que pudieran arrojar datos sobre el funcionamiento real de los SUDS en lo que respecta a la reducción del caudal punta, el retraso temporal de dicho caudal punta o la reducción de la contaminación de la escorrentía.

En esta investigación se ha diseñado una planta piloto de pavimentos permeables donde se han construido, específicamente para el objeto de la investigación, distintos módulos de pavimento permeable y pavimento convencional (usado como ámbito de control), así como una serie de arquetas donde recoger y monitorizar el agua de lluvia filtrada y escurrida. De esta forma, se busca caracterizar el comportamiento hidráulico de los pavimentos permeables a escala real y bajo condiciones reales. Estos datos permitirán realizar la calibración de un modelo hidráulico-hidrológico, que es fundamental para planificar adecuadamente la futura implantación de nuevos SUDS.

3. DESIGN OF THE WORKS AND MONITORING

The experimental area of permeable pavements occupies 180 m², is located in the recently built urbanization of Txomin-Enea, in San Sebastian (see Figure 1) and its layout is shown in Figure 2. Half of the area is sidewalk, built with tiles or pavers (called P surfaces) and the other half is a parking area, built with asphalt (called A surfaces).

1. The pavement package used in each case has been made independent of the grading, i.e., the surface in contact with the natural soil has been waterproofed, in order to control the volume of water managed by the different sections. Specifically, three different sections or configurations were used (see figure 2):
2. The first section, called the control zone, has been built with conventional materials, and therefore, impermeable. Thus, in the sidewalk area, the typical hexagonal tiles used by the city of San Sebastian (Pimp) have been used, and in the parking area, traditional asphalts (Aimp) have been used.
3. In the second section, permeable pavers (P) and porous asphalt (A) have been used over the usual gravel layers in permeable pavements.
4. The last section is identical to the previous one, except that plastic cells have been placed at the bottom to increase the hydraulic capacity of the section. These sections have been identified as Pcell and Acell respectively.

In order to evaluate the performance of the permeable pavements installed in their different configurations as well as that of the control section, six manholes have been installed on site. Two of them collect the surface runoff water and have been named R: Rimp collects the surface runoff water corresponding to the control area (Aimp and Pimp) and Rperv collects the surface runoff corresponding to the permeable pavement areas (A, P, Acell and Pcell). The other four boxes collect the infiltrated water for each type of permeable pavement and section, that is:

- Dp: Subsurface drainage of the permeable pavers of the first section (P).
- Da: Subsurface drainage of the porous asphalt of the first section (A)
- Dpcell: subsurface drainage of permeable pavers with cells in the subbase of the second section (Pcell)
- Dacell: Subsurface drainage of porous asphalt with cells in the subbase of the second section (Acell).

A thin-walled weir with rectangular geometry has been installed in each of these pits to measure the outflow. In addition, in order to carry out continuous monitoring, 6 pressure sensors have been installed, one in each chamber, which allow the level, and therefore the flow rate, to be determined remotely. To collect rainfall data, a rain gauge was used, which could not be installed safely in the urbanization itself, and was installed on the roof of the School of Engineering of Gipuzkoa, which is located just 2 km from the study area.

3. DISEÑO DE LA OBRA CIVIL Y LA MONITORIZACIÓN

El área experimental de pavimentos permeables ocupa 180 m², se ubica en la urbanización de reciente construcción de Txomin-Enea, en San Sebastián(ver figura 1) y su esquema se recoge en la figura 2. La mitad de la superficie es acera, construida en baldosa o adoquinado (se han denominado superficies P) y la otra mitad es zona de aparcamiento, construido con asfalto (se han denominado superficies A).

Figure 1: Location of Txomin-Enea in San Sebastian and of the experimental area in the new urbanization executed in Txomin Enea.

Figura 1: Localización de Txomin-Enea en San Sebastián y del área experimental en la nueva urbanización ejecutada en Txomin Enea.

1. El paquete de firme empleado en cada caso ha sido independizado de la explanación, es decir, se ha impermeabilizado la superficie de contacto con el suelo natural, con objetivo de controlar el volumen de agua gestionado por las distintas secciones. En concreto, se han utilizado tres secciones o configuraciones diferentes (ver figura 2):

2. La primera sección, denominada zona de control, se ha construido con materiales convencionales, y por tanto, impermeables. Así, en la zona de acera se han utilizado las típicas baldosas hexagonales empleadas por el ayuntamiento de San Sebastián (Pimp) y en la zona de aparcamiento se han utilizado asfaltos tradicionales (Aimp).
3. En la segunda sección, se han utilizado adoquines permeables (P) y asfalto poroso (A) sobre las capas de grava habituales en los pavimentos permeables.
4. La última sección es idéntica a la anterior, salvo por que se han colocado unas celdas de plástico en la parte inferior, con el objetivo de aumentar la capacidad hidráulica de la sección. A estas secciones se las ha identificado como Pcell y Acell respectivamente.

Figure 2: Scheme of the different configurations installed in Txomin-Enea (Madrazo et al., 2022) and image of the finished work.

Figura 2: Esquema de las distintas configuraciones instaladas en Txomin-Enea (Madrazo et al., 2022) e imagen de la obra finalizada.

Con objeto de evaluar el funcionamiento de los pavimentos permeables instalados en sus diferentes configuraciones así como el de la sección de control, se han ejecutado en obra seis arquetas. Dos de ellas recogen el agua que escurre superficialmente y se han denominado R: Rimp recoge el agua de escorrentía superficial correspondiente a la zona de control (Aimp y Pimp) y Rperv recoge la escorrentía superficial correspondiente a las zonas de pavimentos permeables (A, P, Acell y Pcell). Las otras cuatro arquetas recogen el agua infiltrada por cada tipo de pavimento permeable y sección, esto es:

- Dp: Drenaje subsuperficial de los adoquines permeables de la primera sección (P)
- Da: Drenaje subsuperficial del asfalto poroso de la primera sección (A)
- Dpcell: Drenaje subsuperficial de los adoquines permeables con celdas en la subbase de la segunda sección (Pcell)
- Dacell: Drenaje subsuperficial del asfalto poroso con celdas en la subbase de la segunda sección (Acell)

En cada una de estas arquetas se ha instalado un vertedero de pared delgada y geometría rectangular que permite medir el caudal de salida. Además, con objeto de realizar una monitorización continua, se han instalado 6 sensores de presión, uno en cada arqueta, que permiten determinar el nivel, y por tanto, el caudal de forma remota. Para la toma de datos de la pluviometría, se ha empleado un pluviómetro cuya instalación no fue posible realizar en la propia urbanización en condiciones de seguridad, y fue instalado en la cubierta de la Escuela de Ingeniería de Gipuzkoa que se sitúa apenas a 2 km de la zona de estudio.

Figure 3: Three of the manholes built in Txomin-Enea. Weirs can be noted as well as the pressure sensors located in each manhole. Pluviometer installed on the roof of the School of Engineering of Gipuzkoa.

Figura 3: Tres de las arquetas construidas en Txomin-Enea. Pueden observarse los vertederos así como los sensores de presión ubicados en cada arqueta. Pluviometro instalado en la cubierta de la Escuela de Ingeniería de Gipuzkoa.

4. RESUL AND DISCUSSION

The period analyzed runs from July 2021 to December 2021. During this period, the sensors take data every 10 minutes and the most intense storm occurs on November 15 (see Figure 4). As an example, the data obtained for a rainfall episode of Imax=4.8mm/h and 3h duration on September 3rd is shown (see figure 5).

As can be seen in the data obtained from the rain gauge (Figure 5, right), the maximum rainfall intensity on September 3 is between 7:20 and 7:40 am, although from 9:10 to 9:30 am there is another peak, just before the end of the episode at 9:50 am. This rainfall generates a surface runoff on the impervious surface (Rimp) that can be seen in Figure 5 (left). Likewise, the sensors located in the other five manholes, which record water level data in the permeable sections (Rperv, Da, Dacell, Dp, Dpcell) hardly record any measurements, and when they do, it is towards the end of the period analyzed, at values much lower than the surface runoff in the control zone.

It is evident that all the rainwater is filtered by the permeable pavements, hardly generating any outflow. The infiltrated rainwater is absorbed by the material itself and retained in the manholes, without generating subsurface runoff at any time.

4. RESULTADOS Y DISCUSIÓN

El periodo analizado va desde julio de 2021 hasta diciembre de 2021. En este periodo, los sensores toman datos cada 10 minutos y la tormenta de mayor intensidad se da el día 15 de noviembre (ver figura 4). A modo de ejemplo, se muestran los datos obtenidos para un episodio de lluvia de Imax=4,8mm/h y 3h de duración el día 3 de septiembre (ver figura 5).

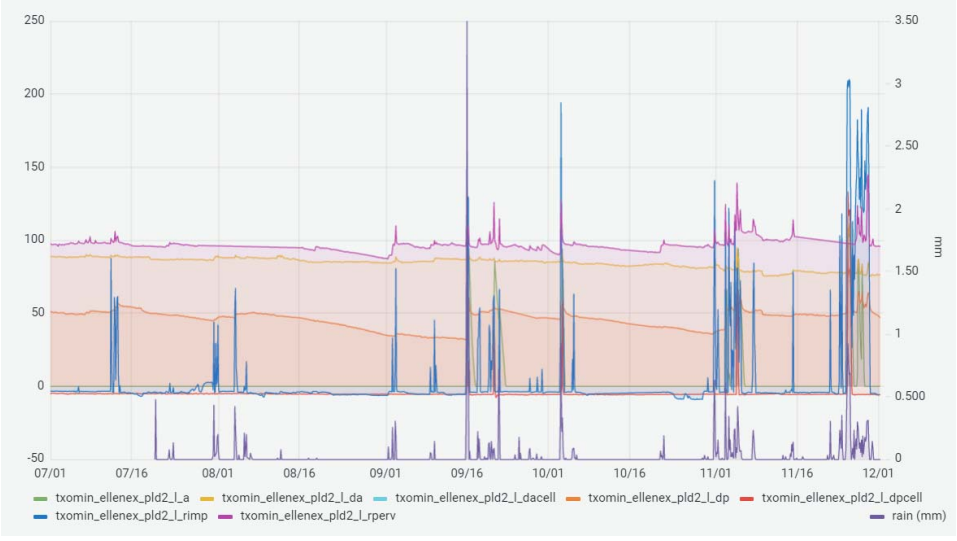

Figure 4: Raw data collected by the pressure sensors and the rain gauge.

Figura 4: Datos en bruto recogidos por los sensores de presión y el pluviómetro.

Tal y como se puede observar en los datos obtenidos del pluviómetro (figura 5, dcha), la intensidad máxima de lluvia el día 3 de septiembre se da entre las 7:20 y las 7:40h de la mañana, si bien de 9:10 a 9:30h se vuelve a dar otro pico, justo antes de terminar el episodio a las 9:50h. Esta lluvia genera una escorrentía superficial en la superficie impermeable de control (Rimp) que se puede apreciar en la figura 5 (izq). Así mismo, los sensores ubicados en las otras cinco arquetas, que registran los datos de nivel de agua en las secciones permeables (Rperv, Da, Dacell, Dp, Dpcell) apenas registran medidas, y cuando lo hacen es hacia el final del periodo analizado, en valores muy inferiores al de la escorrentía superficial en la zona de control.

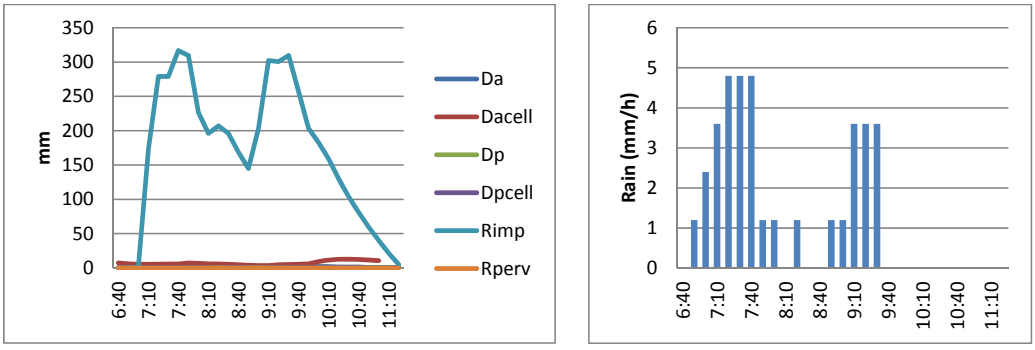

Figure 5: Water levels in the Txomin water boxes and rainfall collected by the rain gauge during the rainfall event analyzed on September 3, 2021.

Figura 5: Nivel de agua en las arquetas instaladas en Txomin y lluvia recogida por el pluviómetro durante el episodio de lluvia analizado el día 3 de septiembre de 2021

Es evidente que toda el agua de lluvia es filtrada por los pavimentos permeables, no llegando apenas a generar un caudal de salida. El agua de lluvia infiltrado es absorbida por el propio material y retenida en las arquetas, sin llegar a generar escorrentía subsuperficial en ningún momento.

5. CONCLUSIONS AND FUTURE RESEARCH

This work has made it possible to establish a methodology for monitoring SUDS in relation to the hydraulic response of permeable pavements. The work carried out and its monitoring makes it possible to measure the infiltrated flows and determine the retention capacity of the infrastructure with real rainfall data. From the data obtained, it is possible to conclude the capacity of a permeable pavement to reduce peak flow and laminate runoff. In any case, it will be necessary to analyze the data over a longer period of time and with higher rainfall

intensities in order to have more conclusive results, although the preliminary results are consistent with the results published to date.

The final objective of this project is the development of a generalized model for urban catchments to analyze the hydraulic and pollutant retention behavior of any urbanization project where the use of permeable pavements is foreseen through the application of SUDS techniques. The data obtained in this work will serve as the basis for a more exhaustive study that will feed and validate the modeling to be carried out. As a future line of research, the storage of infiltrated rainwater by permeable pavements for subsequent reuse is proposed, especially as an alternative in areas where for various reasons (clayey or impermeable soils, high groundwater level, contaminated soils, etc.) the water captured by SUDS cannot or should not infiltrate into the natural ground.

5. CONCLUSIONES Y FUTURAS LÍNEAS DE INVESTIGACIÓN

Este trabajo ha permitido establecer una metodología para la monitorización de los SUDS en relación a la respuesta hidráulica de los pavimentos permeables. La obra ejecutada y su monitorización permiten medir los caudales infiltrados y determinar la capacidad de retención de la infraestructura con datos de lluvia reales. De los datos obtenidos, se puede concluir la capacidad que posee un pavimento permeable de reducir el caudal punta y laminar la escorrentía. En todo caso será necesario analizar los datos durante un periodo de tiempo más largo y con intensidades de lluvia más elevadas para poder tener resultados más concluyentes, si bien, los resultados preliminares son coherentes con los resultados publicados hasta la fecha.

El objetivo final de este proyecto es el desarrollo de un modelo generalizado para cuencas urbanas que permita analizar el comportamiento hidráulico y de retención de contaminantes de cualquier proyecto de urbanización donde se prevea el empleo de pavimentos permeables mediante la aplicación de técnicas SUDS. Los datos obtenidos en este trabajo, servirán de base a un estudio más exhaustivo que permitirá alimentar y validar las modelizaciones a realizar. Como futura línea de investigación, se plantea el almacenamiento del agua de lluvia infitrada por los pavimentos permeables para su posterior reutilización, especialmente como alternativa en las zonas donde por diversas circunstancias (suelos arcillosos o impermeables, nivel freático elevado, suelos contaminados, etc.) el agua captada por los SUDS no pueda o no deba infiltrarse al terreno natural.

ACKNOWLEDGMENTS

The authors are grateful for the financial support of the UPV/EHU through the project US19/17. The project has also received the support of the City Council of San Sebastian, to whom we are grateful for their collaboration throughout the project.

AGRADECIMIENTOS

Los autores agradecen el apoyo económico de la UPV/EHU a través del proyecto US19/17. También ha contado con el apoyo del Ayuntamiento de San Sebastián, a quien agradecemos su colaboración a lo largo del proyecto.

REFERENECES

REFERENCIAS

[1] M. E. Dietz, Low impact development practices: A review of current research and recommendations for future directions, Water, air, and soil pollution, 186 (1-4), 351-363, 2007.

[2] B. Woods Ballard, S. Wilson, H. Udale-Clarke, S. Illman, R. Ashley, R. Kellagher, The SUDS manual (C753). Ciria, London, 2015. Available at: https://www.ciria.org/

[3] M. Shafique, R. Reeho, Low Impact Development Practices: a Review of Current Research and Recommendations for Future Directions. Ecological Chemistry and Engineering, 2015 https://doi.org/10.1515/eces-2015-0032

[4] C.Y. Liu, T.F.M. Chui, Factors Influencing Stormwater Mitigation in Permeable Pavement, WATER, 2017. https://doi.org/10.3390/w9120988

[5] I. Andres-Domenech, S. Perales-Momparler, A. Morales-Torres, I. Escuder-Bueno, Hydrological performance of green roofs at building and city scales under mediterranean conditions, Sustainability 10 (2018). https://doi.org/10.3390/su10093105.

[6] L. A. Sañudo-Fontaneda, D. Jato-Espino, C. Lashford, & S. J. Coupe, Simulation of the hydraulic performance of highway filter drains through laboratory models and stormwater management tools. Environmental Science and Pollution Research, 25(20), 19228-19237, 2018.

[7] E. Salvadore, J. Bronders, O. Batelaan, Hydrological modelling of urbanized catchments: A review and future directions, Journal of Hydrology 529 (2015) 62–81. https://doi.org/10.1016/j.jhydrol.2015.06.028

[8] M.I. Rodríguez-Rojas, F. Huertas-Fernández, B. Moreno, G. Martínez, Middle-Term Evolution of Efficiency in Permeable Pavements: A Real Case Study in a Mediterranean climate, International Journal of Environmental Research and Public Health 17 (2020). https://doi.org/10.3390/ijerph17217774

[9] D. Castro-Fresno, V.C. Andrés-Valeri, L.A. Sañudo-Fontaneda, J. Rodriguez-Hernandez, Sustainable drainage practices in Spain, specially focused on pervious pavements, Water (2013). https://doi.org/10.3390/w5010067

[10] I. Andrés-Doménech, J. Anta, S. Perales-Momparler, J. Rodriguez-Hernandez, Sustainable Urban Drainage Systems in Spain: A Diagnosis, Sustainability 13 (2021). https://doi.org/10.3390/su13052791

[11] A.I. Abellán García, N. Cruz Pérez, J.C. Santamarta, Sustainable Urban Drainage Systems in Spain: Analysis of the Research on SUDS Based on Climatology, Sustainability 13 (2021). https://doi.org/10.3390/su13137258

[12] E. Madrazo-Uribeetxeberria, M. Garmendia, M. Meaurio (2022) Zoladura iragazkorrak hirietako drainatze sarean txertaturiko elementu gisa, Ekaia, DOI: https://doi.org/10.1387/ekaia.23083

Appendix C: Performance

This appendix presents some preliminary findings related to the monitored permeable pavements in Txominenea. In particular, the findings related to the first analysis of the hydraulic performance of the permeable pavements at a 1:1 scale. The reported findings were presented in the international congress entitled Novatech, held in Lyon in 2023.

Permeable pavement flood control performance for several layouts in an Atlantic climate site

Performance des chaussées perméables contre les inondations pour plusieurs aménagements en climat atlantique

Eneko Madrazo-Uribeetxebarria[1], Maddi Garmendia Antín[1], Ignacio Andrés-Doménech[2], Ainhoa Lekuona Orkaizagirre[3], Maite Meaurio[3], Ainara Gredilla[4]

1. Gipuzkoa Engineering Faculty, University of the Basque Country UPV/EHU, eneko.madrazo@ehu.eus / maddi.garmendiaa@ehu.eus
2. Instituto Universitario de Investigación de Ingeniería del Agua y del Medio Ambiente (IIAMA), Universitat Politècnica de València, igando@hma.upv.es
3. Faculty of Chemistry, University of the Basque Country UPV/EHU, ainhoa.lekuona@ehu.eus / maite.meaurio@ehu.eus
4. Faculty of Science and Technology, University of the Basque Country UPV/EHU, ainara.gredi@ehu.eus

RÉSUMÉ

Les chaussées perméables sont un type de technique alternative de gestion des eaux de ruissellement urbain, dont l'un des avantages est qu'elles nécessitent peu d'espace supplémentaire, ce qui les rend avantageuses dans les zones urbaines où l'espace est limité. Les chaussées perméables fournissent un instrument supplémentaire de contrôle des inondations, caractérisé par la réduction du volume et des pics de ruissellement. Cependant, des données supplémentaires sont encore nécessaires pour tester leur performance à long terme dans diverses conditions climatiques. Par conséquent, cet article explore la performance de quatre agencements différents de chaussées perméables situés dans un climat atlantique. Le débit de ces aménagements, tous conçus sans infiltration, a été collecté par un tuyau poreux et dirigé vers des regards individuels où le débit a été mesuré toutes les 10 minutes, et les données ont été comparées au ruissellement mesuré sur un site complètement imperméable. Les résultats montrent que tous les aménagements constituent une mesure très efficace pour contrôler le volume et le pic de ruissellement. Le volume de ruissellement est réduit de plus de 80 % dans tous les cas, et le pic de ruissellement est réduit de plus de 70 % pour les aménagements considérés. Cette réduction est très significative, car les tempêtes considérées atteignent 117 mm et le site perméable est conçu sans infiltration.

ABSTRACT

Permeable pavements are a Sustainable Urban Drainage System (SUDS) technique. One of its advantages is that it requires little additional space, which makes them advantageous in urban areas with limited space. Permeable pavements, as other SUDS techniques, provide an additional instrument for flood control, characterised by its runoff volume reduction and peak flow reduction. However, more data is still required to test their long-term performance under various climatic conditions. Hence, this article explores the performance of four different permeable pavements layouts located in an Atlantic climate. Outflow from those layouts, all designed with no infiltration, has been collected through a porous pipe and directed into individual manholes were flow was measured every 10 minutes. This data was compared with runoff measured in a completely impervious site. Results show that all layouts are a very effective measure to control runoff volume and peak. Runoff volume is reduced over 80 % in all cases, and runoff peak is reduced over 70 % for considered layouts. This reduction is very significant, as considered storms are up to 117 mm and the permeable site is designed with no infiltration.

KEYWORDS

SUDS, permeable asphalt, permeable pavers, urban runoff, flood control

1 INTRODUCTION

Permeable pavements are a Sustainable Urban Drainage System (SUDS) technique, which can be implemented, among other areas, in walkways, parking lots, roads or playgrounds. One of its advantages is that they require little additional space compared to other SUDS types, which makes them advantageous in urban areas with limited space and high land price (Kuruppu et al., 2019).

Hydraulic performance of permeable pavements is an important factor for flood control, being total volume reduction and peak reduction two typical indicators to characterise their performance (Tirpak et al., 2021). However, these indices are considerably sensitive to rainfall (Zhu eta al., 2021), and, by extension, to climate conditions.

On the other hand, further investigation is still required regarding stormwater runoff quantity and weather patterns (Liu et al., 2021). In that regard long-term performance of surface runoff can provide valuable information for the design of permeable pavements (Abdalla et al., 2022). Hence, this study explores the performance of permeable pavements that was characterised by the peak and volume reduction of runoff compared to the runoff produced by an impervious site.

2 METHODOLOGY

2.1 Site design

The experimental permeable pavement site is located by the Bay of Biscay, in Donostia/San Sebastián (Spain), as shown in Figure 1. The city, according to Köppen classification, has a temperate climate without dry season and mild summer (Abellán García et al., 2021). Annual average precipitation is 1507 mm, with 141 days per year with rainfalls higher than 1 mm. Average temperature is 13.5°C.

Figure 1. Location of the permeable pavement site.

The city council has a combined sewer network where, during high storms, overflows occur. In order to analyse the effect of permeable pavements, an experimental site was implemented in a new urban plot. The experimental area has 180 m^2, with 80 m^2 corresponding to a walkway and 100 m^2 to a parking lot. Additionally, the site has been divided in three equal areas: standard pavement (impervious), permeable pavement and permeable pavement with subsurface cells. Hence the plot has 6 different areas: impervious walkway and parking, permeable walkway and parking, and permeable walkway and parking with subsurface cells.

Each of the four permeable pavement areas, walkway/parking and with/without subsurface cells, was designed to avoid infiltration into the natural soil. Hence, all the water infiltrated into the pavement section was collected by a porous tube pipe and directed to a manhole in order to be measured. Thus, the analysis focuses exclusively on the permeable pavement structure.

2.2 Monitored data

The site was designed to measure surface flow on the impervious standard site, with a combination of walkway and asphalt, and infiltrated rain into four different permeable areas. All flows were derived into individual channels, five in total (impervious, asphalt, pavers, asphalt with cells and pavers with cells), where flow was controlled by rectangular weirs previously calibrated at the laboratory. Sensor data was collected by level

sensors with an error of 0.25 mm. Rain data was collected from Miramon weather station, located 2,5 km from the site, with public accessible data gathered in a 10-minute interval.

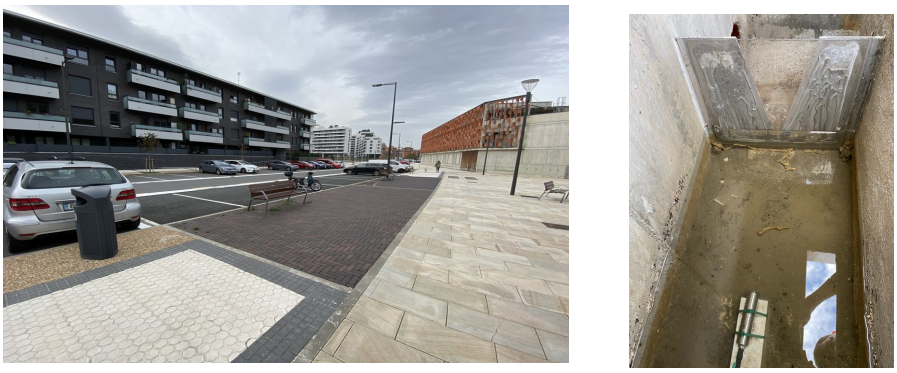

Figure 2. Image of the pavement site (left), with a parking area (darker asphalt) and walkway area (red pavers), and manholes for flow control (right).

3 RESULTS AND DISCUSSION

13 storms were selected and analysed from gathered data. Storms depths ranged from 3 mm to 118 mm. Two of those storms are given in Figure 3 and Figure 4 as examples, which are considered illustrative enough for a low precipitation volume, (8.4 mm for the storm given in Figure 3), and a high precipitation volume, (117.8 mm for the storm given in Figure 4, which is the highest of all selected storms).

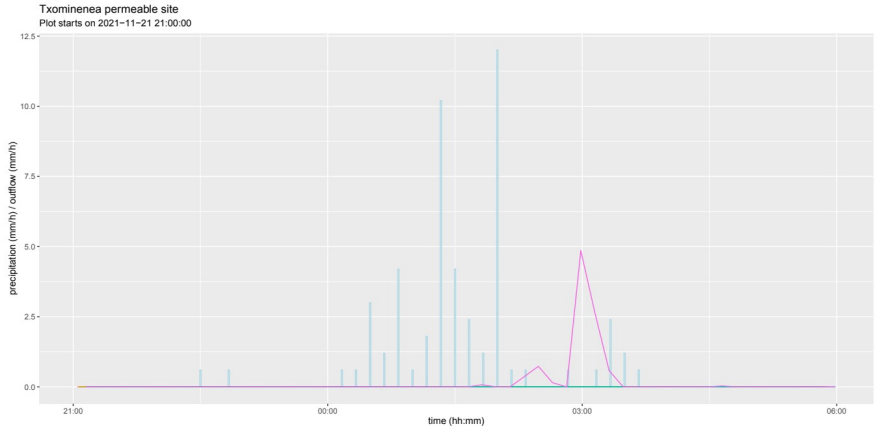

Figure 3. Precipitation (blue bars) and drain outflow for the impervious site (pink) and four permeable sites (orange, brown, green and blue) for a storm of 8.4 mm. Notice that the orange, brown, green and blue lines are completely flat.

The first result that obtained data clearly shows is that there is a considerable reduction of the runoff volume and peak in those sites where permeable pavement has been implemented. For runoff volume, storm depths lower than 40 mm have a runoff volume reduction higher than 90%, if compared with the impermeable site. Many of those lowest storms measured very little flow, or no flow at all. In addition, even for higher storms, the volume reduction is always higher than 80%. Accordingly, peak reduction is almost 100% for storms with volumes lower than 40 mm. For higher storms, peak reduction is considerably high, but the lowest reduction is 70%, lower than volume reduction, as may be expected.

The runoff reduction, both peak and volume, are effective in all four considered layouts. However, there are some little differences. For instance, drain outflow is higher for pavers than for asphalt sites. Also, flow from sites with a subsurface cell is higher than flow from sites without any cell.

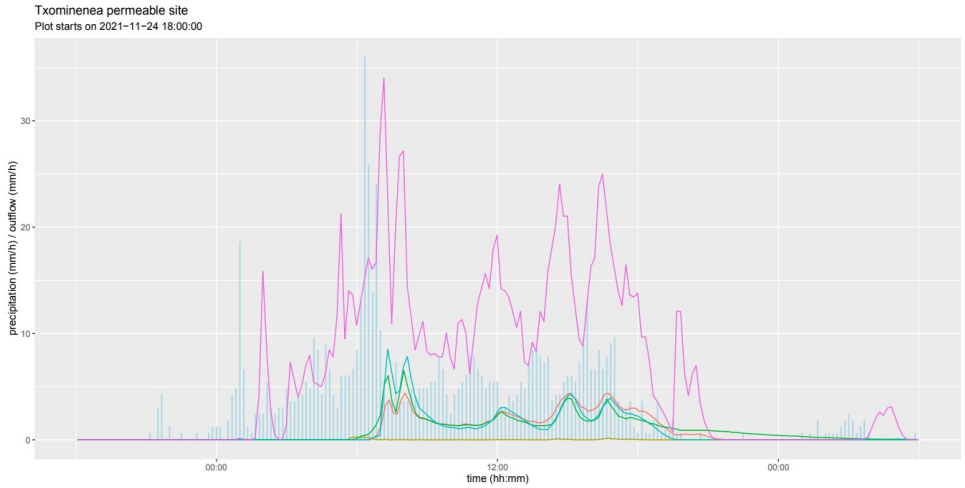

Figure 4. Precipitation (blue bars) and drain outflow for the impervious site (pink) and four permeable sites (red for asphalt, green for pavers, brown for asphalt with cells and blue for pavers with cells) for a storm of 117,8 mm.

4 CONCLUSIONS

This study analyses the effectiveness of permeable pavements for flood control in an experimental site located in an Atlantic climate area, based on data collected during 6 months, from June to December. Measured storms are representative enough to conclude the effectiveness of permeable pavements for flood control in an Atlantic climate. Most of the storms are well controlled by the permeable pavement, as no runoff is created for storms lower than 40 mm.

The runoff reduction, both peak and volume, is effective in all four considered layouts, although there are some slight differences. Nevertheless, there are only a couple of high storms where outflow from the permeable site has been measured, which makes it difficult to compare the performance of several pavement designs. Although the lack of data from the permeable sites being positive, it means that they fulfil their purpose, makes it hard to compare how different designs affect flood control. Further measurements will continue, so more detailed conclusions can be drawn.

LIST OF REFERENCES

Abdalla, E. M. H., Muthanna, T. M., Alfredsen, K., and Sivertsen, E. (2022). *Towards improving the hydrologic design of permeable pavements*. Blue-Green Systems, 4(2), 197–212.

Abellán García, A., Noelia Cruz Pérez, I. and C. Santamarta, J. (2021). *Sustainable Urban Drainage Systems in Spain: Analysis of the Research on SUDS Based on Climatology*. Sustainability 13(13).

Kuruppu, U., Rahman, A., and Rahman, M. A. (2019). *Permeable pavement as a stormwater best management practice: A review and discussion*. In Environmental Earth Sciences 7, 327. Springer

Liu, T., Lawluvy, Y., Shi, Y., and Yap, P.-S. (2021). *Low Impact Development (LID) Practices: A Review on Recent Developments, Challenges and Prospects*. Water, Air, & Soil Pollution, 232(9), 344.

Tirpak, R. A., Winston, R. J., Feliciano, M., Dorsey, J. D., and Epps, T. H. (2021). *Impacts of permeable interlocking concrete pavement on the runoff hydrograph: Volume reduction, peak flow mitigation, and extension of lag times*. Hydrological Processes, 35(4), e14167.

Zhu, Y., Li, H., Yang, B., Zhang, X., Mahmud, S., Zhang, X., Yu, B., and Zhu, Y. (2021). *Permeable pavement design framework for urban stormwater management considering multiple criteria and uncertainty*. Journal of Cleaner Production, 293, 126114.

Appendix D: Implementation analysis

This appendix presents some of the preliminary findings related to the SUDS implementation at a municipal level. In particular, the findings related to the necessary space allocation for implementing SUDS in the early stages of urban development. The reported findings were presented in the national conference entitled 39th IAHR World Congress in Granada in 2022.

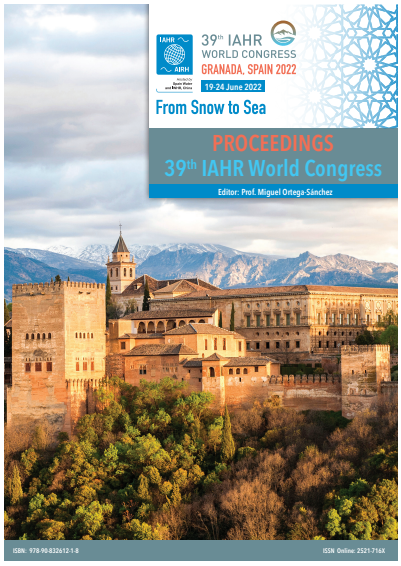

39th IAHR WORLD CONGRESS GRANADA, SPAIN 2022 From Snow to Sea 19-24 June 2022

Proceedings of the 39th IAHR World Congress
19–24 June 2022, Granada, Spain
doi://10.3850/IAHR-39WC2521716X2022282

Influence of SUDS Allocated Area on Runoff Reduction in Developing Urban Catchments: a Case Study in San Sebastian (Spain)

Eneko Madrazo-Uribeetxebarria[(1)], Maddi Garmendia Antín[(2)], Jabier Almandoz Berrondo[(2)] and Ignacio Andrés-Doménech[(3)]

[(1)] Faculty of Engineering in Bilbao, University of the Basque Country UPV/EHU, Spain
eneko.madrazo@ehu.eus

[(2)] Faculty of Engineering in Gipuzkoa, University of the Basque Country UPV/EHU, Spain
maddi.garmendiaa@ehu.eus

jabier.almandoz@ehu.eus

[(3)] Instituto Universitario de Investigación de Ingeniería del Agua y Medio Ambiente (IIAMA), Universitat Politècnica de València, Spain
igando@hma.upv.es

Abstract

Despite the increasing use of Sustainable Urban Drainage System (SUDS) techniques, it is still difficult for urban planners to identify how many shall they implement, especially when planning new developments. In addition, most agencies or public authorities limit runoff outflows to the greenfield or undeveloped conditions, but planners do not have the capacity to link this objective to the level of SUDS implementation. Thus, the objective of the present study is to analyse the relation between the implementation level of SUDS and the reduction of urban catchment ouflows (peak flow and volume), compared to greenfield condition. For that purpose, a hydrological model was created with the Storm Water Management Model (SWMM), based on a case study of 3.2 ha in Donostia/San Sebastián (Spain). The greenfield scenario was characterised with a CN equal to 78. Pervious and impervious areas were identified into the urbanised plot, as well as the existing drainage network. Finally, certain area of SUDS was assigned to each subcatchment randomly, and hydraulic variables were compared at the outlet with the ones in the greenfield situation. As the area is a dense urban area, the considered SUDS for this study were green roofs, permeable pavements and bio-retention cells. Four storm scenarios were used, with a 30 minutes duration but different return periods: 2, 5, 10 and 20. Results show how SUDS application is more effective with the peak than with the volume, and that surface with SUDS applied on a 35% of the surface may reduce the outflow peak to its greenfield value.

Keywords:SUDS; SWMM; urban planning; SUDS allocation.

1. INTRODUCTION

Urbanisation and varying precipitation regimes derived from climate change threaten long-term reliability of urban drainage networks. Sustainable Urban Drainage Systems (SUDS), which manage surface runoff at source by enhancing infiltration, evaporation and detention, are helpful instruments to address those future challenges.

Although there are several SUDS practices with different hydraulic and quality performances, space limitations constraint those that can be applied in highly urbanised environments without reducing the operating area for pedestrians and vehicles. Permeable pavements, for example, allow runoff control without reducing the hard surface, especially important if there is little available space for stormwater detention (Kuruppu et al., 2019). On the other hand, and although bioretention cells do not meet that requirement, bioretention systems are some of the most commonly used SUDS practices (Skorobogatov et al., 2020).

Urban environments often have two very different types of plots, private and public, with very different design and development processes. In that regard, an increasing number of authorities are supporting the use of green roofs in private buildings. In addition, as private plots also have areas with surface use easement, permeable pavements may also be applied in those private plots.

But, regardless the SUDS or plot type, SUDS selection, design, and location is a high-level complexity problem (Ferrans et al., 2022). In that regard, strategic planning approaches can be very helpful tools to help in the spatial allocation of SUDS, but the urban planners are reluctant to use them (Kuller et al., 2019).

On the other hand, as flood control will be a critical planning issue in the future (Kong et al., 2017), hydrological issue will play a critical role in that allocation process. Hence, it is common to analyse SUDS requirements hydrologically, usually comparing it with a greenfield scenario with no urbanisation in it.

Previously, Palla and Gnecco (2015) studied how some hydrologic performance parameters varied under several SUDS application scenarios. Just considering one single scenario for permeable pavements and four scenarios for green roofs, they established a linear relation between the applied SUDS area and the peak and volume reduction, compared to a scenario where no SUDS was applied. They found that peak reduction was 45% and volume reduction was 24% when implemented SUDS occupied 36% of the area.

This study deepens on the reduction of those parameters (runoff volume and peak) with the random application of different SUDS percentages. The performance of the SUDS application percentage is compared with a greenfield baseline scenario. This analysis is made to help urban planners deciding how much space shall be allocated for SUDS in a new urban development if certain hydraulic objectives are to be fulfilled, in the very early stages of the planning, when there is limited information about the drainage network or even the space type distribution.

2. METHODS

2.1 Case study

The case study has been conducted in a new development located in the city of Donostia/San Sebastián (Spain), as shown in Figure 1. The new development was built in a plot with some buildings, lawns and gardens, with a total area of 15.5ha. The area had numerous flooding problems in the past, as it is located at the Urumea river mouth. The study was conducted because the city council aims to promote the use of SUDS at the municipal level.

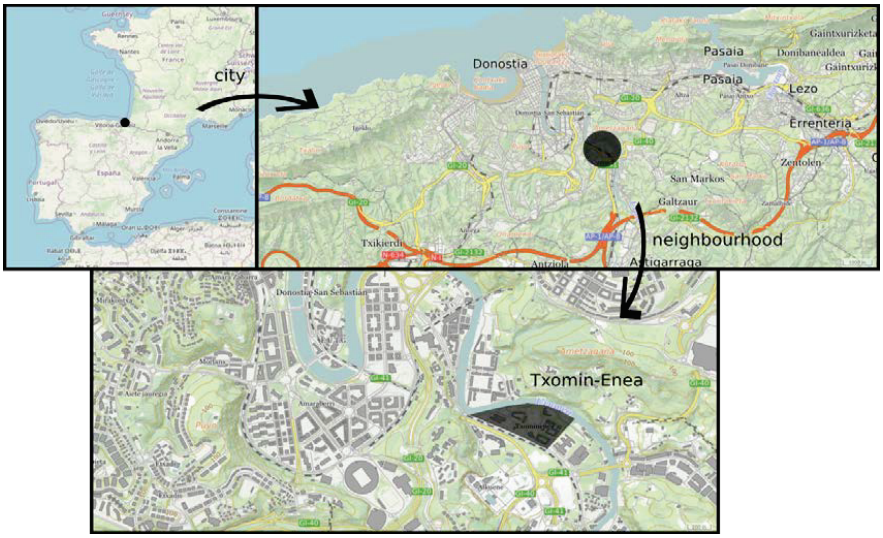

Figure 1. Case study location.

Donostia/San Sebastian has an Atlantic climate, and average annual rainfall is 1474 mm. Rainfall is evenly distributed throughout the year, the monthly average is between 90-120 mm in the less rainy months, and between 140-175 mm in the rainiest months. For this study, IDF curves from Igeldo weather station were selected, as it has a long historical record. For the analysis, 30 minutes duration constant rainfalls were considered, with these intensities for each return period (Tr): 40 mm/h (Tr = 2 years), 52 mm/h (Tr = 5 years), 61 mm/h (Tr = 10 years) and 70 mm/h (Tr = 20 years).

As the new development is located by the Urumea river, it has several drainage outflows to the river, with 3 independent subcatchments on the plot that direct the flow to the river. For this study, only the area contributing to one of the catchments has been selected, with a total of 3.2 ha(see Figure 2, where the area contour is drawn in red).

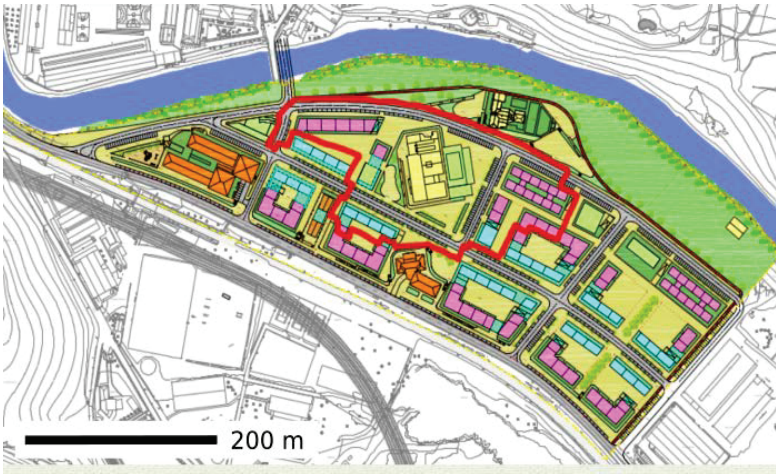

Figure 2. New development and the area selected for the analysis (contour is drawn in red).

2.2 SUDS implementation analysis

To carry out the analysis, a detailed model of the catchment was created in SWMM, with 372 subcatchments (see Figure 3). Private and public spaces were considered in the urban plot. The private ones, which were 55% of the total area, included private plots with public use easement on the surface. Public space was divided in sidewalks (24%), roads and parking lots (19%), bike lines (1%), and green areas (1%). Except the last one, all of them were sealed with conventional pavement on the surface. For the analysis, bike lines were considered as pathways.

The drainage network of the area has a total of 152 pipes and 153 manholes. The pipe diameter ranges from 0.25 m to 0.80 m. The smallest ones are PVC pipes located in the begging of the network, to direct water from the catchment basins to the main pipes. Water from private lots is collected in PVC pipes with a diameter of 0.30 m. Rest of the pipes are the ones from the main pipe, which direct water to the river outlet (on the left upper side of Figure 3). Biggest pipes, from 0.50 m diameter, are concrete pipes.

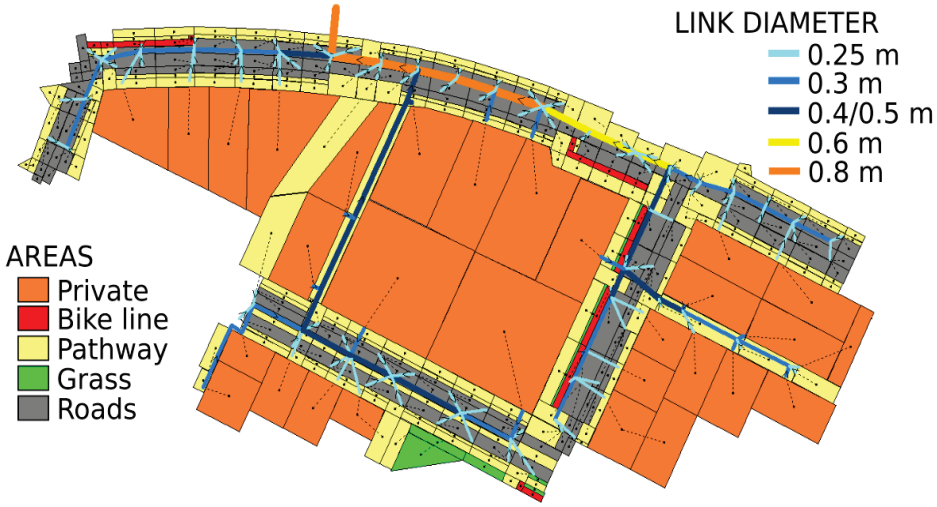

Figure 3. SWMM model of modelled area, with different colours for each considered subcatchment typology and pipe diameter.

The SUDS implementation analysis was made based on a greenfield scenario, which was considered as a baseline to compare runoff volumes and peak values in the outflow from the subcatchment. That greenfield scenario was characterised by a CN equal to 78, correspondent to a cultivated land, with conservation treatment and an hydrologic soil group C.

For SUDS application scenarios, it was considered a CN equal to 98 for all impervious surfaces (road, pathways, cycle paths and private plots), and 78 for green spaces (same as greenfield case). For application of the CN method, a depression storage of 2.5 mm was used over green areas, 1.6 mm for impervious areas and 6 mm for greenfield case (Rossman and Huber, 2016a).

For SUDS implementation analysis, three SUDS types were considered: permeable pavement, green roof and bioretention cell. Used parameters are given in Table 1, which are commonly used for SUDS design (Rossman and Huber, 2016b) No drain was considered for any of the SUDS, neither clogging conditions.

Table 1. SWMM parameters for considered SUDS types.

LAYER / PARAMETER	UNITS	GREEN ROOF (GR)	PERMEABLE PAVEMENT (PP)	BIORETENTION CELL (BR)
SURFACE				
BERM HEIGHT	mm	10	0	100
VEGETATION VOLUME	fraction	0.15	0	0.1
SURFACE ROUGHNESS	$s/m^{1/3}$	0.1	0.1	0.1
SURFACE SLOPE	%	1	1.5	1
PAVEMENT				
THICKNESS	mm	-	80	-
VOID RATIO	V/S	-	0.97	-
IMPERVIOUS SURFACE	fraction	-	0.9	-
PERMEABILITY	mm/h	-	10000	-
SOIL				
THICKNESS	mm	100	0	400
POROSITY	fraction	0.5	-	0.4
FIELD CAPACITY	fraction	0.2	-	0.2
WILTING POINT	fraction	0.1	-	0.1
CONDUCTIVITY	mm/h	100	-	100
CONDUCTIVITY SLOPE	-	30	-	40
SUCTION HEAD	mm	60		60
STORAGE				
THICKNESS	mm	-	400	300
VOID RATIO	V/S	-	0.80	0.75
SEEPAGE RATE	mm/h	-	10	10
DRAIN MATERIAL				
THICKNESS	mm	3	-	-
VOID FRACTION	fraction	0.5	-	-
ROUGHNESS	$s/m^{1/3}$	0.1	-	-

The SUDS application was done considering different plot types and SUDS percentages (see Table 2). In private plots two types of SUDS were applied: green roof and permeable pavement. In public spaces two types of SUDS were also applied: permeable pavement (just on pathways and bikes lines) and bioretention cells (just in road surfaces). The SUDS implementation analysis was done selecting a percentage of application for each type, done randomly, and that SUDS was applied to all subcatchments of the same type (road, sidewalk, etc.). Each percentage was selected independently (four in total), and the global SUDS percentage calculated later. This last value was the only one considered in the following analyses.

Table 2. Percentage ranges applied in the subcatchments for each SUDS type.

	PRIVATE PLOT MINIMUM	PRIVATE PLOT MAXIMUM	PUBLIC SPACE MINIMUM	PUBLIC SPACE MAXIMUM
GREEN ROOF	0%	50%	-	-
PERMEABLE PAVEMENT (PP)	0%	20%	0%	40%
BIO-RETENTION CELL (BRC)	-	-	0%	10%

Some SUDS were designed to collect a certain amount of impervious area of the same type, considering regular design standards. Permeable pavement collected an impervious surface equal to its area (Woods Ballard, 2015). For bioretention cells, the collected extra impervious surface was 4 times the biorentention area.

Analysis of SUDS scenario was done comparing these hydrologic performance indexes for all simulations: runoff peak and runoff volume. The considered parameters for the analysis were the increase of peak and volume over the greenfield scenario, given as a percentage. The simulations were performed 50 times for each return period, thus, a total of 200 simulations were performed.

3 RESULTS AND DISCUSSION

3.1 Outflow peak

If a new urban plot is designed without any SUDS solution in it, see Figure 4, peak flow is increased between 75% and 150% for a certain storm event, compared to greenfield scenario. Those two values correspond to 0% of SUDS implementation for returns periods equal to 20 and 2.Figure shows how that peak increase, compared to greenfield scenario, decreases with the application of SUDS into the urban catchment. The relation between the applied SUDS percentage and the peak flow is linear and, obviously, decreases if the percentage of applied SUDS is increased.

The figure also shows that greater return periods give lower peak increases over greenfield scenario. That is probably related to the precipitation intensity, as greenfield scenario can not manage high water volumes in low time intervals. Hence, peak increase over greenfield scenario is lower for higher return periods. The figure also reveals that the smaller the return period, the faster the peak is reduced with the application of SUDS or, graphically, that decreasing slope is higher for lower return periods.

The figure also shows that, for the analysed three highest return periods, the flow peak is equal to the greenfield case when the SUDS application is around 35%, although the value is a bit different for each return period. However, that value is considerably higher for the lowest return period, which is around 45%. In any case, it can be concluded that an application of a SUDS surface equivalent to the 45% of the total area shall not increase the peak volume compared to greenfield case.

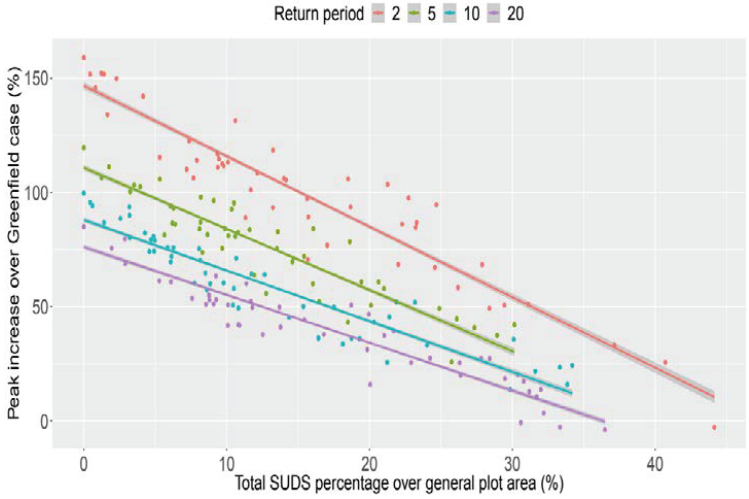

Figure 4. Relation between peak flow and SUDS percentage application into a urban plot, with different colours for considered return periods.

3.2 Outflow volume

Similarly to peak analysis, Figure 5 shows how the runoff volume increases, compared to greenfield scenario, from 175% to 400% if no SUDS solution is applied (value corresponding to 0% of SUDS implementation). Thus, runoff volume increase over the greenfield scenario is considerably higher than the

peak increase. Also, in this case, volume increase over greenfield scenario decreases with SUDS application, and it does faster for lower return periods. But, contrary to what happens with the peak, a SUDS application within the 35-45% range does not reduce the outflow volume to the greenfield case. For the volume case, that value only decreases the volume until it doubles the greenfield case, which corresponds to the 100% value in theordinate axis of the figure.

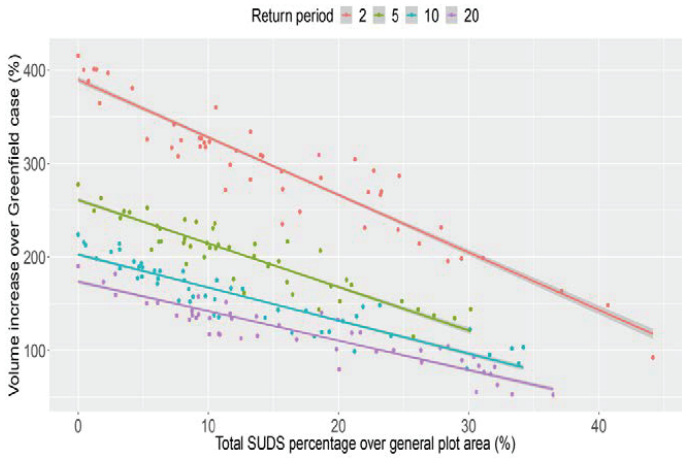

Figure 5. Relation between runoff volume and SUDS percentage application into a urban plot, with different colours for considered return periods.

If both peak and volume results are compared with those obtained by Palla and Gnecco (2015), it can be observed that SUDS are effective even if the implementation level is low, although Palla and Gnecco identified a minimum reduction of 5% was required to obtain noticeable hydrologic benefits. As Palla and Gnecco (2015) compared the reduction based on 0% SUDS implementation, or “do nothing” scenario, comparison is not direct, but findings are in line with those obtained previously.

4 CONCLUSIONS

This study has analysed how SUDS application influences outflow from a dense urban plot. The results show, consideringthe bioretention cell as the only one reducing available space, that it is not necessary to allocate a huge amount of space to get some reasonable reduction on runoff peak and volumes. With these results, urban planners have one more tool to decide, in the very initial stages of urban developments, how much space shall be dedicated to SUDS. Planners can further detail SUDS implementationin future planning stages: what type, management trains, exact location, and other specific details, which are difficult to set in the very beginning of the planning process.

However, this study has some limitations. First, the analysis has been performed with three types of SUDS, but it shall be interesting to check how the output shall perform with other types of SUDS. In addition, SUDS were applied uniformly into the subcatchments, effect shall be different if SUDS were applied randomly over the different subcatchments. Also, this study has just introduced one type of SUDS that decreases the available space for pedestrians and vehicles in dense urban environments: the bioretention cell. Other types of SUDS do not have such limitations, and it would be interesting to analyse this factor. Secondly, the analysis was based on a constant single event storm, but the effect of a continuous modelling should be explored. The study was limited to a certain urban plot and drainage network as well, the effect those late is also recommend to be explored. Finally, individual devices were explored, but management trains shall improve obtained results.

5 ACKNOWLEDGEMENTS

This research was supported by Donostia/San Sebastián City Council, to which we are very grateful.

6 REFERENCES

Ferrans, P., Torres, M.N., Temprano, J., & Rodríguez Sánchez, J. P. (2022). Sustainable Urban Drainage System (SUDS) modeling supporting decision-making: A systematic quantitative review. *Science of The Total Environment*, 806, 150447. https://doi.org/10.1016/j.scitotenv.2021.150447

Kong, F., Yulong, B., Haiwei, Y, Philip, J., and Iryna Dronova. (2017). Modeling Stormwater Management at the City District Level in Response to Changes in Land Use and Low Impact Development. *Environmental Modelling and Software* 95: 132–42. https://doi.org/10.1016/j.envsoft.2017.06.021.

Kuller, M., Bach, P.M., Roberts, S., Browne, D., and Deletic, A. (2019). A Planning-Support Tool for Spatial Suitability Assessment of Green Urban Stormwater Infrastructure. *Science of The Total Environment* 686: 856–68. https://doi.org/https://doi.org/10.1016/j.scitotenv.2019.06.051

Kuruppu, U., Rahman, A., & Rahman, M.A. (2019). Permeable pavement as a stormwater best management practice: a review and discussion. *Environmental Earth Sciences*, 78(10). https://doi.org/10.1007/s12665-019-8312-2

Palla, A., and Gnecco, I. (2015). Hydrologic Modeling of Low Impact Development Systems at the Urban Catchment Scale. *Journal of Hydrology* 528: 361–68. https://doi.org/10.1016/j.jhydrol.2015.06.050

Rossman, L.A., & Huber, W.C. (2016a). Storm Water Management Model Reference Manual Volume I Hydrology (Revised): Vol. I

Rossman, L.A., & Huber, W.C. (2016b). Storm Water Management Model Reference Manual Volume III Water Quality (Vol. III).

Skorobogatov, A., He, J.X., Chu, A., Valeo, C., & van Duin, B. (2020). The impact of media, plants and their interactions on bioretention performance: A review. *Science of the Total Environment*, 715. https://doi.org/10.1016/j.scitotenv.2020.136918

Woods Ballard, B., Wilson, S., Udale-Clarke, H., Illman, S., Ashley, R., Kellagher, R., Martin, P., Jefferies, C., Bray, R., Shaffer, P., & Wallingford, H. R. (2015). The SUDS manual. In CIRIA, London, UK.

